การแยกอิแนนทิโอเมอร์ของแอมีนด้วยแก๊สโครมาโทกราฟีที่ใช้อนุพันธ์แอซีทิลบีตาไซโคลเดกซ์ทรินเป็นเฟสคงที่

นางสาวสายทิพย์ เจริญชัยวรกิจ

วิทยานิพนธ์นี้เป็นส่วนหนึ่งของการศึกษาตามหลักสูตรปริญญาวิทยาศาสตรมหาบัณฑิต
สาขาวิชาเคมี ภาควิชาเคมี
คณะวิทยาศาสตร์ จุฬาลงกรณ์มหาวิทยาลัย
ปีการศึกษา 2557

ENANTIOMERIC SEPARATION OF AMINES BY GAS CHROMATOGRAPHY USING ACETYL-DERIVATIZED BETA-CYCLODEXTRIN AS STATIONARY PHASE

Miss Saithip Charoenchaiworakit

A Thesis Submitted in Partial Fulfillment of the Requirements
for the Degree of Master of Science Program in Chemistry
Department of Chemistry
Faculty of Science
Chulalongkorn University
Academic Year 2014

Thesis Title	ENANTIOMERIC SEPARATION OF AMINES BY GAS CHROMATOGRAPHY USING ACETYL-DERIVATIZED BETA-CYCLODEXTRIN AS STATIONARY PHASE
By	Miss Saithip Charoenchaiworakit
Field of Study	Chemistry
Thesis Advisor	Assistant Professor Aroonsiri Shitangkoon, Ph.D.

Accepted by the Faculty of Science, Chulalongkorn University in Partial Fulfillment of the Requirements for the Master's Degree

.....Dean of the Faculty of Science

(Professor Supot Hannongbua, Dr.rer.nat.)

THESIS COMMITTEE

.....Chairman

(Associate Professor Paitoon Rashatasakhon, Ph.D.)

.....Thesis Advisor

(Assistant Professor Aroonsiri Shitangkoon, Ph.D.)

.....Examiner

(Monpichar Srisa-Art, Ph.D.)

.....External Examiner

(Assistant Professor Jongkolnee Jongaramruong, Ph.D.)

สายทิพย์ เจริญชัยวรกิจ : การแยกอิแนนทิโอเมอร์ของแอมีนด้วยแก๊สโครมาโทกราฟีที่ใช้อนุพันธ์แอซีทิลบีตาไซโคลเดกซ์ทรินเป็นเฟสคงที่ (ENANTIOMERIC SEPARATION OF AMINES BY GAS CHROMATOGRAPHY USING ACETYL-DERIVATIZED BETA-CYCLODEXTRIN AS STATIONARY PHASE) อ.ที่ปรึกษาวิทยานิพนธ์หลัก: ผศ. ดร.อรุณ ศิริ ชิตางกูร, 77 หน้า.

ศึกษาการแยกคู่อิแนนทิโอเมอร์ของอนุพันธ์ไตรฟลูออโรแอซีทิลของแอมีนทั้งหมด 49 ตัว ด้วยแก๊สโครมาโทกราฟีที่ใช้ เฮปตะคิส(2,3-ได-โอ-แอซีทิล-6-โอ-เทอร์ต-บิวทิลไดเมทิลไซลิล)บีตาไซโคลเดกซ์ทริน (หรือ BSiAc) เป็นเฟสคงที่ชนิดไครัล โดยศึกษาอิทธิพลของอุณหภูมิและโครงสร้างของแอมีน (ชนิดและตำแหน่งของหมู่แทนที่) ที่มีผลต่อรีเทนชันและค่าการแยกอิแนนทิโอเมอร์ พบว่า BSiAc สามารถแยกอิแนนทิโอเมอร์ของแอมีนได้ 45 ชนิด สำหรับกลุ่ม 1-ฟีนิลเอทิลลามีน พบว่าตำแหน่งของหมู่แทนที่มีผลต่อการแยกมากกว่าชนิดของหมู่แทนที่ โดยแยกอิแนนทิโอเมอร์ของสารที่มีหมู่แทนที่ในตำแหน่งเมตาได้ดี อีกทั้งได้ศึกษาผลของชนิดของหมู่แทนที่ที่ตำแหน่งสเทอริโอเจนิก พบว่า BSiAc แยกอิแนนทิโอเมอร์ของสารกลุ่ม 1-ฟีนิลโพรพิลลามีนและกลุ่ม 1-แอมิโนอินเดน ได้ดีกว่ากลุ่ม 1-ฟีนิลเอทิลลามีน แต่ BSiAc แยกอิแนนทิโอเมอร์ของสารกลุ่มฟีนิลฟีนิลเมทานามีนไม่ได้หรือแยกได้ไม่ดี ซึ่งมีหมู่แทนที่ขนาดใหญ่ เช่น ฟีนิล จากสารที่นำมาศึกษาทั้งหมด พบว่าอุณหภูมิมีผลต่อการแยกอิแนนทิโอเมอร์ของ 3CF3 มากที่สุด และสามารถแยกสารนี้สมบูรณ์ภายในเวลาน้อยที่สุด

ภาควิชา เคมี ลายมือชื่อนิสิต .....

สาขาวิชา เคมี ลายมือชื่อ อ.ที่ปรึกษาหลัก .....

ปีการศึกษา 2557

5572137023 : MAJOR CHEMISTRY

KEYWORDS: GAS CHROMATOGRAPHY / ENANTIOMER / AMINE

SAITHIP CHAROENCHAIWORAKIT: ENANTIOMERIC SEPARATION OF AMINES BY GAS CHROMATOGRAPHY USING ACETYL-DERIVATIZED BETA-CYCLODEXTRIN AS STATIONARY PHASE. ADVISOR: ASST. PROF. AROONSIRI SHITANGKOON, Ph.D., 77 pp.

The enantioseparation of 49 trifluoroacetyl amine derivatives was studied by gas chromatography using heptakis(2,3-di-*O*-acetyl-6-*O*-*tert*-butyldimethylsilyl)-beta-cyclodextrin (or BSiAc) as a chiral stationary phase. The effects of temperature and amine structure (type and position of substitution) on retention and enantioselectivity were studied. BSiAc could resolve enantiomers of 45 amines. For 1-phenylethylamines, the position of substitution played a major role on enantioseparation than the type of substitution: analytes with *meta*-substitution showed good enantioseparation. The effect of type of substitution at the stereogenic center was also investigated. BSiAc showed better enantioseparation towards 1-phenylpropylamines or 1-aminoindans than 1-phenylethylamines. However, BSiAc showed poor or no enantioseparation towards phenyl phenyl methanamines which have a large phenyl group at the stereogenic center. Among all analytes tested in this study, 3CF3 showed strong temperature dependency and could be completely enantioseparated with the shortest analysis time.

Department: Chemistry Student's Signature .....

Field of Study: Chemistry Advisor's Signature .....

Academic Year: 2014

ACKNOWLEDGEMENTS

First of all, I would like to express my gratitude to my advisor, Assistant Professor Dr. Aroonsiri Shitangkoon, for her support and guidance throughout the course of this research. I would not have achieved this far and this work would not have been completed without her. I also would like to thank Associate Professor Dr. Paitoon Rashatasakhon, Assistant Professor Dr. Jongkolnee Jongaramruong and Dr. Monpichar Srisa-Art for serving as the thesis committee and for their valuable comments.

I am especially thankful to Professor Gyula Vigh (Texas A & M University, USA) for providing cyclodextrin derivative used in my research.

I am grateful to Department of Chemistry, Chulalongkorn University for providing instrumentations, facilities and partial financial support for this research.

Finally, I would like to give my heartfelt thanks to my beloved family, my friends and all members in chiral separation group for encouragement and help during the period of this research.

CONTENTS

Page

Page

LIST OF TABLES

LIST OF FIGURES

CHAPTER I

INTRODUCTION

Amines are important class of compounds for living systems. They are substances for several chemical syntheses and are essential components in amino acids and many drugs. For some amines with chiral property in their structures, each enantiomer may show different or opposite biological activity to its optical isomer. For example, (*S*)-(+)-amphetamine is more active towards the nervous system than (*R*)-(–)-amphetamine (Figure 1.1). Dextro-isomer of propoxyphene (Figure 1.1) is an analgesic drug, but levo-isomer is an anti-tussive drug [1-3]. Thus, separation techniques or synthetic schemes leading to purely single enantiomer of drugs are useful. In addition, fast and reliable analytical techniques are important for the determination of enantiomeric purity of the desired compounds before any usage.

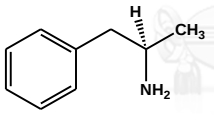

(*R*)-(+)-amphetamine

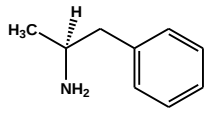

(*S*)-(–)-amphetamine

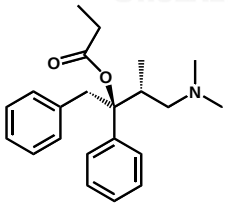

dextropropoxyphene

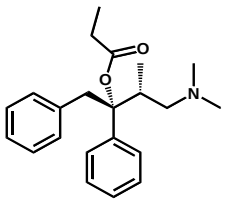

levopropoxyphene

Figure 1.1 Structure of *(R)*- and *(S)*-enantiomers of amphetamine and propoxyphene.

In this work, 1-phenylethylamines (1-PEAs) are the compounds of interest as they have been widely used as a key moiety in chiral synthetic drugs, as a chiral auxiliary or ligand for asymmetric synthesis, or a resolving agent to convert chiral

compounds to diastereoisomers [4]. Analytical techniques frequently used to separate the enantiomers of amines include gas chromatography (GC) [5-7], high performance liquid chromatography (HPLC) [8], and capillary electrophoresis (CE) [9-11] employing different types of chiral selectors as stationary phase, mobile phase additive, or modifier. Cyclodextrins (CDs) and their derivatives are among the most commonly used chiral selectors [12] as they are chiral and can form inclusion complexes with many types of compounds. There are reports on the enantiomeric separation of 1-PEA and other amines of related structures using CD derivatives as chiral selectors. However, small changes in analyte structure as well as CD structure greatly affect the enantioselectivity. Thus, the enantiomeric separation of new analytes is still difficult to predict. The derivatized CDs with large *tert*-butyldimethylsilyl group at 6-*O*-position and small alkyl or acyl substituents at 2-*O*- and 3-*O*-positions were shown to be good chiral selectors in GC for enantiomeric separation of compounds with various structures [5, 13-15].

The objective of this work was therefore to study the enantiomeric separation as a function of temperature of forty-nine trifluoroacetyl derivatives of amines by GC using heptakis(2,3-di-*O*-acetyl-6-*O*-*tert*-butyldimethylsilyl)-β-CD (or BSiAc) as a chiral selector. Total of forty-nine 1-PEAs and other amines of related structure with different types and positions of substitution were selected to examine the influence of analyte structure on enantioselectivity. To study the effect of type of CD substitution, the results obtained from BSiAc were compared to those previously reported using heptakis(2,3-di-*O*-methyl-6-*O*-*tert*-butyldimethylsilyl)-β-CD (or BSiMe) [16].

CHAPTER II

THEORY

2.1 Analyses of enantiomers

Qualitative and quantitative analyses of enantiomers were generally performed by spectroscopic technique, such as nuclear magnetic resonance (NMR), or separation techniques, such as gas chromatography (GC), high performance liquid chromatography (HPLC) or capillary electrophoresis (CE). The separation of enantiomers could be achieved either by indirect or direct approach [17]. For indirect approach, enantiomers were reacted with highly pure chiral reagent to form diastereomers which have different physical and chemical properties. Diastereomers were then analyzed by NMR or separated by chromatographic techniques using non chiral stationary phases. Disadvantages of the indirect approach include the requirement of high purity chiral reagents for specific reactions as well as complete and similar conversion of both enantiomers into diastereomers without loss or decomposition. For direct approach, enantiomers were directly analyzed by separation techniques without changing to diastereomers. However, these techniques require the use of chiral selector as chiral stationary phase (GC, HPLC) or modifier in mobile phase (HPLC) or background electrolyte (CE). Cyclodextrin derivatives, either in pure form or as a mixture in polysiloxane, are among the most popular chiral GC stationary phases [3].

2.2 Cyclodextrins and their derivatives

Cyclodextrins (CDs) are cyclic oligosaccharides with the shape of a truncated cone (Figure 2.1). CDs are composed of several D-glucose units connected by α-1,4-linkages (Figure 2.2). Secondary hydroxyl groups (at C2 and C3) of the glucose unit are at the wider edge, while primary hydroxyl groups (at C6) are at the narrower rim. The cavity of CDs is relatively hydrophobic, while the outside is relatively hydrophilic.

Three commonly used CDs are α-, β- and γ-CDs, containing 6, 7 and 8 glucose units, respectively. Their properties are compared in Table 2.1.

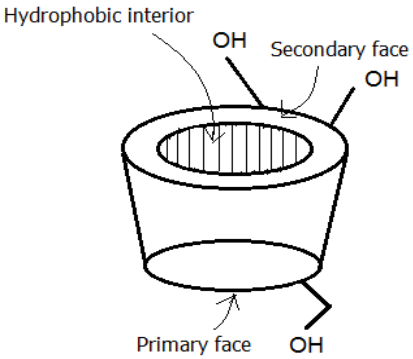

Figure 2.1 Structure on side view of β-CD [18].

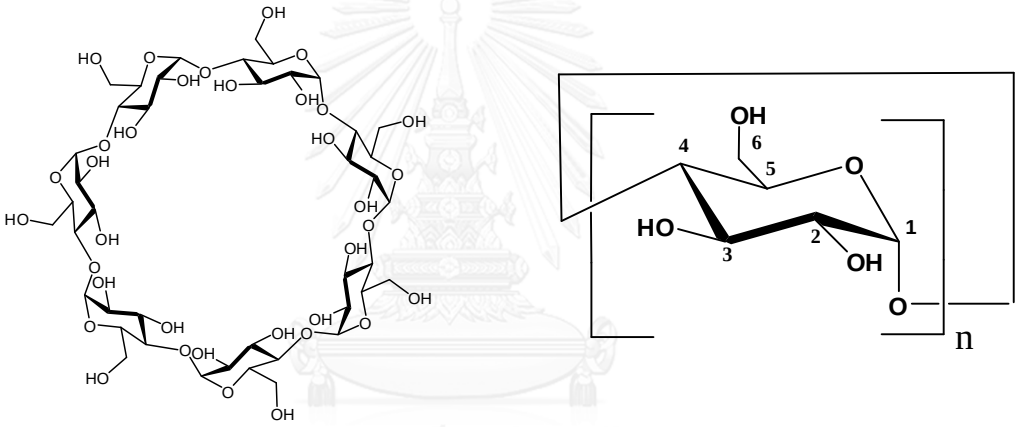

(a) (b)

Figure 2.2 (a) Chemical structure of β-CD and (b) a repeating unit of CD.

Table 2.1 Properties of α-, β- and γ-CDs [18].

property	α-CD	β-CD	γ-CD
number of glucose units	6	7	8
molecular weight (g/mol)	972	1135	1297
solubility in water at 25 °C (% w/v)	14.5	1.85	23.2
outer diameter (Å)	14.6	15.4	17.5
cavity diameter (Å)	4.7-5.3	6.0-6.5	7.5-8.3
height of torus (Å)	7.9	7.9	7.9
cavity volume ($Å^3$)	174	262	427

CDs have chiral property as they have many chiral carbons in their molecules, thus they can be useful as chiral selector or chiral stationary phase. Derivatization of hydroxyl groups at C2, C3 and C6 of the glucose unit can change CD physical properties (e.g. solubility, polarity and thermal stability), their types of interaction with analytes as well as their abilities to resolve different type of enantiomers. Changing the size of CD ring can also alter enantioselectivity.

CD molecules also have a cavity in their structures. This characteristic structure can provide the "inclusion complex formation" (Figure 2.3) between the analyte (guest molecule) and CD (host molecule). Guest molecule with suitable structure and polarity can enter into CD cavity. The strength of complex formation relies on the size of host-guest and interaction between functional groups of host and guest. Although, inclusion complex formation is an important mechanism in chiral separation using CD derivatives, separation of enantiomers may occur without inclusion complex formation [12, 18, 19].

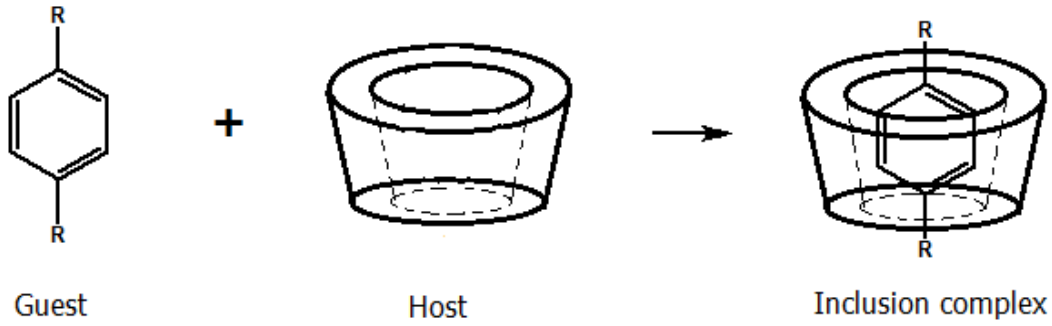

Figure 2.3 Cyclodextrin inclusion complex formation [18].

2.3 Enantiomer and 1-phenylethylamine

Enantiomers are stereoisomers of a chiral molecule. They are mirror images of each other and their structures are not superimposable (Figure 2.4). Enantiomers have identical chemical and physical properties, but may have different biological and pharmaceutical activities [3]. Due to these dissimilarities, only pure single enantiomeric forms are preferred in industries. Thus, many researches aimed for

asymmetric syntheses towards enantiopure compounds. However, these reactions required chiral auxiliaries, reagents or catalysts [20].

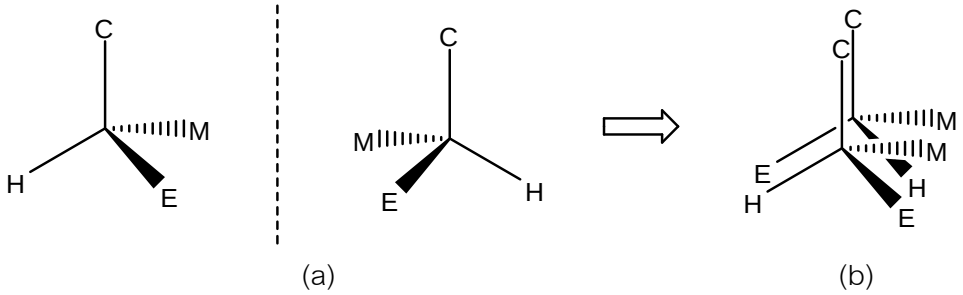

Figure 2.4 (a) A mirror image of an enantiomer; (b) non-superimposable structures.

1-Phenylethylamine (1-PEA) is one of general chiral amines that is a commercially available reagent. Individual enantiomers of 1-PEA are useful for various industrial processes. For instance, (*R*)- or (*S*)-1-PEA is used as a chiral ligand for asymmetric catalyses or as a resolving agent for the resolution of racemic products via diastereomeric salt formation (Figure 2.5) [4].

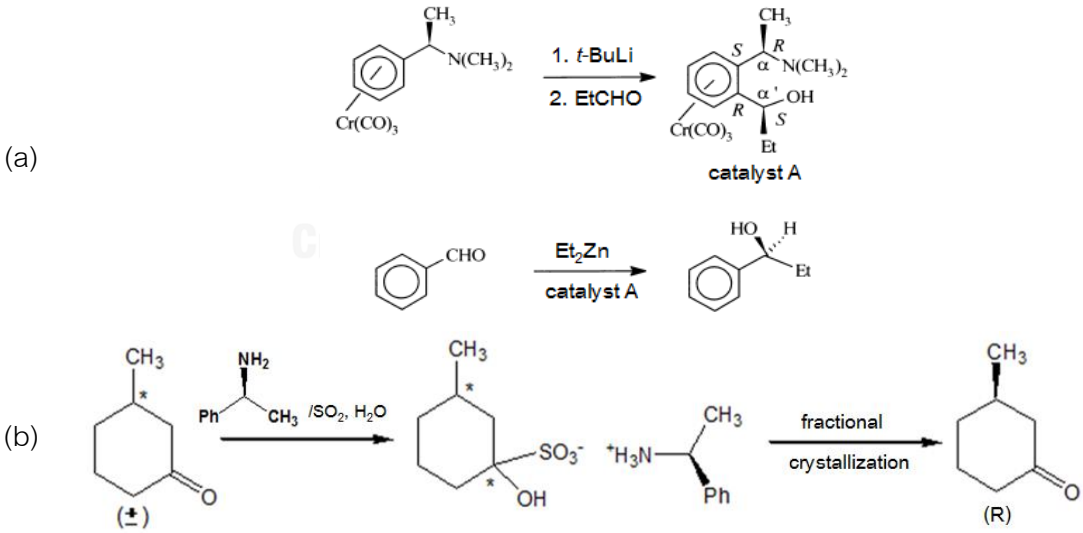

Figure 2.5 The use of 1-PEA as (a) a chiral ligand for asymmetric catalysis and (b) a resolving agent.

1-PEA could be synthesized by many methods [21-23] but a generally simple and efficient method is the reductive amination [23]. This reaction involved the conversion of a carbonyl group to an amino group via an intermediate imine. In this

work, racemic amines with different types of substitution were prepared by modified procedure of Miriyala et al. [23]. The ketone was used as a substrate and the reaction proceeded via a titanium (IV) complex or a transient imine before it was reduced to an amine product (Figure 2.6). The synthetic procedure required simple work-up and the pure products were obtained without further purification.

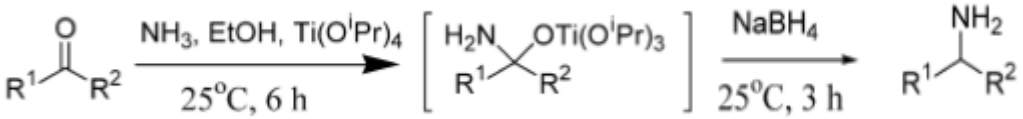

Figure 2.6 Scheme for the synthesis of primary amines from ketones [23].

2.4 Derivatization of amines before GC analysis [24, 25]

In many cases, direct GC analyses of polar compounds containing active hydrogens, such as alcohols and amines, usually yield tailing or asymmetric peaks with low detector sensitivity. Thus, the derivatization of these compounds before GC analysis is required. Derivatization provides the following advantages for GC analyses:

- increase the volatility of non-volatile or less volatile compounds,
- improve detector response,
- reduce adsorption of polar compounds to active surface of column, and
- provide better peak shape and improve resolution between peaks.

Derivatization reactions should be fast, efficient, reproducible and non-hazardous. Generally, there are three reaction types for GC derivatization: silylation, alkylation and acylation.

For silylation, a silyl group is introduced into a molecule to substitute at the active hydrogens of analyte. A variety of reagents are commercially available for the introduction of trimethylsilyl group such as trimethylchlorosilane (TMCS), trimethylsilylimidazole (TMSI), bistrimethylsilylacetamide (BSA), bistrimethylsilyltrifluoroacetamide (BSTFA), etc. These reagents differ in their reactivity, selectivity and reaction by-products. However, both the reagents and the

trimethylsilyl derivatives are moisture sensitive. The reaction and the product must be kept dry.

For alkylation, the active hydrogens of analyte are replaced by an alkyl group. Alkylation is commonly used to transform compounds with acidic hydrogens, such as carboxylic acids and phenols. Common derivatization reagents for this type include dialkylacetals, BF_3 in methanol, pentafluorobenzyl bromide (PFBBr) and tetrabutylammonium hydroxide (TBH). The resulting products are rather stable, but the reaction conditions are quite severe and the reagents are mostly toxic.

For acylation, compounds containing active hydrogens will react with carboxylic acid or carboxylic acid derivative (acyl anhydride or acyl halide). Common reagents for acylation are trifluoroacetic anhydride (TFAA), pentafluoropropionic anhydride (PFPA), N-methyl-bis(trifluoroacetamide) (MBTFA) and trifluoroacetylimidazole (TFAI). Although the reagents are moisture sensitive, the reactions are fast and easy. Nevertheless, excess reagents and by-products must be removed before GC analysis otherwise they might damage the capillary GC column.

2.5 Enantiomeric separation of amines using cyclodextrin derivatives

Enantiomeric separations of chiral analytes have been performed by GC using various types of CD derivatives as chiral stationary phases. It was shown that there are several factors affecting enantioselectivity such as type and size of CD derivatives, analyte structure, and temperature. Studies related to enantiomeric separation of 1-phenylethylamine and other amines by GC using CD derivatives are summarized below.

Juvancz et al. [26] analyzed enantiomers of arylalkyl amines and alcohols derivatives (Figure 2.7) GC using a 10 m long, 0.1 mm i.d. fused-silica column coated with a mixture of permethylated β-cyclodextrin in polysiloxane (Chirasil-Dex) as a stationary phase. Amines and alcohols were analyzed as acetyl (Ac) and trifluoroacetyl (TFA) derivatives. The results showed that Ac derivatives provided higher enantioselectivities than TFA derivatives. However, for arylalkyl amines, analysis times of Ac amines were 2-5 times longer than those of TFA amines.

Interestingly, most TFA amines and Ac amines provided opposite elution order for (*R*)- and (*S*)-enantiomers.

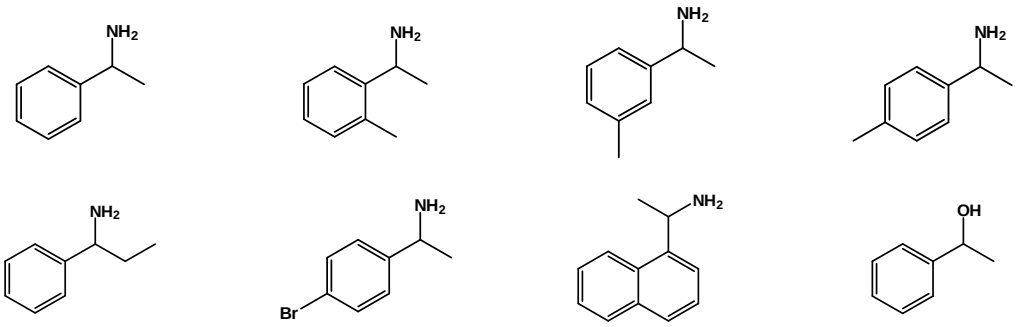

Figure 2.7 Structures of chiral analytes studied by Juvancz et al. [26].

Shitangkoon and Vigh [5] studied the effect of the 6-*O*-substituent of 2,3-di-*O*-methyl-β-CD on the enantioselectivity by GC. The results showed that 6-*O*-*tert*-butyldimethylsilyl was the most appropriate substituent. This CD derivative showed the ability to separate the enantiomers of various compounds of different functional groups such as hydrocarbons, alkylhalides, ethers, epoxides, ketones, lactones, esters, aldehydes, alcohols, hydroxy acid esters, amides and amines (Figure 2.8).

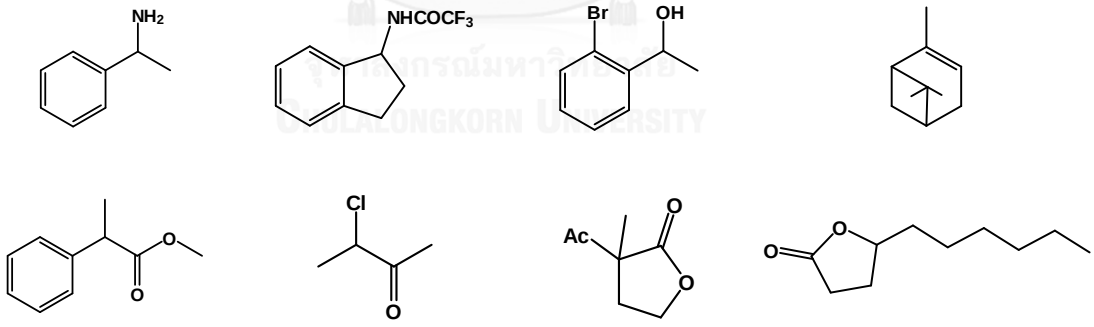

Figure 2.8 Structures of chiral analytes studied by Shitangkoon and Vigh [5].

Nie et al. [6] separated the enantiomers of amines, alcohols, diols, carboxylic acids, amino acids, epoxides, halohydrocarbons and ketones (Figure 2.9) by GC. The effect of alkyl chain length substituted at C2 and C6 of the glucose unit of (3-*O*-trifluoroacetyl)-β-CDs on enantioselectivity was studied. The results revealed that both nonyl and pentyl substituents could separate a large number of chiral analytes

but nonyl group provided better enantioselectivity than pentyl group.

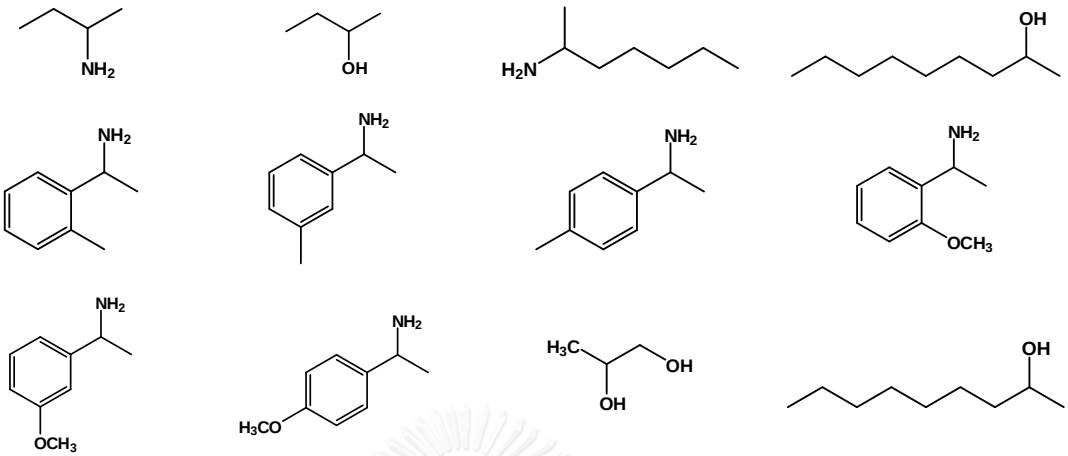

Figure 2.9 Structures of chiral analytes studied by Nie et al. [6].

Shen et al. [27] synthesized heptakis[2,6-di-*O*-pentyl-3-*O*-(4'-chloro-5'-pyridylmethyl)]-β-CD and used it as a new stationary phase in capillary GC. Several tested compounds included amines, alcohols, esters, alkyl halides, aldehydes and positional isomers of aromatic compounds (Figure 2.10). The results showed that the enantiomers could be successfully separated even compounds with several stereogenic centers. The introduction of pyridyl group probably increased a variety of the interaction between analyte and β-CD. They also reported that hydrogen bonding interaction between CD derivative and analytes extremely influenced the enantioselectivities.

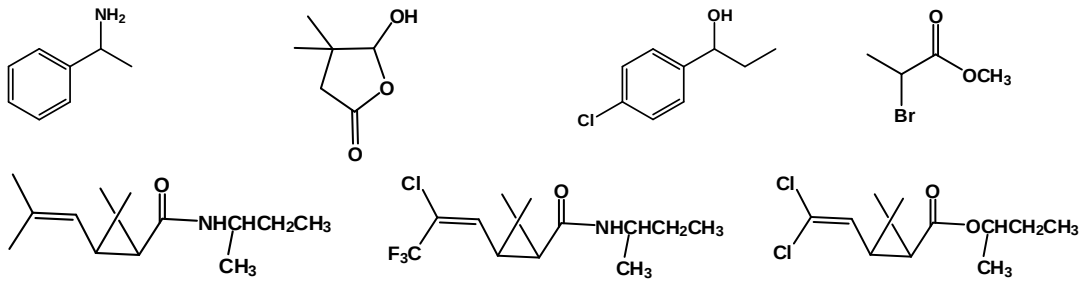

Figure 2.10 Structures of chiral analytes studied by Shen et al. [27].

Nie et al. [28] studied the enantiomeric separation of chiral compounds such as 1-phenylethylamine derivative, styrene oxide, pyrethroid insecticides and other

carboxylates using a single CD derivative and a mixture of CD derivatives as stationary phases. CD derivatives included permethylated β-CD (or PMBCD), heptakis(2,6-di-*O*-butyl-3-*O*-butyryl)-β-CD (or DBBBCD) and heptakis(2,6-di-*O*-nonyl-3-*O*-trifluoroacetyl)-β-CD (or DNTBCD). They found that the mixed CD stationary phase gave better resolution than the single CD stationary phase for some analytes. The synergistic effect was also studied. For example, enantiomers of 1-phenylethylamine derivative could be separated with good resolution on DBBBCD column, but could not be separated on PMBCD column. However, the enantioseparation was very much improved on the mixed CD (PMBCD + DBBBCD) column. It implied that 1-phenylethylamine derivative showed the positive synergistic effect on this mixed column.

Armstrong et al. [29] used 2,6-di-*O*-pentyl-3-*O*-trifluoroacetyl-α-, β-, γ-CDs as chiral GC stationary phases for 10 m long, 0.25 mm i.d. capillary column to separate 150 pairs of enantiomers. The analytes included chiral alcohols, diols, polyols, halohydrocarbons, lactones, and amines including 1-phenylethylamine (Figure 2.11). All alcohols and amines were analyzed as TFA derivatives. The results showed that γ-CD column were more useful than α- and β-CDs. The γ-CD column could resolve about 80 % of analytes, while α- and β-CDs could resolve 30 and 60 % of analytes, respectively.

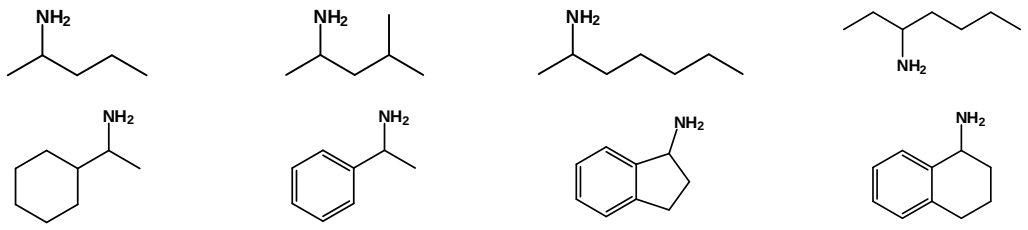

Figure 2.11 Structures of chiral analytes studied by Armstrong et al. [29].

CHAPTER III

EXPERIMENTAL

3.1 Chiral analytes

Thirty-two chiral amines used in this study were previously purchased and synthesized by Issaraseriruk [16]. Additional seventeen chiral amines were synthesized from their corresponding ketones by reductive amination [23]. Most chemicals and solvents were purchased from commercial vendors (Aldrich, Fluka, Merck or J.T. Baker) and were used without further purification. Starting materials (ketones) used in this work are listed as follows:

- 1-acetonaphthone, [941-98-0] 98% (Fluka)
- 4-acetylbiphenyl, [92-91-1] 99% (Aldrich)
- 4-bromobenzophenone, [90-90-4] 98% (Aldrich)
- 4'-butylacetophenone, [37920-25-5] 95% (Aldrich)
- butyrophenone, [495-40-9] 99% (Aldrich)
- 4-chlorobenzophenone, [134-85-0] 99% (Aldrich)
- cyclohexyl phenyl ketone, [712-50-5] 98% (Aldrich)
- 4'-ethylacetophenone, [937-30-4] 97% (Aldrich)
- 4-fluorobenzophenone, [345-83-5] 97% (Aldrich)
- hexanophenone, [942-92-7] 99% (Aldrich)
- isobutyrophenone, [611-70-1] 97% (Fluka)
- 4-methoxybenzophenone, [611-94-9] 97% (Aldrich)
- 4-methylbenzophenone, [134-84-9] 99% (Aldrich)
- 4'-tert-butylacetophenone, [943-27-1] 97% (Aldrich)

- α-tetralone, [529-34-0] 98% (Aldrich)
- β-tetralone, [530-93-8] 98% (Aldrich)
- 2,2,2-trifluoroacetophenone, [434-45-7] 99% (Aldrich)

The synthesis procedure is summarized as follows. The ketone (5 mmol) was dissolved in 20 mL of isopropanol. Titanium (IV) isopropoxide (10 mmol, 2 equiv) was added to the stirred solution under flowing ammonia gas. The solution was stirred for 5-7 h at room temperature. Sodium borohydride (7.5 mmol, 1.5 equiv) was added into the reaction mixture and the stirring was continued for another 2 h. The reaction mixture was quenched by adding 2 M ammonium hydroxide (25 mL) and the precipitate was filtered off. The filtrate was extracted with dichloromethane (2 x 25 mL). The combined organic layer was then extracted with 2 M hydrochloric acid (30 mL). The acidic aqueous layer was adjusted to pH 10-12 with 2 M sodium hydroxide and re-extracted with dichloromethane (2 x 25 mL). The combined organic extract was washed with saturated sodium chloride (30 mL) and dried with anhydrous sodium sulfate. The solvent was evaporated using a rotary evaporator to obtain the desired amine. The structure of product was characterized by ^{1}H and ^{13}C-NMR techniques. Abbreviation, structure and name of chiral amines used in this study are listed in Table 3.1.

Table 3.1 Abbreviation, structure and name of all amines used in this study.

No.	abbreviation	structure	name
1	H	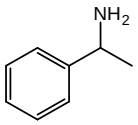	1-phenylethylamine
2	2F	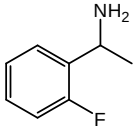	1-(2′-fluorophenyl)ethylamine
3	3F	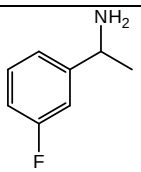	1-(3′-fluorophenyl)ethylamine

No.	abbreviation	structure	name
4	4F	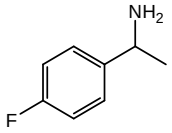	1-(4′-fluorophenyl)ethylamine
5	2Cl	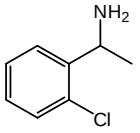	1-(2′-chlorophenyl)ethylamine
6	3Cl	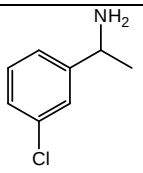	1-(3′-chlorophenyl)ethylamine
7	4Cl	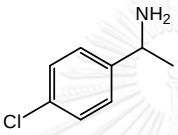	1-(4′-chlorophenyl)ethylamine
8	2Br	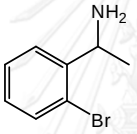	1-(2′-bromophenyl)ethylamine
9	3Br	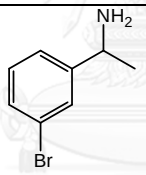	1-(3′-bromophenyl)ethylamine
10	4Br	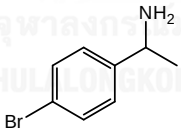	1-(4′-bromophenyl)ethylamine
11	2Me	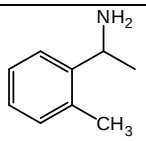	1-(2′-methylphenyl)ethylamine
12	3Me	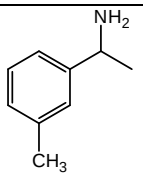	1-(3′-methylphenyl)ethylamine
13	4Me	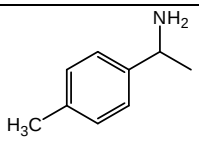	1-(4′-methylphenyl)ethylamine

No.	abbreviation	structure	name
14	2OMe	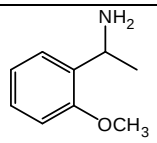	1-(2′-methoxyphenyl)ethylamine
15	3OMe	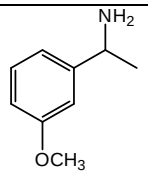	1-(3′-methoxyphenyl)ethylamine
16	4OMe	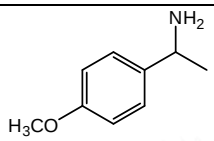	1-(4′-methoxyphenyl)ethylamine
17	2CF3	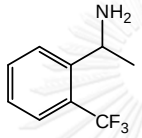	1-(2′-trifluoromethylphenyl)ethylamine
18	3CF3	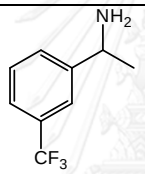	1-(3′-trifluoromethylphenyl)ethylamine
19	4CF3	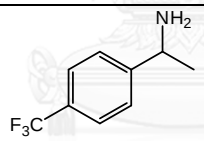	1-(4′-trifluoromethylphenyl)ethylamine
20	P	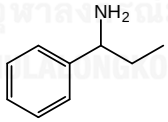	1-phenylpropylamine
21	4FP	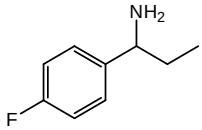	1-(4′-fluorophenyl)propylamine
22	4ClP	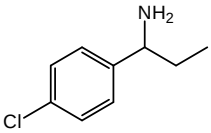	1-(4′-fluorophenyl)propylamine
23	4BrP	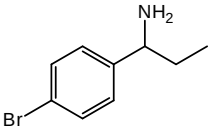	1-(4′-bromophenyl)propylamine

No.	abbreviation	structure	name
24	4MeP	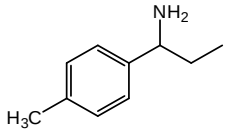	1-(4′-methylphenyl)propylamine
25	4OMeP	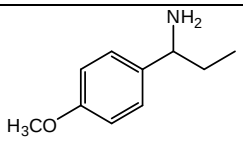	1-(4′-methoxyphenyl)propylamine
26	4CF3P	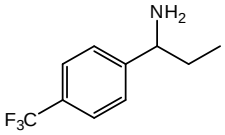	1-(4′-trifluoromethylphenyl)propylamine
27	A	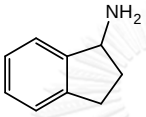	1-aminoindan
28	5FA	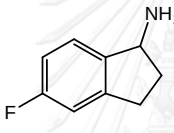	5′-fluoro-1-aminoindan
29	5ClA	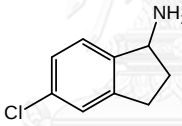	5′-chloro-1-aminoindan
30	5BrA	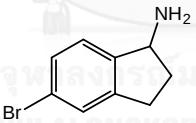	5′-bromo-1-aminoindan
31	5MeA	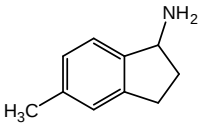	5′-methyl-1-aminoindan
32	5OMeA	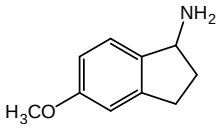	5′-methoxy-1-aminoindan
33	4FPh	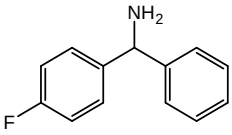	(4-fluorophenyl)(phenyl)methanamine
34	4ClPh	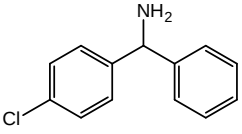	(4-chlorophenyl)(phenyl)methanamine

No.	abbreviation	structure	name
35	4BrPh	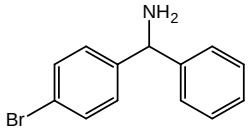	(4-bromophenyl)(phenyl)methanamine
36	4MePh	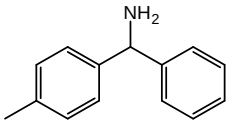	phenyl(*p*-tolyl)methanamine
37	4OMePh	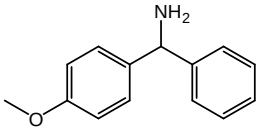	(4-methoxyphenyl)(phenyl)methanamine
38	4Et	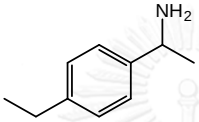	4-ethylphenylethylamine
39	4Bu	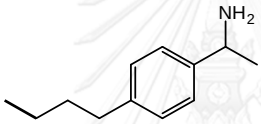	4-butylphenylethylamine
40	4tBu	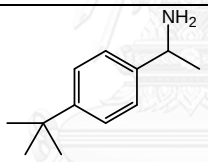	4-tert-butylphenylethylamine
41	4Ph	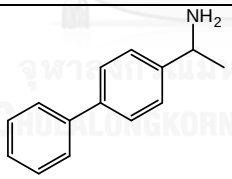	1-(4-biphenylyl)ethylamine
42	Nap	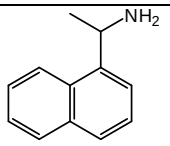	1-(1-naphthyl)ethylamine
43	CF3	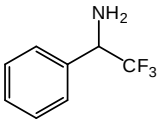	2,2,2-trifluoro-1-phenylethylamine
44	.Bu	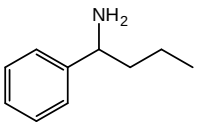	phenylbutylamine

No.	abbreviation	structure	name
45	iBu	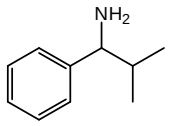	phenylisobutylamine
46	Hex	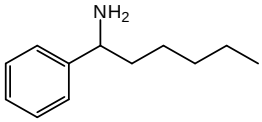	phenylhexylamine
47	Cy	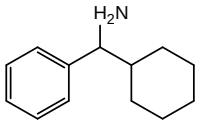	phenylcyclohexylamine
48	ATL	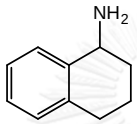	1-aminotetralin
49	2ATL	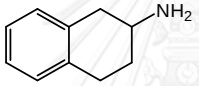	2-aminotetralin

All amines were derivatized into trifluoroacetyl (TFA) derivatives before GC analysis [25]. The mixture of amine (20 μL) and trifluoroacetic anhydride (TFAA, 100 μL) in dichloromethane (300 μL) was allowed to react for 1-2 h at room temperature. Dry nitrogen was flowed through the solution to remove excess reagent and solvent. Finally, the product was re-dissolved in 0.5-1 mL of dichloromethane. Approximately 0.4 μL of solution was injected into GC.

3.2 Gas chromatographic column

3.2.1 Preparation of a coated capillary column

A mixture (0.04 g) of 33.5 % heptakis(2,3-di-*O*-acetyl-6-*O*-*tert*-butyldimethyl silyl)-β-CD (or BSiAc) in polysiloxane OV-1701 (Supelco) was dissolved in dichloro-methane (10 mL). The solution was then loaded into the 16 m long, 0.25 mm I.D. deactivated fused silica capillary column (Agilent). The solvent was then evaporated in a controlled-temperature water bath leaving a thin film (0.25 μm) of stationary

phase inside. The capillary column was conditioned at 220 °C until a stable baseline was observed.

3.2.2 Evaluation of the coated capillary column

The properties of a newly coated capillary column were evaluated by Grob Test [28] in terms of inertness, acidity/basicity, and column efficiency (TZ value). A split ratio was adjusted to 40 : 1. The Grob test mixture of 1 μL was injected. The column temperature was programmed from 40 to 180 °C at the rate of 3.16 °C /min. The column efficiency (N) was also regularly determined with *n*-alkanes over the temperature range of 110-220 °C and was found to be over 3,500 plates/m.

3.3 Gas chromatographic analyses

All chromatographic measurements were performed on an Agilent 6890 series gas chromatograph equipped with a split injector and a flame ionization detector (FID). Both injector and detector were set at 250 °C. A split ratio was adjusted to 100 : 1. Hydrogen was used as a carrier gas at an average linear velocity of 50 cm/s. Each analyte solution (~ 0.4 μL) was injected isothermally at least two times (retention times were within 0.003 min). The GC analyses were performed at 7-8 temperature values with 10 °C intervals in the temperature range of 110-220 °C (depending on elution temperature of each analyte). The retention time (t_R) and peak width (w_h) were obtained from chromatograms and were used to calculate retention factor (k'), enantioselectivity (α), and resolution (Rs).

CHAPTER IV

RESULTS AND DISCUSSION

4.1 Syntheses of amines and their derivatives

The reaction of ketones with ammonia gas in the presence of titanium (IV) isopropoxide catalyst, followed by reduction with sodium borohydride led to desired amines in 5-60 % yield (Table 4.1). Most reactions were allowed to react for 5 hours according to the procedure of previous study [16]. When low yields were observed for some analytes, the reaction time was later increased to 6-7 hours. However, the yield of amine products obtained were not under optimized conditions since the quantities of amines were enough for further GC analyses. The obtained products were quite pure and no additional purification was needed. The identities of all products were confirmed by ^{1}H and ^{13}C NMR.

Table 4.1 Yield and reaction time of synthesized amines.

product	% yield	time (h)
Bu	20.5	5
Hex	5.1	5
iBu	40.5	5
Cy	5.3	5
ATL	60.3	5
2ATL	45.9	5
4Et	36.4	5
4tBu	12.6	5
4Bu	5.7	5

product	% yield	time (h)
4Ph	7.3	5
4FPh	21.0	6
4ClPh	7.8	6
4BrPh	7.8	6
4OMePh	16.9	6
Nap	48.2	7
CF_3	17.2	7
4MePh	10.5	7

Attempts to convert amines into their alkyl or silyl derivatives did not proceed well. Amines were subjected to reductive methylation in the presence of aqueous formaldehyde and zinc [30, 31]. However, pure *N*-methyl substituted amines were

not obtained, a mixture of mono and dimethyl substituted amines was observed instead. In addition, the reaction time was long and the work-up procedure was tedious. Attempts to silylate amines using BSTFA + 1% TMCS yielded the desired trimethylsilyl products with impurities. All amines were then derivatized into their trifluoroacetyl (TFA) derivatives using trifluoroacetic anhydride as a reagent. The derivatization procedure was simple and the reaction time was short. The final TFA products were quite clean.

4.2 Evaluation of a coated capillary column

The Grob test mixture contains 12 compounds of different functional groups: *n*-decane (C_{10}), *n*-undecane (C_{11}), methyl decanoate (E_{10}), methyl undodecanoate (E_{11}), methyl dodecanoate (E12), octan-1-ol (ol), nonanal (al), butane-2,3-diol (D), 2,6-dimethylaniline (A), 2,6-dimethylphenol (P), dicyclohexylamine (am) and 2-ethylhexanoic acid (S). The Grob test mixture is used for evaluation of capillary column properties in terms of inertness, acidity/basicity, and column efficiency (TZ value). A chromatogram of Grob test for the BSiAc column was shown in Figure 4.1.

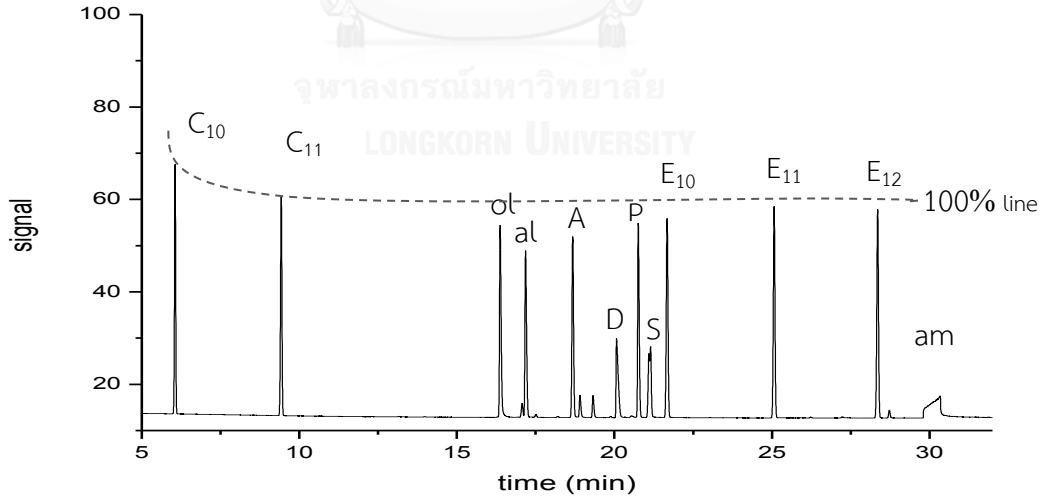

Figure 4.1 Grob test for the BSiAc column.

Column efficiency was determined from the average of TZ values of E_{10}-E_{11} and E_{11}-E_{12} ester peak pairs and was found to be 27.9 (good efficiency). The inertness of the column was characterized by the adsorption of alcohols (ol, D) and aldehyde

(al). All three compounds were symmetrical and tailing peak was not observed. D was observed as 3 peaks due to the ability of BSiAc column to separate isomers and enantiomers of D. Acid-base properties were tested by the P-A pair (weak acid and base) and the S-am pair (strong acid and base). No strong acid-base properties were observed as the heights of P and A were similar. However, the column was weakly acidic since am (strong base) was more strongly adsorbed than S (strong acid). In addition, S was observed as a split peak due to the ability of BSiAc to separate enantiomers of S (incomplete separation). No severe tailing peak was observed for S. Hence, this BSiAc-coated column shows good efficiency and is suitable for analysis of different compound types, except for direct analysis of strong amines.

4.3 Gas chromatographic enantiomeric separation of amine derivatives

The enantiomeric separations of forty-nine TFA derivatives of amines were investigated by GC using BSiAc as a chiral selector. The structures of all 49 amines were based on 1-phenylethylamine with different types and positions of the substituents. The retention (k′), selectivity (α) and resolution (Rs) for each working column temperature were calculated. The influence of temperature and analyte structure toward enantioseparation of these amine analytes were studied and compared. Since the physical properties of amines are quite different, direct comparison of chromatographic parameters among analytes at the same temperature was not possible. Therefore, thermodynamic parameters over a temperature range were used.

Thermodynamic parameters related to the interaction between analytes and stationary phase in GC could be obtained through van't Hoff equation [32].

$$\ln k' = -\frac{\Delta H}{RT} + \frac{\Delta S}{R} - \ln \beta$$

where k' = retention factor of each enantiomer calculated from analyte retention time (t_R) according to

$$k' = \left(\frac{t_R - t_M}{t_M} \right)$$

ΔH = enthalpy change

ΔS = entropy change

T = absolute temperature in Kelvin

R = universal gas constant (1.987 cal/mol·K)

β = phase ratio or the ratio of mobile phase volume to stationary phase volume

According to the van't Hoff equation, the influence of temperature towards retention (k′) of all amines was studied. Plots of ln k′ versus 1/T of each enantiomer for all analytes gave linear relationship, with correlation coefficient (R^2) greater than 0.9951. From these plots, enthalpy change (ΔH) and entropy change (ΔS) for each enantiomer could be determined from its corresponding slope and y-intercept, respectively. Enthalpy change (ΔH) resulted from the interaction between an analyte and the stationary phase. The sharper slope (more negative ΔH value) indicated stronger intermolecular forces between analyte and stationary phase when the temperature decreased. Entropy change (ΔS) represented the loss of degree of freedom related to the interaction between analyte and stationary phase. More negative ΔS value indicated fewer freedom of motion of analyte molecule on stationary phase. When a pair of enantiomers was separated, difference in enthalpy change ($\Delta\Delta H$) and difference in entropy change ($\Delta\Delta S$) of two enantiomers could be determined. Larger $\Delta\Delta H$ and $\Delta\Delta S$ values indicated a higher chance to improve the separation between the two enantiomers with temperature.

Figures 4.2-4.3 showed $-\Delta H_2$ and $-\Delta S_2$ values of the more retained enantiomers of all TFA amines on the BSiAc column. Both $-\Delta H_2$ and $-\Delta S_2$ values showed similar trend. Most halogenated and high electronegative substitution at *meta*- and *para*-position of 1-PEA (compounds **3F**, **4F**, **3Cl**, **4Cl**, **3Br**, **4Br**, **3CF3**, **4CF3**) and at 5-position of 1-aminoindan (compounds **5FA**, **5ClA**, **5BrA**) tended to exhibit larger $-\Delta H_2$ and $-\Delta S_2$ values (stronger interaction) than other compounds of different types and positions of substituents. Retention factors (k′) of these analytes were more temperature dependent than those of other analytes. A decrease in separation temperature would result in a larger increase of analysis time. These results

suggested the influence of analyte structure toward the interaction between analyte and stationary phase.

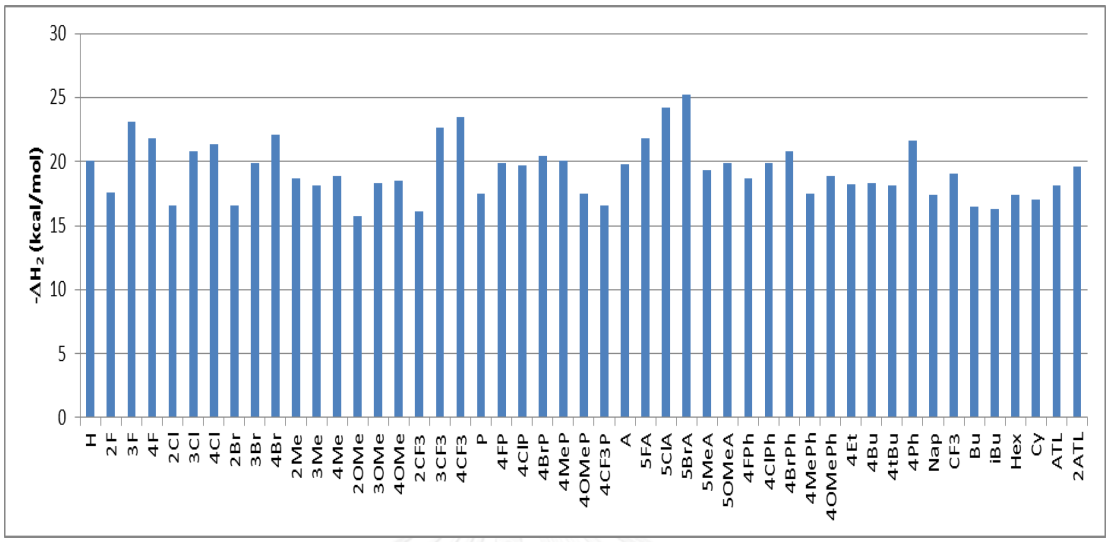

Figure 4.2 Enthalpy change (-ΔH, kcal/mol) of the more retained enantiomers of all TFA amines on the BSiAc column.

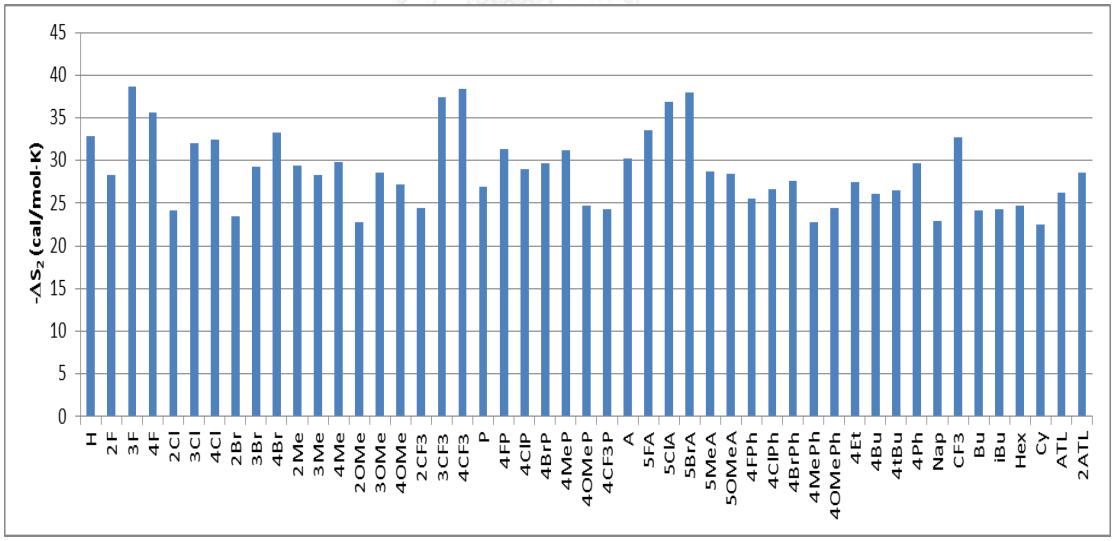

Figure 4.3 Entropy change (-ΔS, cal/mol·K) of the more retained enantiomers of all TFA amines on the BSiAc column.

Figures 4.4-4.5 showed -ΔΔH and -ΔΔS values of all TFA amines separated on the BSiAc column. Both -ΔΔH and -ΔΔS values showed similar trend, but were different from $-\Delta H_2$ and $-\Delta S_2$ values. These results suggested that strong interaction did not necessarily result in high enantioseparation. For example, **5BrA**, **4CF3**, and **3F** had highest $-\Delta H_2$ and $-\Delta S_2$ values (Figures 4.2-4.3). However, **3CF3** had the highest -ΔΔH and -ΔΔS values (Figures 4.4-4.5). The correlation between -ΔΔH and -ΔΔS values of all amines was then constructed and high linearity was observed (R^2 = 0.998) as in Figure 4.6. The results suggested that the enantioseparation on the BSiAc column of all amines in this study was mainly occurred by the same mechanism [6].

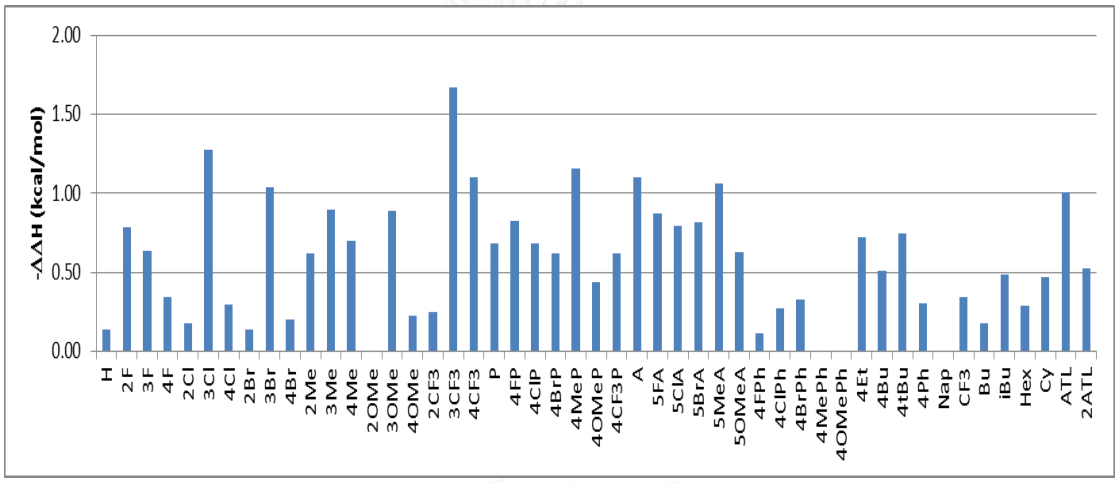

Figure 4.4 Enthalpy difference (-ΔΔH, kcal/mol) of all TFA amines on the BSiAc column.

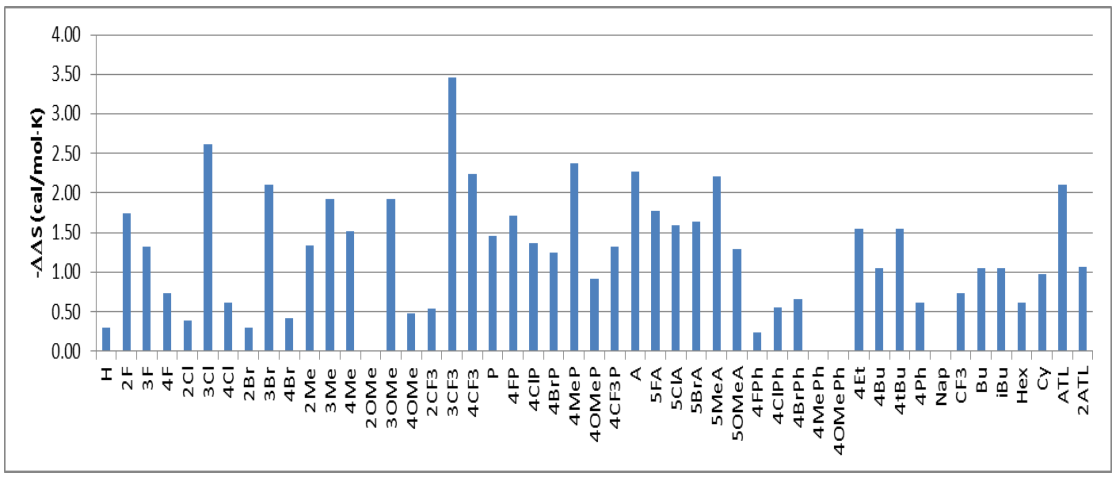

Figure 4.5 Entropy difference (-ΔΔS, cal/mol·K) of all TFA amines on the BSiAc column.

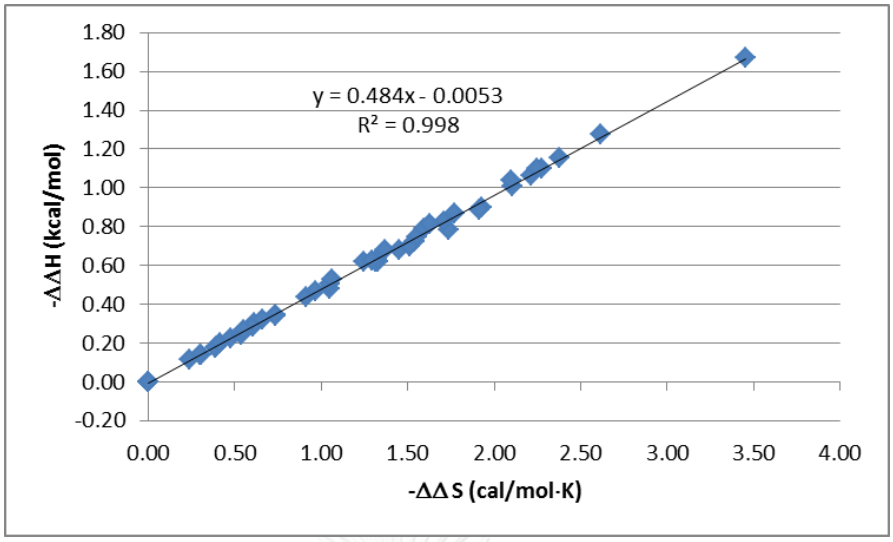

Figure 4.6 Plot of -ΔΔH versus -ΔΔS of all TFA amines on the BSiAc column.

Among 49 TFA derivatives of racemic amines investigated in this work, 45 racemates could be separated into their enantiomers. Four amines that could not be enantioseparated (-ΔΔH and -ΔΔS = 0) were **2OMe**, **4MePh**, **4OMePh** and **Nap**. Since -ΔΔH and -ΔΔS values showed similar trend, the discussion will be referred to -ΔΔH only. The effect of analyte structure and temperature toward enantioselectivity will be discussed according to analytes of similar structures.

Effect of type and position of substitution on the aromatic ring

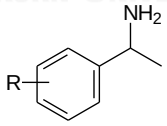

Effect of temperature on the enantioseparation of TFA derivatives of 1-phenylethylamines with different types and positions of substitutions on the aromatic ring was studied. 1-Phenylethylamine (**H**) was used as a reference compound. Other amines were 1-phenylethylamines with mono-substitution of fluoro, chloro, bromo, methyl, methoxy, trifluoromethyl at *ortho*-, *meta*- and *para*-positions. From Figure 4.4, almost all analytes with mono-substitution on the aromatic ring showed similar or greater -ΔΔH values than **H** with varying degree. **2OMe** was the only exception; its enantiomers could not be separated on the BSiAc

column. It could be noticed that the position of substitution seemed to play a major role on enantioseparation than the type of substitution. In most cases, -ΔΔH values were in the order of *meta* >> *para* > *ortho*. These results indicated that temperature had stronger influence on enantioseparation at *meta*-substituted 1-phenylethylamines; therefore, a small decrease in temperature would result in a larger increase in enantioselectivity. Larger substituents at *ortho*-position tended to sterically hinder the interaction around the stereogenic center and lower -ΔΔH values were obtained. **2F**, with smallest substituent, showed the highest -ΔΔH values among all *ortho*-substituted analytes.

Effect of position of substitution on retention and enantioselectivity of three isomers of trifluoromethyl-substituted analytes was compared. Plots of ln k′ versus 1/T and ln α versus 1/T of **2CF3**, **3CF3** and **4CF3** were shown in Figures 4.7-4.8. From Figure 4.7, it was shown that the retention factors (k′) of **3CF3** and **4CF3** were higher than that of **2CF3** at the same temperature. In addition, -ΔH values of the more retained enantiomers of three isomers were in the order of **4CF3** > **3CF3** > **2CF3**, suggesting that a decrease in temperature would result in a larger increase in retention for **4CF3** > **3CF3** > **2CF3**, respectively. However, enantioselectivities at the same temperature as well as their -ΔΔH values were in the order of **3CF3** > **4CF3** > **2CF3** (Figure 4.8), suggesting that temperature has a great influence on the enantioselectivity of **3CF3**. Enantioseparation of three trifluoromethyl-substituted analytes was compared in Figures 4.9.

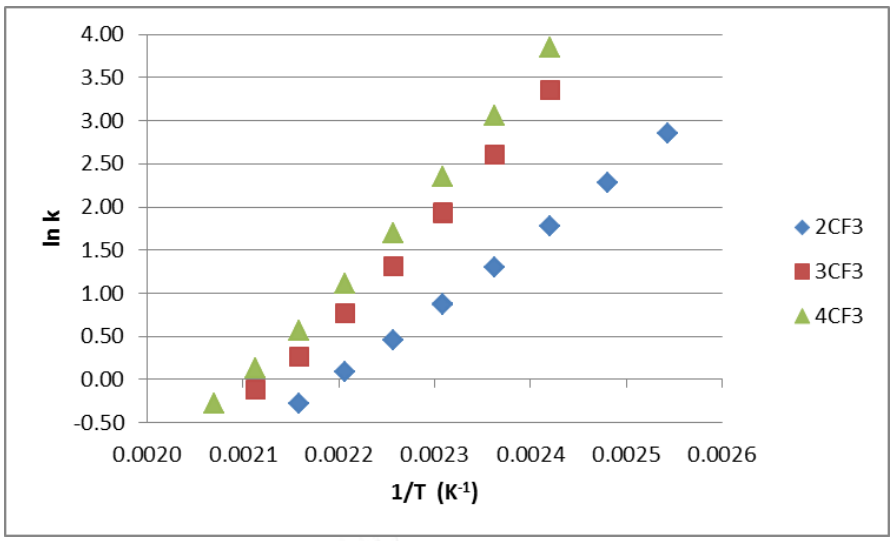

Figure 4.7 Plots of ln k'_2 versus 1/T of **2CF3**, **3CF3** and **4CF3**.

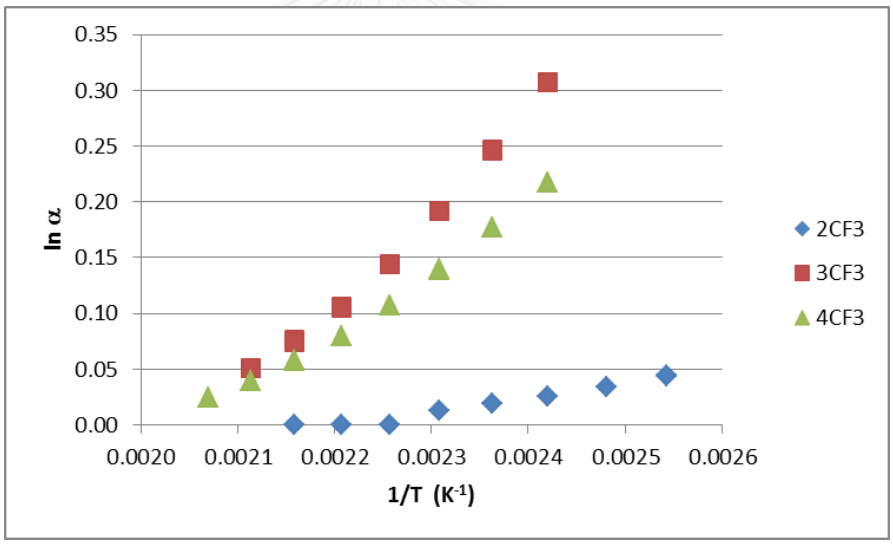

Figure 4.8 Plots of ln α versus 1/T of **2CF3**, **3CF3** and **4CF3**.

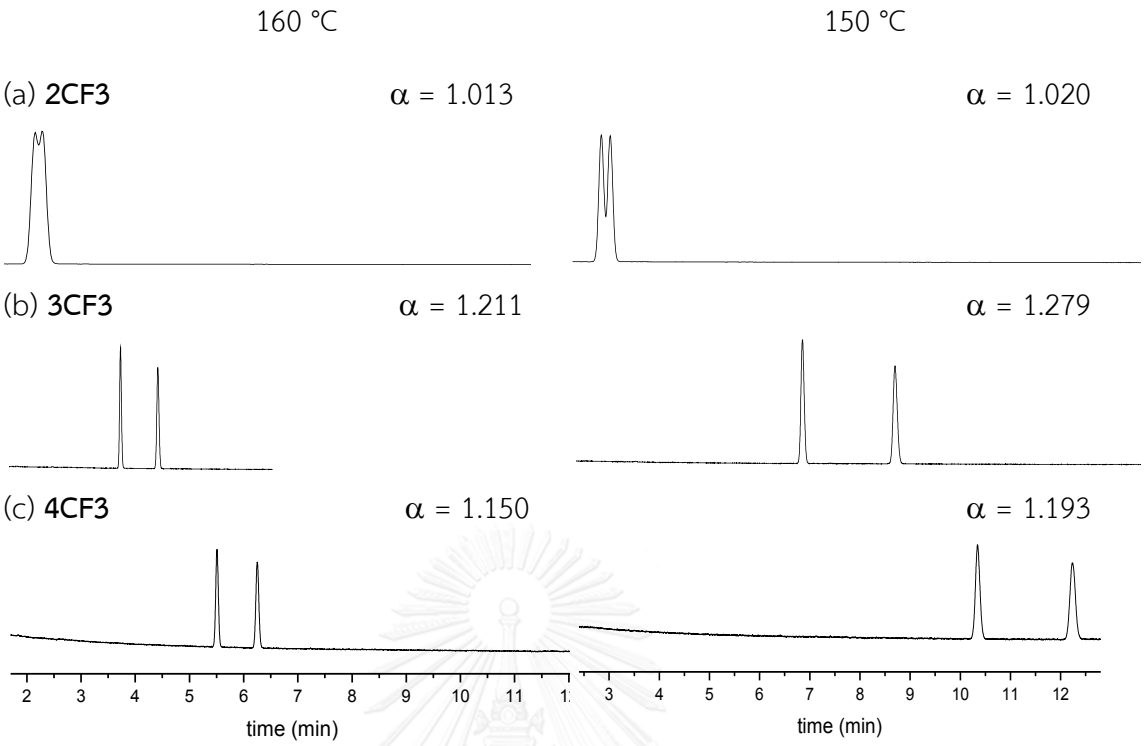

Figure 4.9 Chromatograms of (a) **2CF3**, (b) **3CF3** and (c) **4CF3** at 160 and 150 °C.

A fluorine atom has similar size to a hydrogen atom, but it can provide interesting property. Among 18 analytes in this group, fluoro-substituted analytes showed different trend when compared to other substituents. All fluoro-substituted analytes showed better enantioseparation than **H**. Their -ΔΔH values were in the order of **2F** > **3F** > **4F** > **H**.

The effect of type of substituent on the aromatic ring on enantioseparation was also studied. For *meta*-substituted analytes, their -ΔΔH values were in the order of **3CF3** > **3Cl** > **3Br** > **3Me** ~ **3OMe** > **3F**, according to their electron withdrawing property except for fluoro. Plots of ln k′ versus 1/T and ln α versus 1/T were also shown in Figures 4.10-4.11. Comparison of enantioselectivities, **3CF3** was the highest. In addition, the decrease in temperature by 10 °C greatly improved the enantioselectivity of **3CF3** compared to other *meta*-substituted analytes (Figure 4.12).

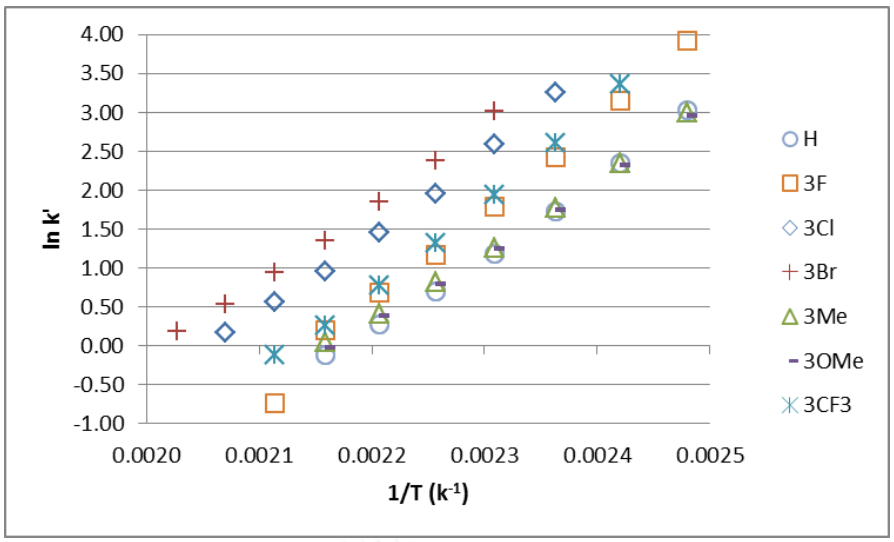

Figure 4.10 Plots of ln k'_2 versus 1/T of **H**, **3F**, **3Cl**, **3Br**, **3Me**, **3OMe** and **3CF3**.

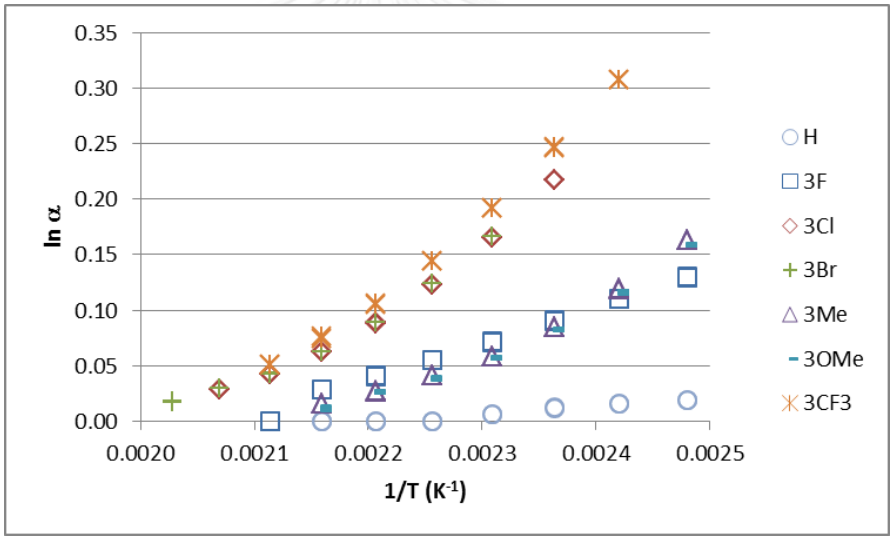

Figure 4.11 Plots of ln α versus 1/T of **H**, **3F**, **3Cl**, **3Br**, **3Me**, **3OMe** and **3CF3**.

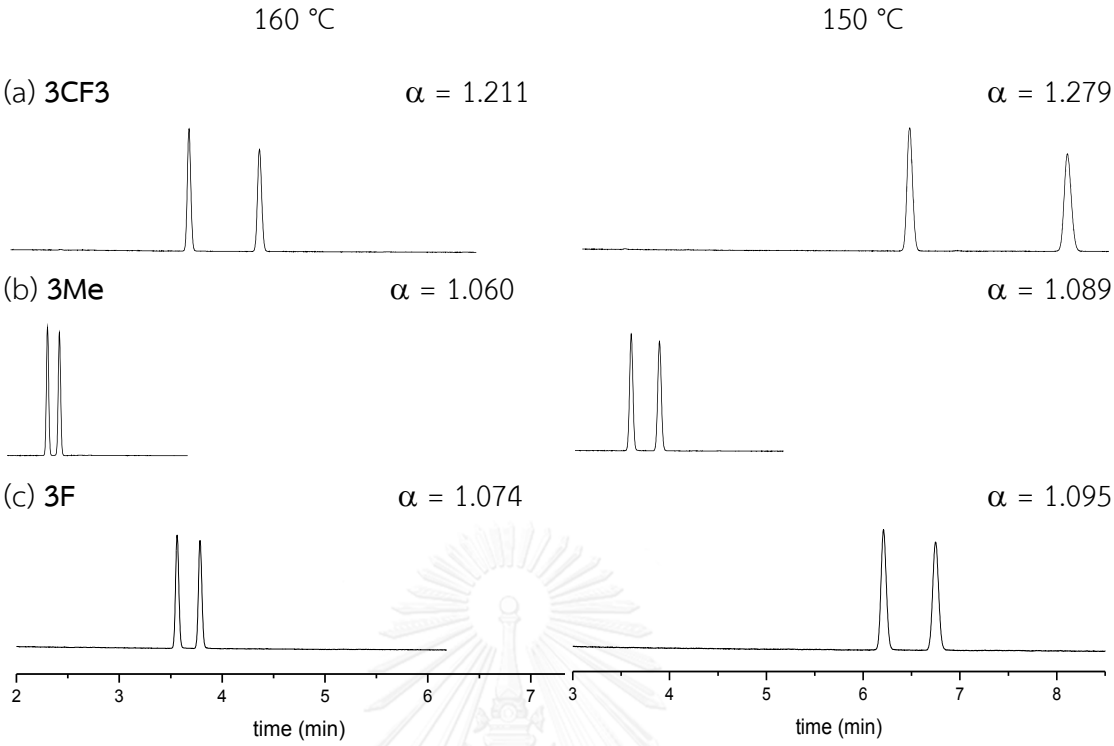

Figure 4.12 Chromatograms of (a) **3CF3**, (b) **3Me** and (c) **3F** at 160 and 150 °C.

The effect of type of substituent on the aromatic ring on enantioseparation of *para*-substituted analytes was different from that of *meta*-substituted analytes. *Para*-substitution with halogen atom (**4F**, **4Cl**, **4Br**) gave low -ΔΔH values. Alkyl substitution either as a straight chain (methyl, trifluoromethyl, ethyl, butyl) or bulky group (*tert*-butyl), however, seemed to improve enantioselectivity at *para*-position, as shown by higher -ΔΔH values of **4Me**, **4CF3**, **4Et**, **4Bu** and **4tBu**. A large phenyl group, as in **4Ph**, gave low -ΔΔH value. A change of the core structure from phenyl (**H**) to naphthyl (**Nap**) resulted in a complete loss of enantioselectivity (-ΔΔH and -ΔΔS = 0).

Effect of the core structure or the type of substitution at the stereogenic center

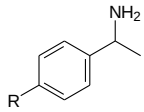

phenylethylamine

PE

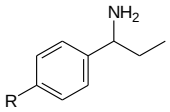

phenylpropylamine

PP

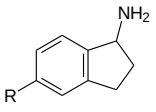

aminoindan

AI

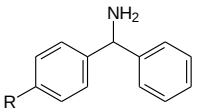

phenyl phenyl methanamine

Ph

Enantiomeric separations of TFA derivatives of *para*-substituted 1-phenylethyl amines (PE), 1-phenylpropylamines (PP), phenyl phenyl methanamines (Ph) and 5-substituted 1-aminoindans (AI), of differing core structure, were compared. Their -ΔΔH values were compared in Figure 4.13. Trifluoromethyl-substituted of Ph and AI were omitted because the starting ketones were not available and their corresponding amines could not be prepared.

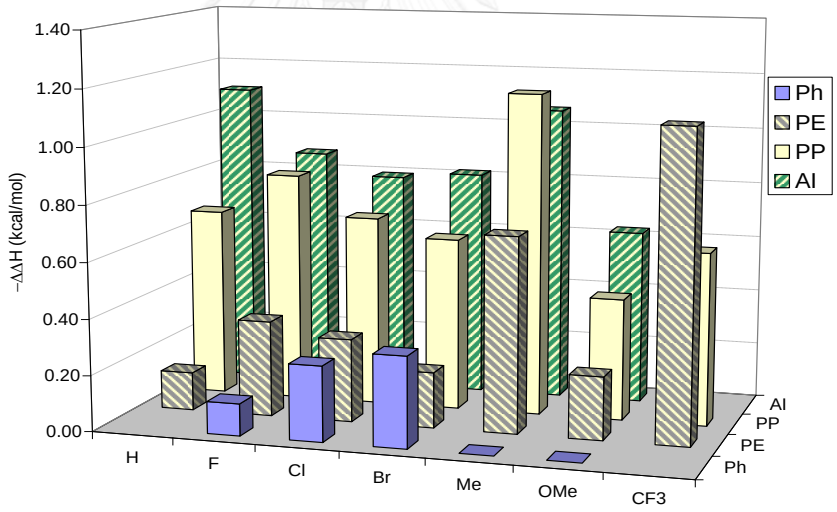

Figure 4.13 Enthalpy difference (-ΔΔH, kcal/mol) of TFA derivatives of PEs, PPs, Phs and AIs on the BSiAc column.

From Figure 4.13, it was quite clear that two phenyl rings substituted at the same stereogenic center (as in Phs) mostly led to a complete loss of enantioselectivity (**4MePh** and **4OMePh**) or low -ΔΔH values (**4FPh** and **4ClPh**). These results may imply that these analytes were too large for the separation using

the medium-size cavity of BSiAc or two phenyl rings sterically hinder the interaction around the stereogenic center.

When a methyl group (PEs) at the stereogenic center was replaced by a longer ethyl group (PPs), -ΔΔH values of most analytes improved. When the side chain ethyl group formed a five-membered ring (AIs), -ΔΔH values of most analytes further improved. This indicated the effect of analyte rigidity towards enantioseparation. Only trifluoromethyl-substituted analytes showed different trend for PE and PP. However, the conclusion could not be obtained for trifluoromethyl substitution because of insufficient number of analytes. Enantioseparation of **4F** and **4FP** was shown in Figure 4.14.

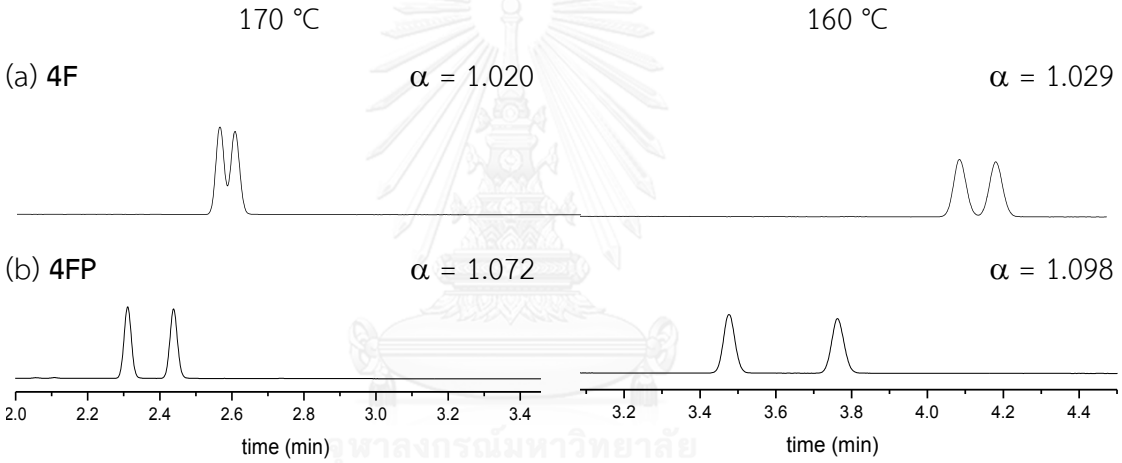

Figure 4.14 Chromatograms of (a) **4F** and (b) **4FP** at 170 and 160 °C.

The influence of type of substitution at the stereogenic center was further examined. The -ΔΔH values of 10 amines with no substitution on the aromatic ring but with varying size and rigidity were compared in Figure 4.15.

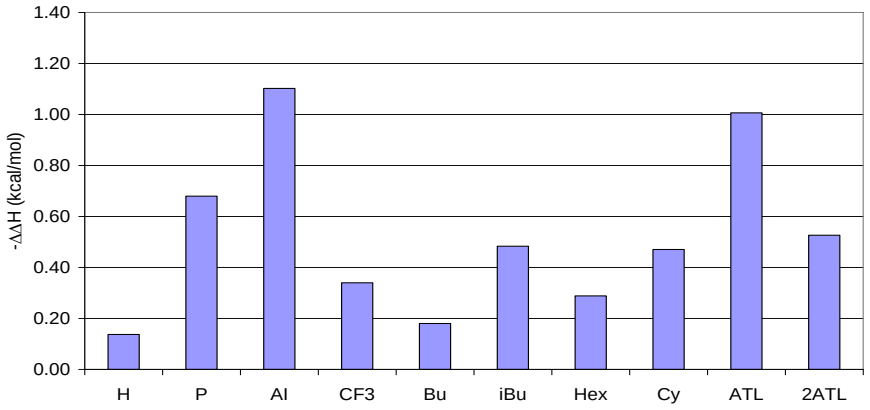

Figure 4.15 Enthalpy difference (-ΔΔH, kcal/mol) of TFA derivatives of **H**, **P**, **AI**, **CF3**, **Bu**, **iBu**, **Hex**, **Cy**, **ATL** and **2ATL** on the BSiAc column.

Using **H** as a reference compound, substitution with longer alkyl group at the stereogenic center seemed to improve enantioseparation as -ΔΔH values of **P**, **Bu**, **iBu**, and **Hex** were higher than **H**. However, the increase in -ΔΔH values did not correlate to alkyl chain length. The highest -ΔΔH value was observed for **P**, with ethyl substitution. Bulky group or cyclic structure with the similar number of carbon substitution seemed to provide better enantioseparation than their corresponding straight chain substitution, as -ΔΔH values of **iBu** > **Bu** and **Cy** > **Hex**. In addition, more rigid structure seemed to provide better enantioseparation than their corresponding straight chain substitution, as -ΔΔH values of **AI** > **P** and **ATL** > **Bu**. Nevertheless, a small change in analyte structure (**H** vs. **CF3** and **ATL** vs. **2ATL**) might result in a big difference in enantioseparation and the enantioseparation of new compounds is still difficult to predict.

As shown above, temperature and analyte structure are important factors for enantioseparation. In general, a decrease in temperature results in an improved enantioselectivity as well as an increase in retention or longer analysis time. In this study, retention factors of the more retained enantiomer (k'_2) of all analytes that provided complete baseline separation of enantiomers (at Rs = 1.5) were compared and shown in Figure 4.16.

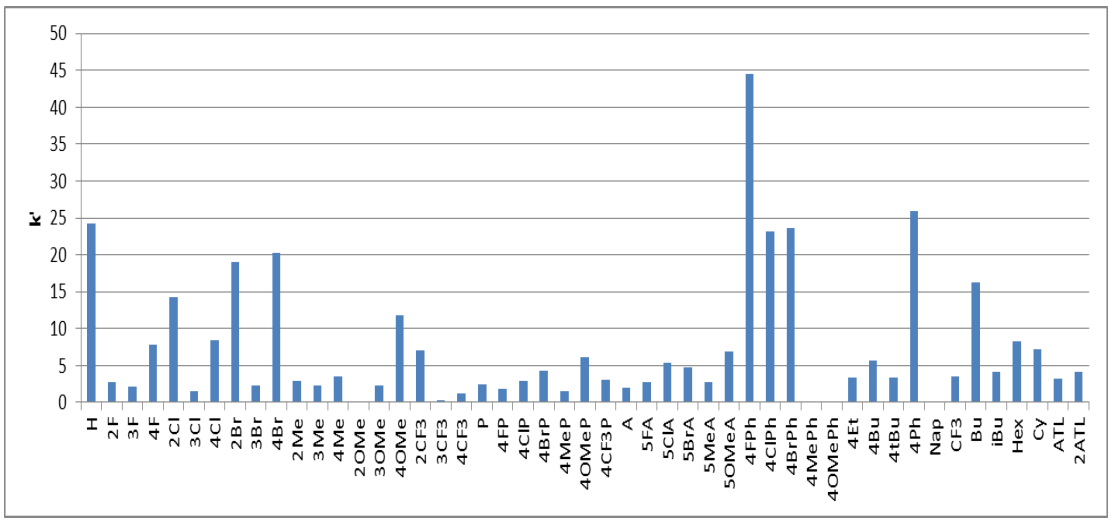

Figure 4.16 k'_2 of all TFA amines at Rs = 1.5 on the BSiAc column.

From all 49 amines in this study, 4 analytes (**2OMe**, **4MePh**, **4OMePh** and **Nap**) could not be enantioseparated. Complete enantioseparation with short analysis time ($k'_2 \leq 5$) could be achieved with 27 analytes. The analyte that required shortest analysis time ($k'_2 = 0.36$) to achieve complete enantioseparation was **3CF3**. Complete enantioseparation of other analytes could be achieved within k'_2 of 25. The analyte that required longest analysis time ($k'_2 = 45$) to achieve complete enantioseparation was **4FPh**. For most cases, analytes with high $-\Delta\Delta H$ values showed complete enantioseparation with short analysis time. The results agreed with retention of **3CF3** and **4FPh**, having the highest and lowest $-\Delta\Delta H$ values, respectively. For most analytes that complete enantioseparation could be achieved with $k'_2 \leq 5$, they have $-\Delta\Delta H$ values greater than 0.48 kcal/mol (**iBu**). For **5OMeA**, even it has high $-\Delta\Delta H$ value (0.63 kcal/mol), it has high $-\Delta H_2$ value (19.9 kcal/mol) as well. Therefore, the complete enantioseparation of **5OMeA** could be achieved at longer analysis time ($k'_2 = 6.8$). Substituted phenyl phenyl methanamine (Ph) was the only group of amine in this study that showed no enantioseparation or enantioseparation with long analysis time.

An interesting result was found with **CF3**. It has lower $-\Delta\Delta H$ value (0.34 kcal/mol) and high $-\Delta H_2$ value (19.0 kcal/mol), however, complete enantioseparation could be achieved with a very short analysis time ($k'_2 = 3.5$). The structure of **CF3** is

very similar to **H**. Both of their $-\Delta\Delta H$ and $-\Delta H_2$ values were quite similar. However, **H** required k'_2 of 24.2 to achieve complete enantioseparation. Plots of ln k′ versus 1/T and ln α versus 1/T of **CF3** and **H** were then compared in Figures 4.17-4.18. It can be seen that, the same temperature, k′ of **CF3** was lower than that of **H** but its α was higher than that of **H**. These results showed the attractive characteristic of this analyte in chiral discrimination. The enantioseparation of **H** and **CF3** was shown in Figure 4.19.

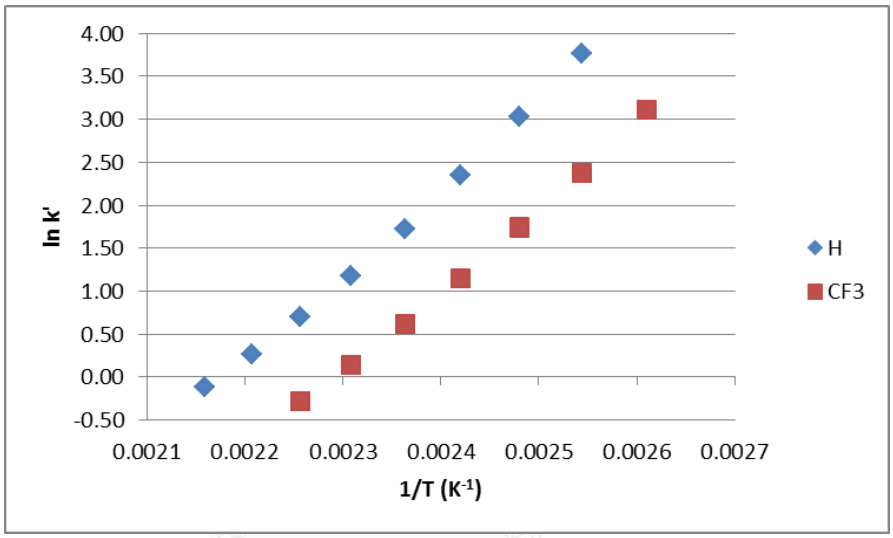

Figure 4.17 Plots of ln k'_2 versus 1/T of **H** and **CF3**.

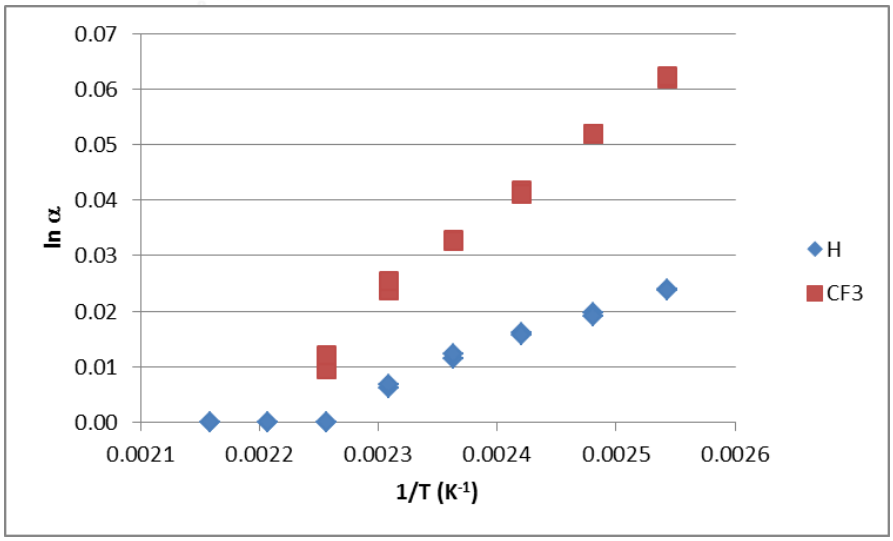

Figure 4.18 Plots of ln α versus 1/T of **H** and **CF3**.

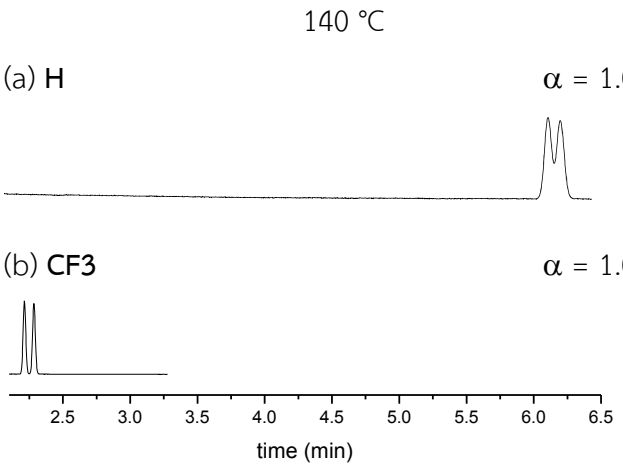

Figure 4.19 Chromatograms of (a) **H** and (b) **CF3** at 140 °C.

4.4 Comparison of enantiomeric separation with other β-cyclodextrin derivative

The enantiomeric separations of TFA derivative of amines using BSiAc as a chiral selector in GC stationary phase were compared with previous results using other type of β-CD derivatives. Enantiomeric separations as a function of temperature of 32 TFA derivative of amines using heptakis(2,3-di-*O*-methyl-6-*O*-*tert*-butyldimethylsilyl)-β-CD (or BSiMe) as a chiral selector have been reported [16]. The effect of type of substitution at the C2 and C3 positions of glucose unit of CD ring will be studied. The $-\Delta H_2$ and $-\Delta\Delta H$ values of 32 analytes obtained from both BSiMe and BSiAc were compared in Figures 4.20-4.21.

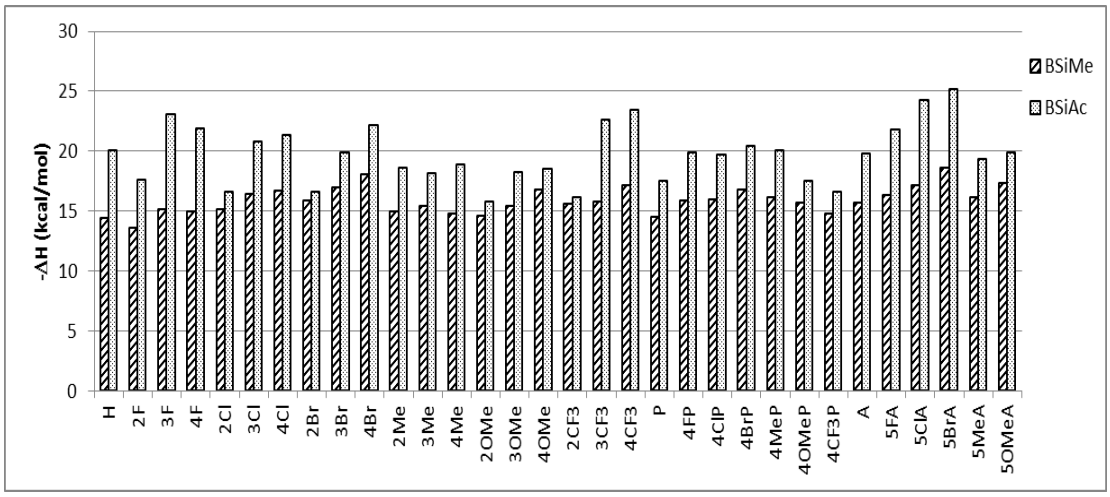

Figure 4.20 Enthalpy change ($-\Delta H$, kcal/mol) of the more retained enantiomers of 32 TFA amines on BSiMe and BSiAc columns.

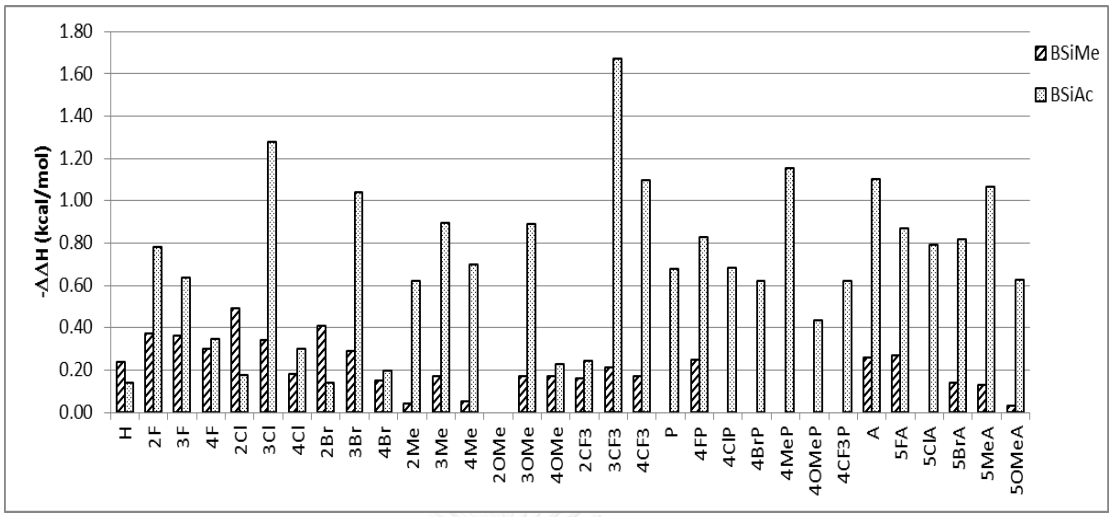

Figure 4.21 Enthalpy difference (-ΔΔH, kcal/mol) of 32 TFA amines on BSiMe and BSiAc columns.

From Figure 4.20, it can be seen that $-\Delta H_2$ values of all 32 analytes obtained from BSiAc were higher than those from BSiMe. The increase in $-\Delta H_2$ values would result from the interaction between amine analytes with more polar acetyl groups of BSiAc. The retention of analytes was more temperature dependent on BSiAc than on BSiMe. However, the trend of $-\Delta H_2$ values for both columns was similar, suggesting that the same influence of analyte substitution on retention for both columns.

Enantioseparation on both columns did not show the same trend. From Figure 4.21, it can be seen that -ΔΔH values of most analytes obtained from BSiAc were higher than those from BSiMe, suggesting that the enantioselectivity of analytes was more temperature dependent on BSiAc than on BSiMe. A decrease in temperature would result in a larger increase in enantioselectivity on BSiAc than on BSiMe. The exceptions were **H**, **2Cl** and **2Br**, whose -ΔΔH values were higher on BSiMe. **2OMe** was the only analyte that could not be separated into their enantiomers on both columns. Phenylpropylamines (PPs) and aminoindans (AIs) could not be enantioseparated or had poor enantioseparation on BSiMe, they showed higher -ΔΔH values and could be well separated with BSiAc. These results suggested the influence of substitution on CD towards enantioseparation. The acetyl groups of BSiAc introduced more polar interaction and the size of acetyl group might lead to a

change in CD cavity. BSiMe showed good enantioseparation for phenylethylamines with no or small substituent at *ortho*-position.

CHAPTER V

CONCLUSION

Forty-nine TFA derivative of racemic amines were prepared and separated into their enantiomers by GC using heptakis(2,3-di-*O*-acetyl-6-*O*-*tert*-butyldimethylsilyl)-β-CD (or BSiAc) mixed with polysiloxane OV-1701 as a stationary phase. The influences of separation temperature and analyte structure on enantioseparation were investigated. BSiAc were suitable for enantioseparation of TFA amines. Only four analytes could not be enantioseparated: **2OMe**, **4MePh**, **4OMePh** and **Nap**. Forty-five analytes could be enantioseparated on this column at varying degree depending on analyte structure as well as type and position of substitution.

For mono-substituted 1-phenylethylamines, the position of substitution seemed to play a major role on enantioseparation rather than the type of substitution. In most cases, enantioseparation of analytes with *meta*-substitution could be easily improved with temperature, as they showed higher -ΔΔH values than their *para*- or *ortho*-isomers. Among 6 different substituents, **3CF3** provided the best enantioseparation. Larger substituents at *ortho*-position tended to reduce enantioseparation. The effect of type of substituent at *para*-position of the aromatic ring on enantioseparation was examined. Alkyl substitution seemed to improve enantioselectivity, while a large phenyl group or halogen seemed to reduce enantioseparation.

The type of substitution at the stereogenic center was also investigated. A longer ethyl group (PPs) or a less flexible structure (AIs) replacing a methyl group (PEs) seemed to improved enantioseparation. Two phenyl rings substituted at the same stereogenic center (as in Phs) mostly led to a poor or complete loss of enantioseparation. Bulky group or cyclic structure with the similar number of carbon substitution seemed to provide better enantioseparation than their corresponding straight chain substitution.

The effect of temperature toward both retention and enantioselectivity was expressed in term of resolution of enantiomeric peak pair. The retention of the more retained enantiomer of all separable analytes at complete baseline separation was compared. Analytes with high -ΔΔH values showed complete enantioseparation with short analysis time. Among all analytes studied, enantiomers of **3CF3** (highest -ΔΔH value) could be separated with the shortest analysis time.

REFERENCES

[1] Rasmussen, L.B., Olsen, K.H., and Johansen, S.S. Chiral separation and quantification of R/S-amphetamine, R/S-methamphetamine, R/S-MDA, R/S-MDMA, and R/S-MDEA in whole blood by GC-EI-MS. Journal of chromatography. B, Analytical technologies in the biomedical and life sciences 842(2) (2006): 136-41.

[2] Sekhon, B.S. Enantioseparation of chiral drugs – an overview. International Journal of PharmTech Research 2(2) (2010): 1584-1594.

[3] Li, B. and Haynie, D.T. Chiral Drug Separation. Encyclopedia of Chemical Processing 1(2007): 449-458.

[4] Juaristi, E., Escalante, J., León-Romo, J.L., and Reyes, A. Recent applications of α-phenylethylamine (α-PEA) in the preparation of enantiopure compounds. Part 1: Incorporation in chiral catalysts. Part 2: α-PEA and derivatives as resolving agents. Tetrahedron: Asymmetry 9 (1998): 715–740.

[5] Shitangkoon, A. and Vigh, G. Systematic modification of the separation selectivity of cyclodextrin-based gas chromatographic stationary phases by varying the size of the 6-*O*-substituents. Journal of Chromatography A 738(1) (1996): 31-42.

[6] Nie, M.-Y., Zhou, L.-M., Liu, X.-L., Wang, Q.-H., and Zhu, D.-Q. Gas chromatographic enantiomer separation on long-chain alkylated β-cyclodextrin chiral stationary phases. Analytica Chimica Acta 408(1–2) (2000): 279-284.

[7] Ward, T.J. Chiral separations. Analitical Chemistry 74 (2002): 2863-2872.

[8] Zhang, Z.B., Zhang, W.G., Luo, W.J., and Fan, J. Preparation and enantioseparation characteristics of a novel chiral stationary phase based on mono (6(A)-azido-6(A)-deoxy)-per(p-chlorophenylcarbamoylated) beta-cyclodextrin. Journal of Chromatography A 1213(2) (2008): 162-8.

[9] Gong, X.Y. and Hauser, P.C. Enantiomeric separation of 1-phenylethylamine and 1-cyclohexylethylamine in capillary electrophoresis with contactless conductivity detection. Journal of Chromatography A 1094(1-2) (2005): 196-9.

[10] Huang, W.X., Xu, H., Fazio, S.D., and Vivilecchia, R.V. Chiral separation of primary amino compounds using a non-chiral crown ether with beta-cyclodextrin by capillary electrophoresis. Journal of Chromatography B: Biomedical Sciences and Applications 695(1) (1997): 157-62.

[11] Chankvetadze, B., et al. Comparative enantioseparations with native beta-cyclodextrin, randomly acetylated beta-cyclodextrin and heptakis-(2,3-di-*O*-acetyl)-beta-cyclodextrin in capillary electrophoresis. Electrophoresis 24(6) (2003): 1083-91.

[12] Mosinger, J., Tománková, V., Němcová, I., and Zýka, J. Cyclodextrins in analytical chemistry. Analytical Letters 34(12) (2001): 1979-2004.

[13] Takahisa, E. and Engel, K.-H. 2,3-Di-*O*-methoxymethyl-6-*O*-*tert*-butyldimethylsilyl-γ-cyclodextrin: a new class of cyclodextrin derivatives for gas chromatographic separation of enantiomers. Journal of Chromatography A 1063(1-2) (2005): 181-192.

[14] Blanch, G.P. and Ruiz del Castillo, M.L. Semipreparative-scale gas-chromatographic separation of filbertone enantiomers. Journal of Separation Science 29(5) (2006): 691-694.

[15] Kitaura, T., Endo, H., Nakamoto, H., Ishihara, M., Kawai, T., and Nokami, J. Isolation and synthesis of a new natural lactone in apple juice(Malus×domestica var. Orin). Flavour and Fragrance Journal 19(3) (2004): 221-224.

[16] Issaraseriruk, N. Enantiomeric separation of amines by gas chromatography using derivatized cyclodextrins as stationary phases. Doctor of Philosophy Dissertation, Chemistry Chulalongkorn University, 2013.

[17] Gübitz, G. and Schmid, M.G. Chiral Separations: Methods and Protocols. Humana Press, 2004.

[18] Del Valle, E.M.M. Cyclodextrins and their uses: a review. Process Biochemistry 39(9) (2004): 1033-1046.

[19] Juvancz, Z. and Szejtli, J. The role of cyclodextrins in chiral selective chromatography. TrAC Trends in Analytical Chemistry 21(5) (2002): 379-388.

[20] Gawley, R.E. and Aubé, J. Chapter 1 - Introduction, general principles, and glossary of stereochemical terms. in Aubé, R.E.G. (ed.) Principles of Asymmetric Synthesis (Second Edition), pp. 1-62. Oxford: Elsevier, 2012.

[21] Katritzky, A.R., Xie, L., and Zhang, G. Synthesis of primary amines via nucleophilic addition of organometallic reagents to aldimines on solid support Tetrahedron Letters 38(97) (1997): 7011-7014.

[22] Eddine, J.J. and Cherqaoui, M. Chiral quaternary benzophenone hydrazonium salt derivatives; Efficient chiral catalysts for the enantioselective phase-transfer alkylation of imines. Application to synthesis of chiral primary amines. Tetrahedron : Asymmetry 6(95) (1995): 1225-1228.

[23] Miriyala, B., Bhattacharyya, S., and Williamson, J.S. Chemoselective reductive alkylation of ammonia with carbonyl compounds: synthesis of primary and symmetrical secondary amines. Tetrahedron 60(7) (2004): 1463-1471.

[24] Kataoka, H. Derivatization reactions for the determination of amines by gas chromatography and their applications in environmental analysis. Journal of Chromatography A 733(1–2) (1996): 19-34.

[25] Orata, F. Derivatization reactions and reagents for gas chromatography analysis. INTECH Open Access Publisher, 2012.

[26] Juvancz, Z., Kiss, V., Schindler, J., and Bálint, J. Use of achiral derivatization to increase selectivity and reverse the order of elution of enantiomers on chirasil-dex. Chromatographia 60(1) (2004): S161-S163.

[27] Shen, G., Cui, J., Yang, X., and Ling, Y. Capillary GC using pyridyl beta-cyclodextrin stationary phase. Journal of Separation Science 32(1) (2009): 79-87.

[28] Nie, M.Y., Zhou, L.M., Wang, Q.H., and Zhu, D.Q. Gas chromatographic enantiomer separation on single and mixed cyclodextrin derivative chiral stationary phases. Chromatographia 51(11-12) (2000): 736-740.

[29] Li, W.Y., Jin, H.L., and Armstrong, D.W. 2,6-Di-*O*-pentyl-3-*O*-trifluoroacetyl cyclodextrin liquid stationary phases for capillary gas chromatographic

separation of enantiomers. Journal of Chromatography A 509(2) (1990): 303-324.

[30] da Silva, R.A., Estevam, I.H.S., and Bieber, L.W. Reductive methylation of primary and secondary amines and amino acids by aqueous formaldehyde and zinc. Tetrahedron Letters 48(43) (2007): 7680-7682.

[31] Bhattacharyya, S. Borohydride reductions in dichloromethane: a convenient procedure for the methylation of amines. Synthetic Communications 25(14) (1995): 2061-2069.

[32] Guo, H.X., Wu, S., and Sun, J. Influence of temperature on the enantioselectivity of koga tetraamines on amylose chiral stationary phases. Molecules 19(1) (2013): 9-21.

Appendix A

Thermodynamic parameters and chromatographic parameters

Table A1 Slope and y-intercept from ln k′ versus 1/T plots of 49 TFA amines on the BSiAc column.

analytes	temperature range (°C)	less retained enantiomer			more retained enantiomer		
		ln k′ = m(1/T) + c		R^2	ln k′ = m(1/T) + C		R^2
		m	c		m	c	
H	190-120	10048.0	-21.935	0.9959	10117.0	-22.088	0.9959
2F	180-120	8472.6	-18.360	0.9974	8814.5	-19.092	0.9962
3F	190-130	9517.9	-20.039	0.9976	10099.0	-21.236	0.9967
4F	200-140	9414.9	-19.603	0.9969	9969.6	-20.748	0.9960
2Cl	200-130	9183.8	-18.866	0.9974	9718.9	-19.982	0.9966
3Cl	210-150	8201.0	-17.501	0.9986	8291.5	-17.700	0.9986
4Cl	220-160	7972.5	-17.191	0.9981	8215.5	-17.719	0.9978
2Br	200-140	8616.0	-17.661	0.9977	9122.3	-18.720	0.9967
3Br	220-160	8816.8	-18.604	0.9975	9181.1	-19.380	0.9970
4Br	220-160	8763.6	-18.055	0.9981	9138.2	-18.836	0.9975
2Me	190-130	8945.7	-18.131	0.9978	9200.1	-18.658	0.9973
3Me	190-130	10736.0	-20.184	0.9985	10888.0	-20.494	0.9985
4Me	190-130	8734.1	-17.028	0.9992	8734.1	-17.028	0.9992
2OMe	190-120	8788.8	-16.995	0.9996	8788.8	-16.995	0.9996
3OMe	190-130	9072.1	-19.667	0.9953	9383.6	-20.337	0.9956
4OMe	210-150	8677.9	-18.772	0.9972	9129.2	-19.743	0.9964
2CF3	190-120	9166.4	-19.740	0.9969	9517.5	-20.501	0.9966
3CF3	200-140	8467.9	-18.889	0.9976	8860.9	-19.764	0.9972
4CF3	210-140	11294.0	-24.303	0.9973	11613.0	-24.968	0.9973
P	190-130	10822.0	-23.072	0.9963	10995.0	-23.443	0.9962
4FP	200-140	8254.4	-17.516	0.9974	8343.8	-17.712	0.9968

analytes	temperature range (°C)	less retained enantiomer			more retained enantiomer		
		ln k′ = m(1/T) + c		R^2	ln k′ = m(1/T) + C		R^2
		m	c		m	c	
4ClP	220-160	9844.8	-20.310	0.9962	10487.0	-21.625	0.9954
4BrP	220-160	10597.0	-21.562	0.9960	10747.0	-21.870	0.9960
4MeP	210-150	8268.5	-17.151	0.9982	8337.7	-17.303	0.9978
4OMeP	210-150	9501.1	-19.168	0.9966	10025.0	-20.225	0.9957
4CF3P	200-140	11038.0	-22.071	0.9968	11138.0	-22.279	0.9966
A	210-150	7936.3	-16.985	0.9987	7936.3	-16.985	0.9987
5FA	220-160	8755.8	-18.970	0.9984	9203.4	-19.935	0.9978
5ClA	220-160	9198.2	-18.942	0.9973	9311.6	-19.183	0.9968
5BrA	220-160	7998.7	-17.586	0.9991	8121.9	-17.857	0.9991
5MeA	210-150	10564.0	-22.601	0.9967	11404.0	-24.340	0.9962
5OMeA	220-160	11240.0	-23.698	0.9962	11793.0	-24.828	0.9959
4FPh	220-150	9324.7	-18.289	0.9985	9382.3	-18.409	0.9983
4ClPh	220-170	9877.6	-18.647	0.9989	10013.0	-18.924	0.9989
4BrPh	220-170	10289.0	-19.116	0.9989	10452.0	-19.447	0.9989
4MePh	220-160	9406.0	-21.595	0.9975	9576.9	-21.967	0.9977
4OMePh	220-170	9513.0	-17.830	0.9994	9513.0	-17.830	0.9994
4Et	200-140	11797.0	-23.255	0.9965	12196.0	-24.058	0.9962
4Bu	220-150	9688.0	-19.173	0.9966	10003.0	-19.824	0.9960
4tBu	210-150	12263.0	-23.810	0.9969	12673.0	-24.631	0.9966
4Ph	220-170	8618.5	-17.665	0.9979	8763.5	-17.971	0.9976
CF3	170-110	8313.7	-16.367	0.9987	8550.3	-16.855	0.9983
Nap	220-160	9616.4	-19.354	0.9961	9881.2	-19.889	0.9962
Bu	190-130	9599.7	-20.439	0.9971	10016.0	-21.300	0.9967
iBu	190-130	9982.9	-19.869	0.9967	10295.0	-20.496	0.9964
Hex	210-150	9576.5	-19.418	0.9965	9920.3	-20.108	0.9962
Cy	220-160	8584.2	-17.486	0.9984	8804.0	-17.946	0.9982
ATL	210-150	8047.0	-17.121	0.9980	8358.5	-17.784	0.9977

analytes	temperature range (°C)	less retained enantiomer			more retained enantiomer		
		ln k′ = m(1/T) + c		R^2	ln k′ = m(1/T) + C		R^2
		m	c		m	c	
2ATL	220-160	10530.0	-21.509	0.9953	10968.0	-22.401	0.9951

Table A2 Thermodynamic parameters of 49 TFA amines on the BSiAc column.

analytes	enthalpy term (kcal/mol)			entropy term (cal/mol·K)		
	$-\Delta H_1$	$-\Delta H_2$	$-\Delta\Delta H$	$-\Delta S_1$	$-\Delta S_2$	$-\Delta\Delta S$
H	19.97	20.10	0.14	32.61	32.92	0.30
2F	16.83	17.61	0.78	26.56	28.30	1.74
3F	22.44	23.08	0.63	37.32	38.64	1.32
4F	21.50	21.85	0.34	34.87	35.61	0.74
2Cl	16.40	16.58	0.18	23.83	24.22	0.39
3Cl	19.56	20.84	1.28	29.38	32.00	2.61
4Cl	21.06	21.35	0.30	31.87	32.48	0.61
2Br	16.43	16.57	0.14	23.11	23.41	0.30
3Br	18.88	19.92	1.04	27.12	29.22	2.10
4Br	21.93	22.13	0.20	32.88	33.30	0.41
2Me	18.03	18.65	0.62	28.11	29.44	1.33
3Me	17.24	18.14	0.90	26.33	28.26	1.93
4Me	18.21	18.91	0.70	28.25	29.76	1.51
2OMe	15.77	15.77	0.00	22.78	22.78	0.00
3OMe	17.40	18.29	0.89	26.72	28.64	1.92
4OMe	18.28	18.50	0.23	26.67	27.15	0.48
2CF3	15.89	16.14	0.24	23.97	24.51	0.54
3CF3	20.99	22.66	1.67	33.94	37.39	3.46
4CF3	22.33	23.43	1.10	36.12	38.36	2.25
P	16.84	17.51	0.68	25.51	26.96	1.45
4FP	19.07	19.90	0.83	29.64	31.35	1.71

analytes	enthalpy term (kcal/mol)			entropy term (cal/mol·K)		
	$-\Delta H_1$	$-\Delta H_2$	$-\Delta\Delta H$	$-\Delta S_1$	$-\Delta S_2$	$-\Delta\Delta S$
4ClP	19.03	19.71	0.68	27.61	28.98	1.37
4BrP	19.84	20.46	0.62	28.51	29.75	1.25
4MeP	18.91	20.07	1.15	28.85	31.22	2.38
4OMeP	17.06	17.49	0.44	23.77	24.69	0.91
4CF3P	15.99	16.61	0.62	23.05	24.37	1.32
A	18.71	19.81	1.10	27.98	30.26	2.28
5FA	20.92	21.79	0.87	31.77	33.54	1.77
5ClA	23.44	24.23	0.79	35.24	36.83	1.60
5BrA	24.37	25.18	0.81	36.34	37.97	1.63
5MeA	18.25	19.31	1.06	26.52	28.73	2.22
5OMeA	19.25	19.88	0.63	27.13	28.42	1.29
4FPh	18.53	18.64	0.11	25.37	25.61	0.24
4ClPh	19.63	19.90	0.27	26.08	26.63	0.55
4BrPh	20.44	20.77	0.32	27.01	27.67	0.66
4MePh	17.46	17.46	0.00	22.80	22.80	0.00
4OMePh	18.90	18.90	0.00	24.46	24.46	0.00
4Et	17.52	18.24	0.72	26.00	27.54	1.54
4Bu	17.78	18.28	0.51	25.06	26.10	1.05
4tBu	17.41	18.16	0.74	24.90	26.46	1.55
4Ph	21.33	21.63	0.30	29.13	29.75	0.62
Nap	17.35	17.35	0.00	22.86	22.86	0.00
CF3	18.69	19.03	0.34	31.94	32.68	0.74

analytes	enthalpy term (kcal/mol)			entropy term (cal/mol·K)		
	$-\Delta H_1$	$-\Delta H_2$	$-\Delta\Delta H$	$-\Delta S_1$	$-\Delta S_2$	$-\Delta\Delta S$
Bu	16.30	16.48	0.18	23.80	24.20	0.40
iBu	15.84	16.32	0.48	23.19	24.24	1.05
Hex	17.12	17.41	0.29	24.13	24.74	0.61
Cy	16.52	16.99	0.47	21.55	22.52	0.97
ATL	17.12	18.13	1.01	24.12	26.23	2.10
2ATL	19.11	19.63	0.53	27.49	28.55	1.06

Table A3 The highest operating column temperature and chromatographic parameters for 49 TFA amines where enantiomers are baseline separated (Rs ≥ 1.5) on the BSiAc column.

analyte	temperature (°C)	k'_2	α	Rs
H	120	42.891	1.024	2.01
2F	150	3.047	1.046	1.96
3F	180	1.976	1.042	1.56
4F	150	12.629	1.039	2.14
2Cl	130	21.491	1.037	2.33
3Cl	200	1.746	1.044	1.55
4Cl	170	10.575	1.031	1.72
2Br	140	18.760	1.024	1.54
3Br	200	2.537	1.045	1.81
4Br	160	34.192	1.027	2.03
2Me	160	3.476	1.048	2.13
3Me	160	3.531	1.060	2.74
4Me	160	4.053	1.044	2.06
2OMe	ND	ND	ND	ND
3OMe	160	3.533	1.059	2.71
4OMe	150	18.022	1.033	1.95
2CF3	130	9.829	1.035	1.86
3CF3	190	1.302	1.079	2.30
4CF3	190	1.752	1.059	2.09
P	160	3.303	1.051	2.27

analyte	temperature (°C)	k'_2	α	Rs
4FP	180	2.140	1.053	2.04
4ClP	190	3.430	1.048	2.16
4BrP	190	5.228	1.042	2.14
4MeP	190	1.689	1.050	1.74
4OMeP	170	6.623	1.031	1.70
4CF3P	170	2.842	1.034	1.52
A	190	2.073	1.046	1.73
5FA	190	3.291	1.049	2.19
5ClA	200	5.319	1.036	1.80
5BrA	210	4.998	1.030	1.51
5MeA	190	2.616	1.035	1.53
5OMeA	180	8.864	1.040	2.23
4FPh	150	45.888	1.019	1.49
4ClPh	170	40.605	1.030	2.34
4BrPh	180	37.024	1.029	2.23
4MePh	ND	ND	ND	ND
4OMePh	ND	ND	ND	ND
4Et	170	3.609	1.040	1.92
4Bu	170	7.838	1.042	2.25
4tBu	180	3.600	1.038	1.81
4Ph	180	33.739	1.024	1.88
Nap	ND	ND	ND	ND

analyte	temperature (°C)	k'_2	α	Rs
CF3	140	3.170	1.043	1.80
Bu	130	18.482	1.026	1.51
iBu	150	5.200	1.041	2.03
Hex	160	9.598	1.029	1.64
Cy	180	7.188	1.031	1.64
ATL	180	3.878	1.047	2.22
2ATL	190	3.962	1.036	1.69

Note: ND = No enantioseparation or baseline separation could not be observed.

Table A4 Relationship between Rs (y) vs. k'_2 (x) for 49 TFA amines and the calculated k'_2 values at baseline separation.

analytes	polynomial equation ($y = -ax^2+bx-c$)	k'_2 at Rs = 1.5
H	$y = -0.001x^2 + 0.088x - 0.0446$	24.2
2F	$y = -0.0207x^2 + 0.8577x - 0.6882$	2.7
3F	$y = -0.0045x^2 + 0.4088x + 0.6642$	2.1
4F	$y = -0.004x^2 + 0.2494x - 0.1992$	7.8
2Cl	$y = -0.0027x^2 + 0.1997x - 0.8079$	14.3
3Cl	$y = -0.0155x^2 + 0.951x + 0.1087$	1.5
4Cl	$y = -0.0056x^2 + 0.2633x - 0.3264$	8.5
2Br	$y = -0.0074x^2 + 0.3146x - 1.8054$	19.0
3Br	$y = -0.0229x^2 + 0.9975x - 0.7262$	2.4
4Br	$y = -0.0022x^2 + 0.1511x - 0.662$	20.3
2Me	$y = -0.0165x^2 + 0.6711x - 0.332$	2.9
3Me	$y = -0.0204x^2 + 0.9043x - 0.4451$	2.3
4Me	$y = -0.0069x^2 + 0.5131x - 0.2457$	3.6
2OMe	ND	ND
3OMe	$y = -0.0181x^2 + 0.8749x - 0.4275$	2.3
4OMe	$y = -0.0075x^2 + 0.2915x - 0.8913$	11.8
2CF3	$y = -0.0112x^2 + 0.3707x - 0.5671$	7.1
3CF3	$y = -0.0217x^2 + 1.3001x + 1.0327$	0.4
4CF3	$y = -0.0081x^2 + 0.717x + 0.6794$	1.2
P	$y = -0.0222x^2 + 0.8261x - 0.4278$	2.5
4FP	$y = -0.0237x^2 + 0.9337x - 0.1486$	1.8

analytes	polynomial equation ($y = -ax^2+bx-c$)	k'_2 at Rs = 1.5
4ClP	$y = -0.0203x^2 + 0.7701x - 0.5496$	2.9
4BrP	$y = -0.0052x^2 + 0.4123x - 0.1617$	4.3
4MeP	$y = -0.0414x^2 + 1.3792x - 0.5828$	1.6
4OMeP	$y = -0.0067x^2 + 0.3614x - 0.4636$	6.1
4CF3P	$y = -0.0234x^2 + 0.8154x - 0.7479$	3.0
A	$y = -0.0298x^2 + 1.1523x - 0.6436$	2.0
5FA	$y = -0.0187x^2 + 0.7854x - 0.5383$	2.8
5ClA	$y = -0.0035x^2 + 0.3551x - 0.2841$	5.3
5BrA	$y = -0.0009x^2 + 0.2046x + 0.5592$	4.7
5MeA	y = -0.0159x2 + 0.8325x - 0.6642	2.7
5OMeA	y = -0.002x2 + 0.3013x - 0.4687	6.8
4FPh	$y = -0.0011x^2 + 0.098x - 0.7804$	44.5
4ClPh	$y = -0.0011x^2 + 0.112x - 0.5043$	23.2
4BrPh	$y = -0.0006x^2 + 0.094x - 0.3816$	23.6
4MePh	ND	ND
4OMePh	ND	ND
4Et	$y = -0.0159x^2 + 0.7069x - 0.6723$	3.3
4Bu	$y = -0.0043x^2 + 0.3693x - 0.4584$	5.7
4tBu	$y = -0.0176x^2 + 0.7417x - 0.8023$	3.4
4Ph	$y = -0.0007x^2 + 0.0973x - 0.5495$	25.9
Nap	ND	ND
CF3	$y = -0.0093x^2 + 0.4176x + 0.1643$	3.5

analytes	polynomial equation ($y = -ax^2+bx-c$)	k'_2 at Rs = 1.5
Bu	$y = -0.0073x^2 + 0.2375x - 0.4399$	16.3
iBu	$y = -0.0144x^2 + 0.5577x - 0.5386$	4.1
Hex	$y = -0.0087x^2 + 0.3222x - 0.5818$	8.4
Cy	$y = -0.0053x^2 + 0.3776x - 0.9486$	7.3
ATL	$y = -0.0185x^2 + 0.9082x - 1.2012$	3.2
2ATL	$y = -0.0112x^2 + 0.4938x - 0.3812$	4.2

Note: ND = No enantioseparation or baseline separation could not be observed.

Appendix B

NMR spectra

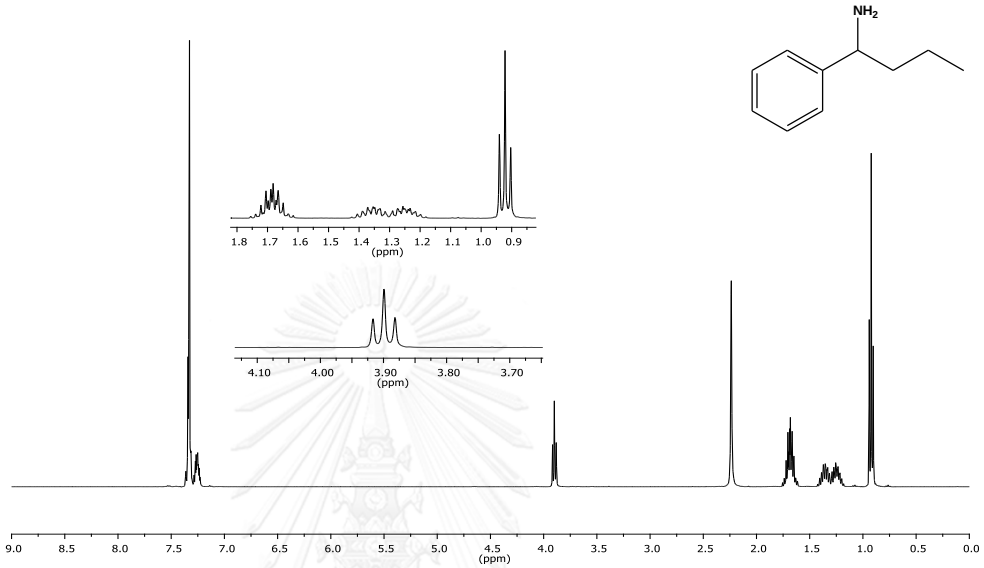

Figure B1 ^{1}H NMR of Bu (400 MHz, $CDCl_3$) δ (ppm): 7.37–7.29 (m, 4H, Ar<u>H</u>), 7.29–7.22 (m, 1H, Ar<u>H</u>), 3.90 (t, *J* = 7.0 Hz, 1H, C<u>H</u>NH_2), 2.24 (br s, 2H, CHN<u>H_2</u>), 1.76–1.60 (m, 2H, CHC<u>H_2</u>), 1.44–1.16 (m, 2H, CH_2C<u>H_2</u>), 0.92 (t, *J* = 7.3 Hz, 3H, CH_2C<u>H_3</u>).

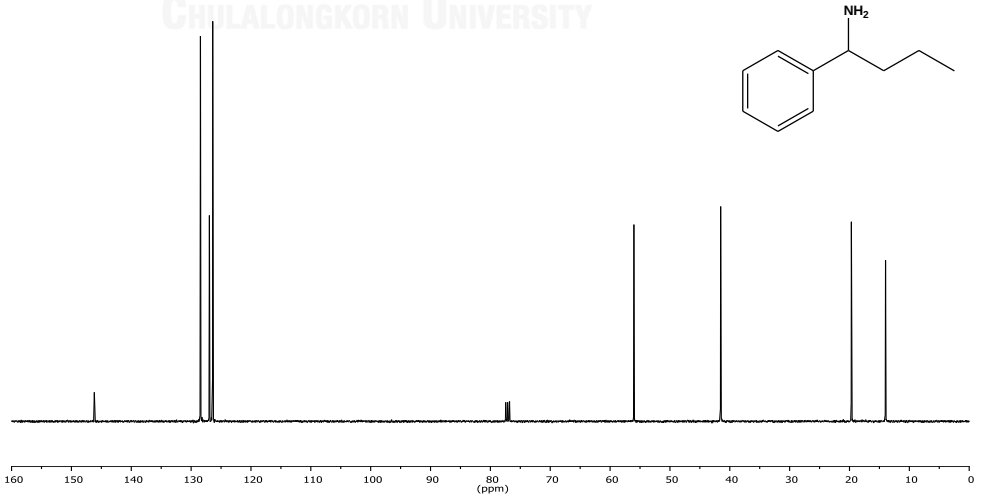

Figure B2 ^{13}C NMR of Bu (100 MHz, $CDCl_3$) δ (ppm): 146.2, 128.4, 126.9, 126.4, 56.0, 41.5, 19.7, 14.0.

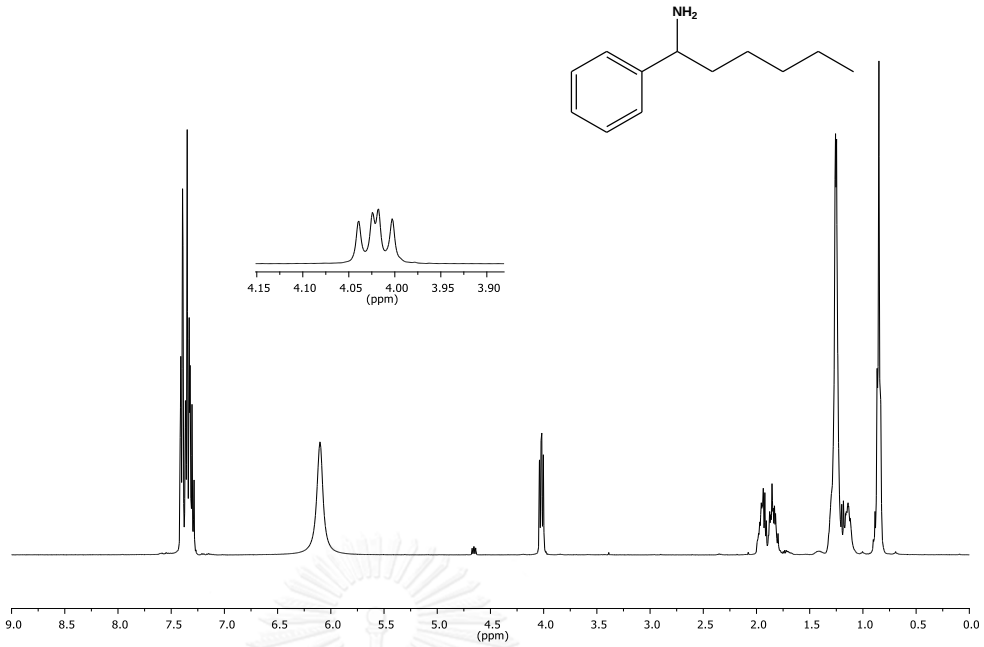

Figure B3 ^{1}H NMR of Hex (400 MHz, $CDCl_3$) δ (ppm): 7.45–7.21 (m, 5H, Ar<u>H</u>), 6.10 (br s, 2H, CHN<u>H</u>$_2$), 4.02 (dd, *J* = 8.6, 6.1 Hz, 1H, C<u>H</u>NH$_2$), 2.03–1.76 (m, 2H, CHC<u>H</u>$_2$), 1.37–1.08 (m, 6H, CH$_2$C<u>H</u>$_2$), 0.85 (t, *J* = 5.9 Hz, 3H, CH$_2$C<u>H</u>$_3$).

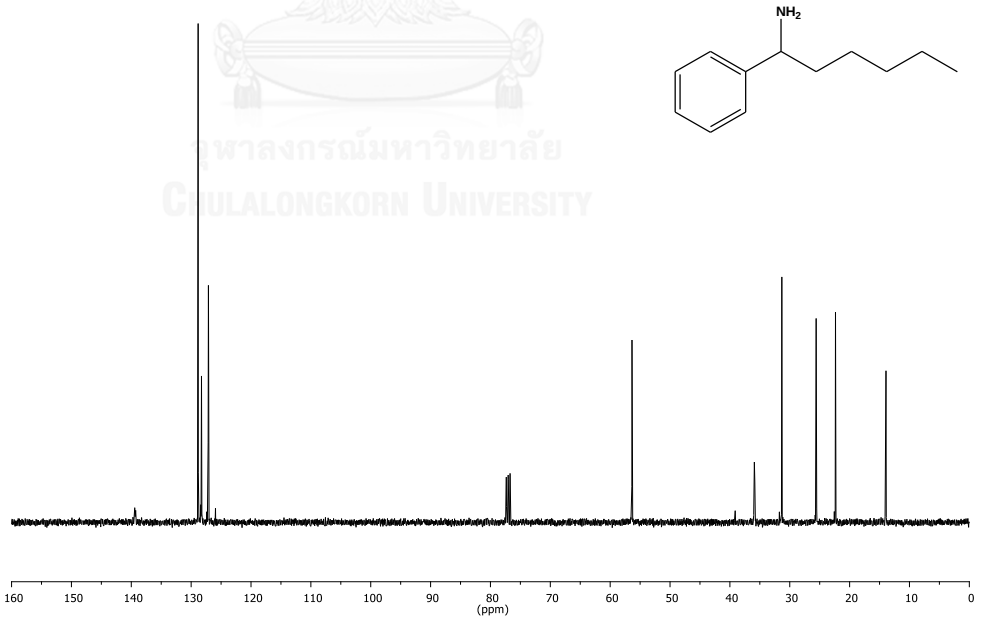

Figure B4 ^{13}C NMR of Hex (100 MHz, $CDCl_3$) δ (ppm): 139.4, 128.8, 128.3, 127.1, 56.4, 35.9, 31.3, 25.6, 22.4, 13.9.

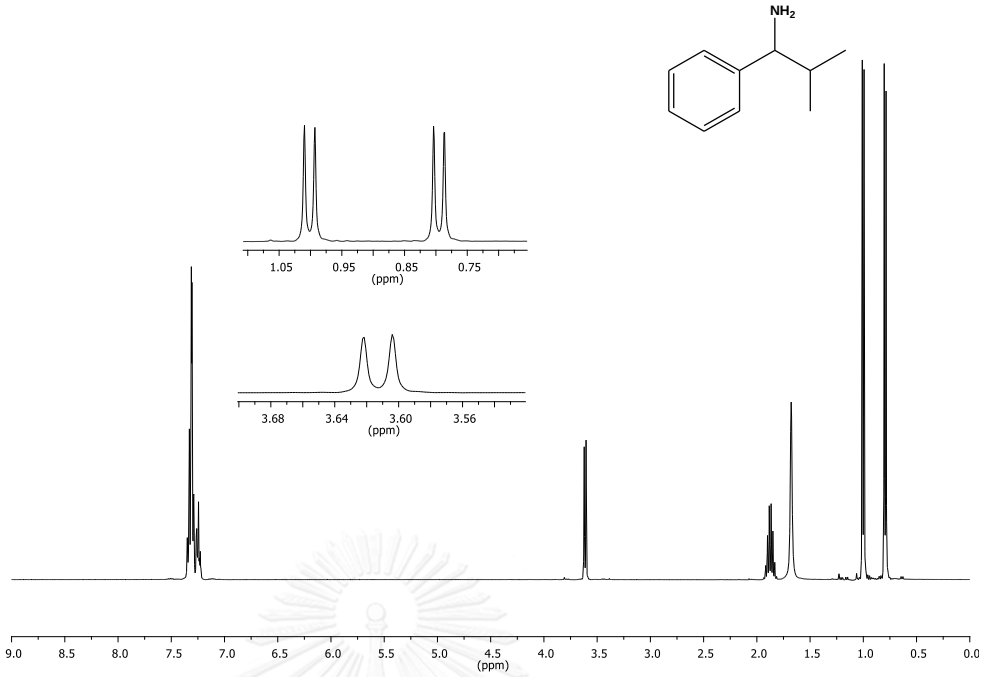

Figure B5 ^{1}H NMR of iBu (400 MHz, $CDCl_3$) δ (ppm): 7.37–7.22 (m, 5H, Ar<u>H</u>), 3.61 (d, *J* = 7.2 Hz, 1H, C<u>H</u>CH), 1.94–1.81 (m, 1H, C<u>H</u>CH_3), 1.68 (br s, 2H, CHN<u>H</u>$_2$), 1.00 (d, *J* = 6.8 Hz, 3H, CHC<u>H</u>$_3$), 0.80 (d, *J* = 6.8 Hz, 3H, CHC<u>H</u>$_3$).

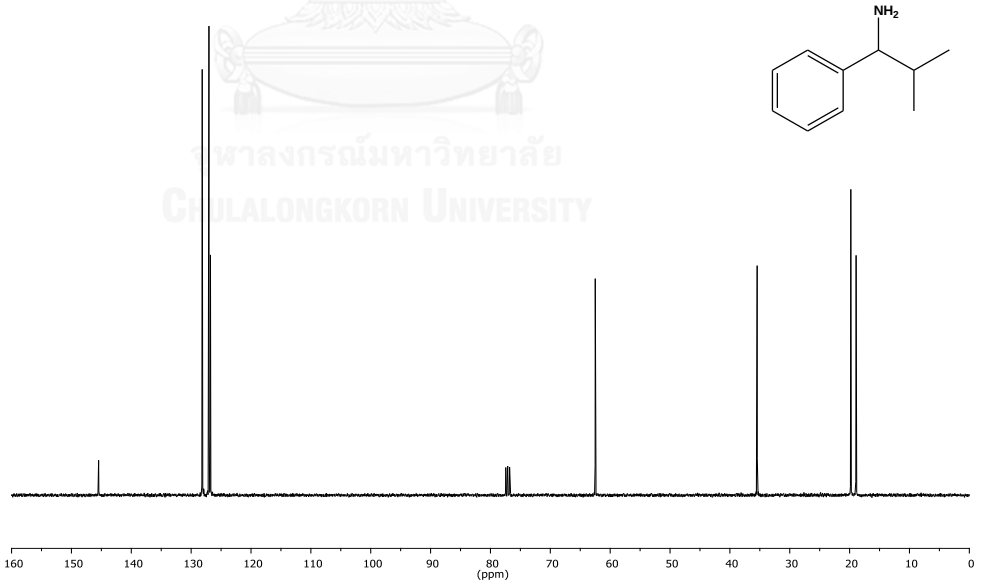

Figure B6 ^{13}C NMR of iBu (100 MHz, $CDCl_3$) δ (ppm): 145.5, 128.2, 127.0, 126.8, 62.5, 35.4, 19.8, 18.9.

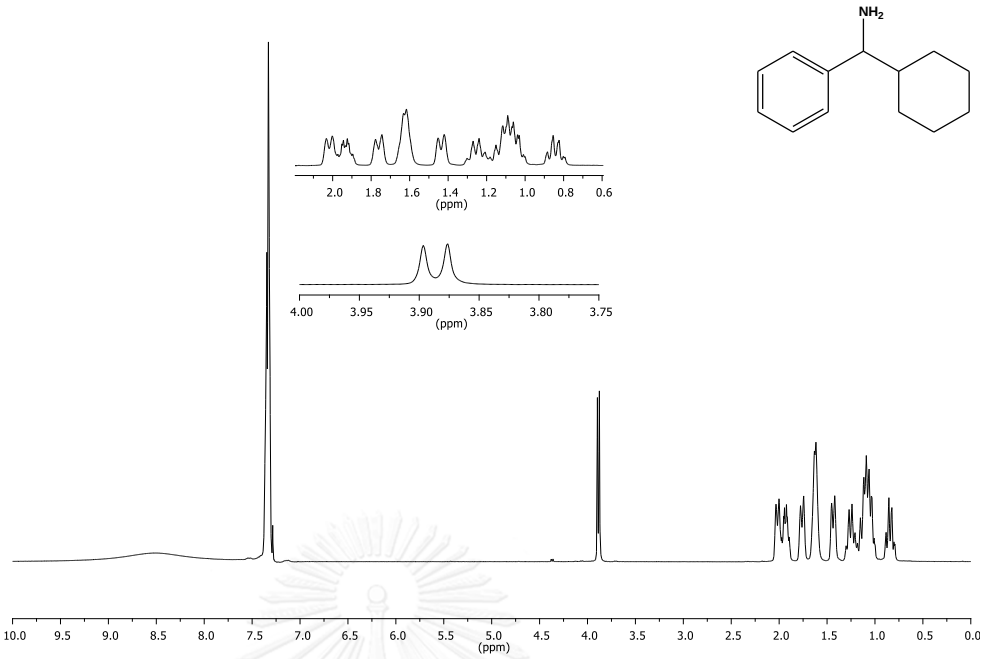

Figure B7 ^{1}H NMR of Cy (400 MHz, $CDCl_3$) δ (ppm): 8.51 (br s, 2H, CHN<u>H</u>$_2$), 7.65 – 7.07 (m, 5H, Ar<u>H</u>), 3.89 (d, *J* = 8.1 Hz, 1H, C<u>H</u>CH), 2.09 – 0.74 (m, 11H, *c*-Hx<u>H</u>).

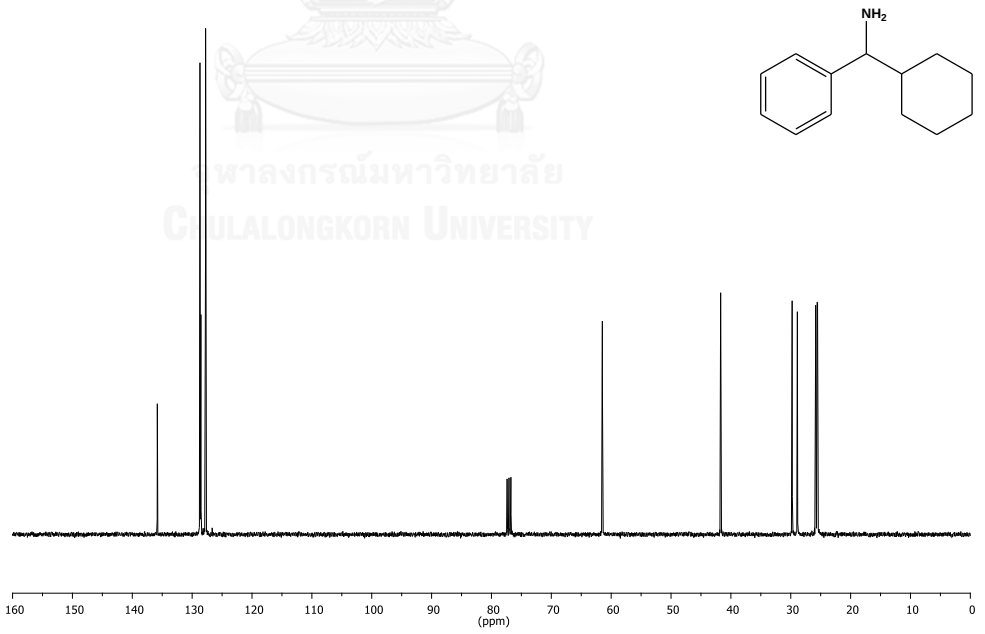

Figure B8 ^{13}C NMR of Cy (100 MHz, $CDCl_3$) δ (ppm): 135.8, 128.7, 128.5, 127.8, 61.5, 41.7, 29.8, 28.9, 25.8, 25.6, 25.5.

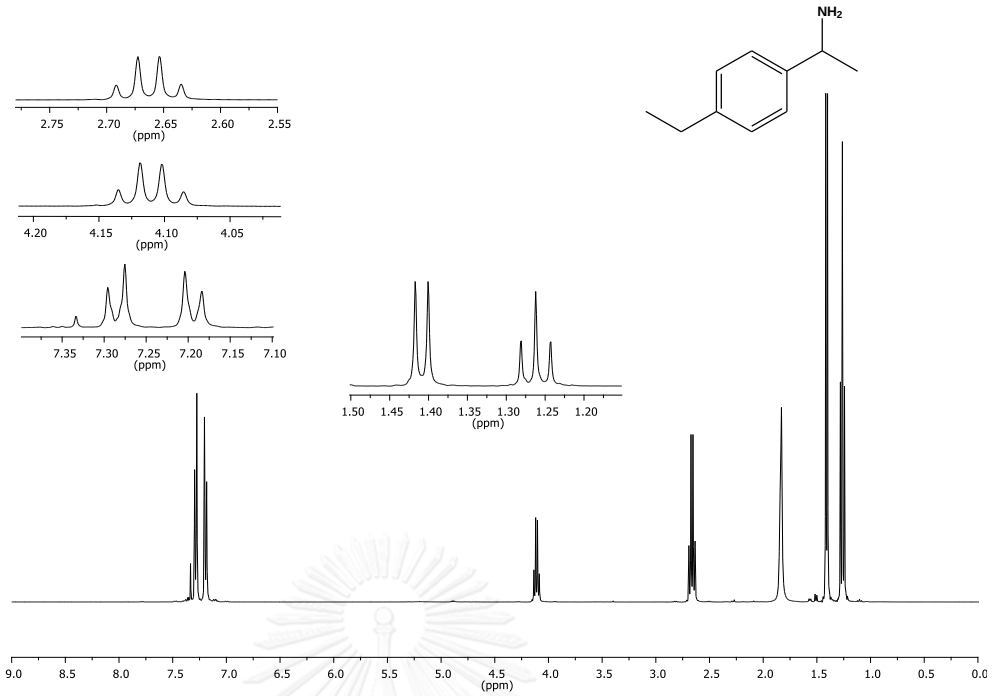

Figure B9 ^{1}H NMR of 4Et (400 MHz, $CDCl_3$) δ (ppm): 7.29 (d, *J* = 8.1 Hz, 2H, Ar<u>H</u>), 7.19 (d, *J* = 8.1 Hz, 2H, Ar<u>H</u>), 4.11 (q, *J* = 6.6 Hz, 1H, C<u>H</u>CH_3), 2.66 (q, *J* = 7.6 Hz, 2H, Ar$C\underline{H}_2$), 1.83 (br s, 2H, $CHN\underline{H}_2$), 1.41 (d, *J* = 6.6 Hz, 3H, $CHC\underline{H}_3$), 1.26 (t, *J* = 7.6 Hz, 3H, $CH_2C\underline{H}_3$).

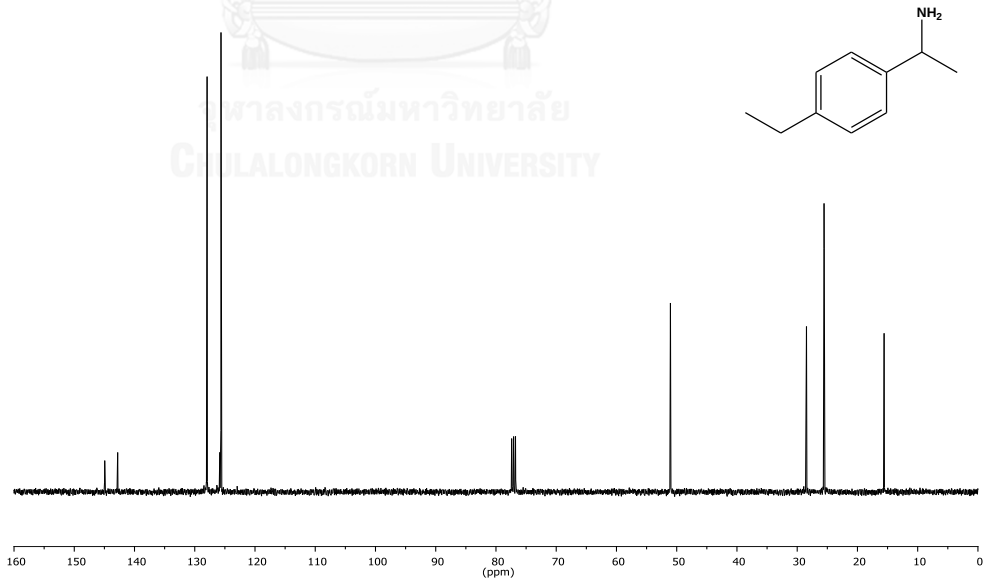

Figure B10 ^{13}C NMR of 4Et (100 MHz, $CDCl_3$) δ (ppm): 145.0, 142.8, 128.0, 125.6, 51.0, 28.5, 25.5, 15.6.

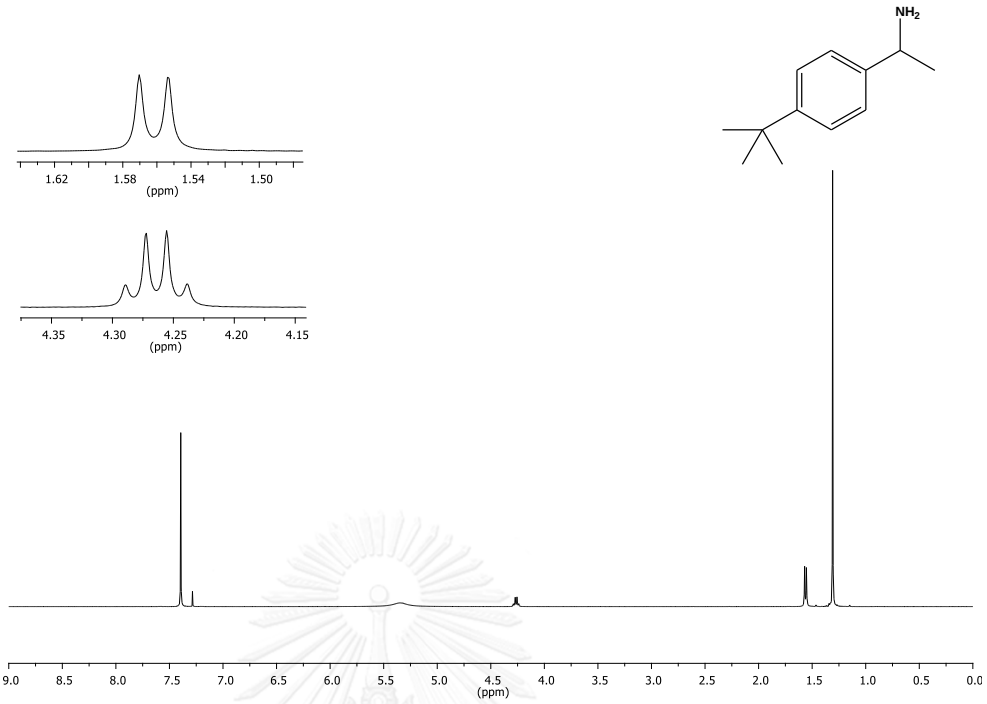

Figure B11 ^{1}H NMR of 4tBu (400 MHz, $CDCl_3$) δ (ppm): 7.39 (s, 4H, Ar<u>H</u>), 5.33 (br s, 2H,CHN<u>H</u>$_2$), 4.26 (q, *J* = 6.8 Hz, 1H, C<u>H</u>CH$_3$), 1.56 (d, *J* = 6.8 Hz, 3H, CHC<u>H</u>$_3$), 1.31 (s, 9H, CC<u>H</u>$_3$).

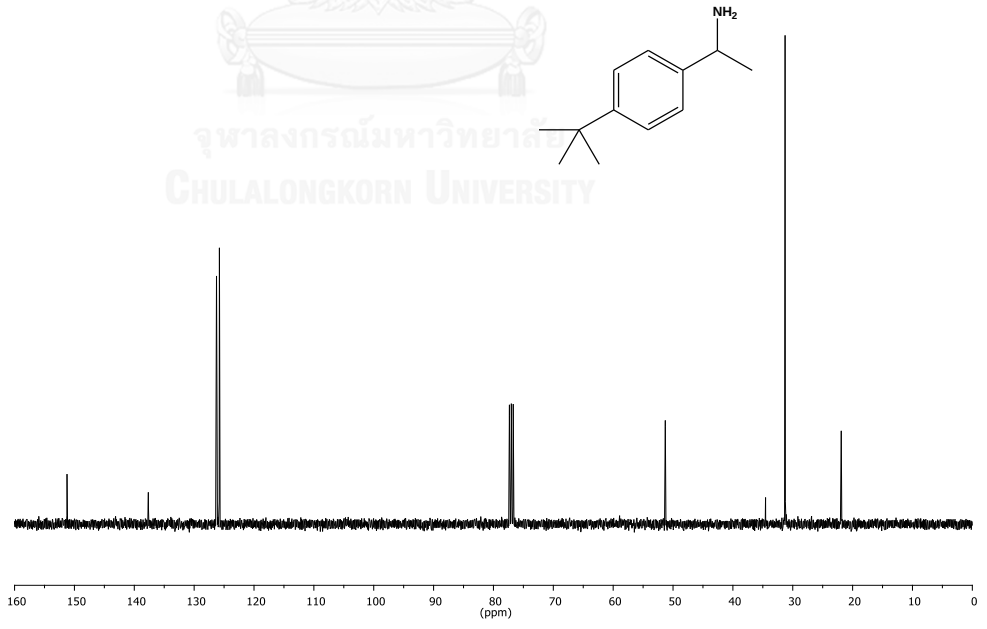

Figure B12 ^{13}C NMR of 4tBu (100 MHz, $CDCl_3$) δ (ppm): 151.2, 137.7, 126.3, 125.8, 51.3, 34.5, 31.3, 21.9.

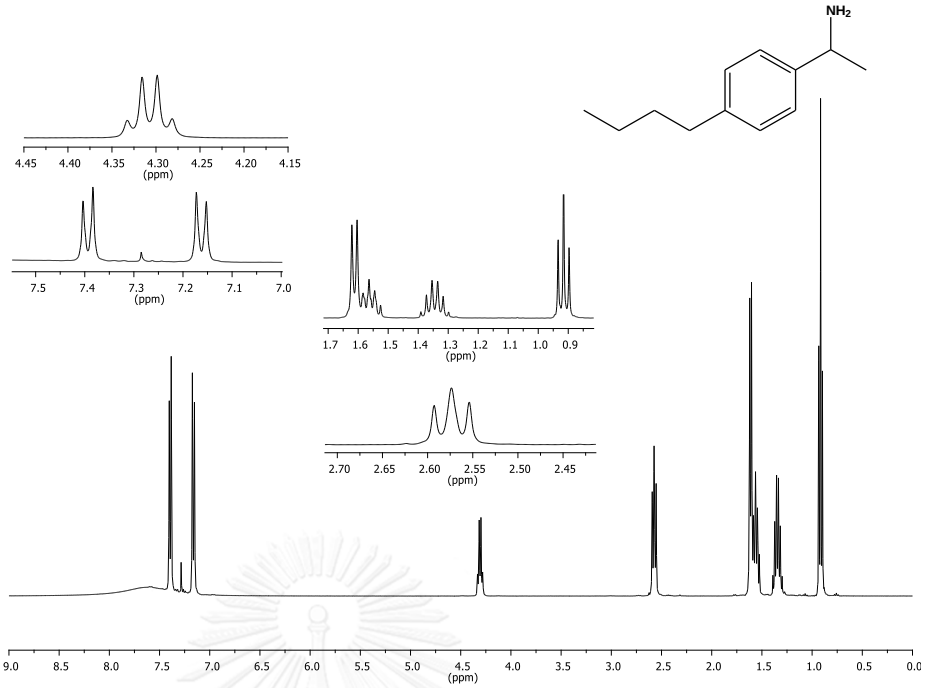

Figure B13 ^{1}H NMR of 4Bu (400 MHz, $CDCl_3$) δ (ppm): 7.59 (br s, 2H, CHN$\underline{H}_2$), 7.39 (d, *J* = 8.1 Hz, 2H, Ar$\underline{H}$), 7.16 (d, *J* = 8.1 Hz, 2H, Ar$\underline{H}$), 4.31 (q, *J* = 6.9 Hz, 1H, C$\underline{H}CH_3$), 2.57 (t, *J* = 7.7 Hz, 2H, ArC$\underline{H}_2$), 1.61 (d, *J* = 6.9 Hz, 3H, CHC$\underline{H}_3$), 1.59 – 1.51 (m, 2H, $CH_2C\underline{H}_2$), 1.40 – 1.29 (m, 2H, C$\underline{H}_2CH_3$), 0.92 (t, *J* = 7.3 Hz, 3H, $CH_2C\underline{H}_3$).

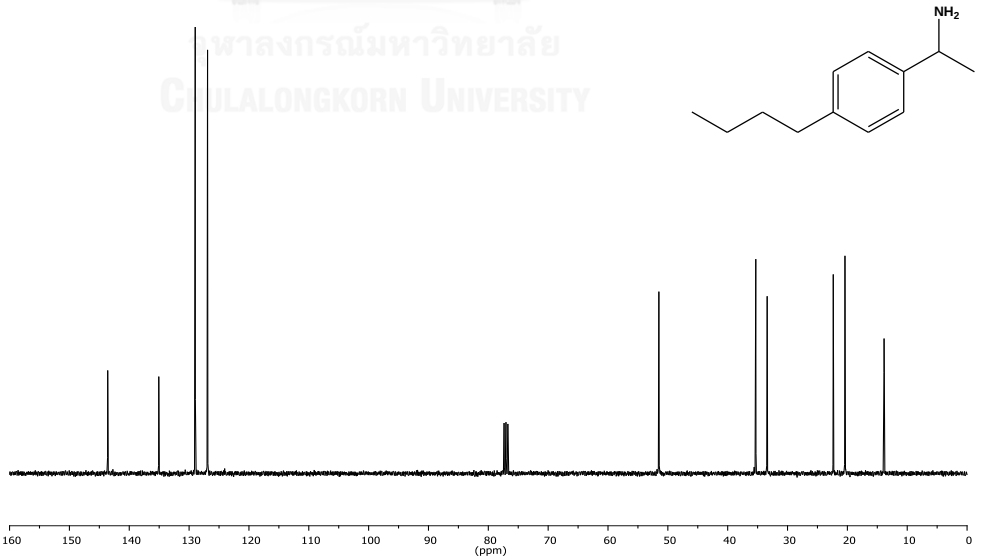

Figure B14 ^{13}C NMR of 4Bu (100 MHz, $CDCl_3$) δ (ppm): 143.6, 135.1, 129.0, 126.9, 51.5, 35.3, 33.4, 22.4, 20.4, 13.9.

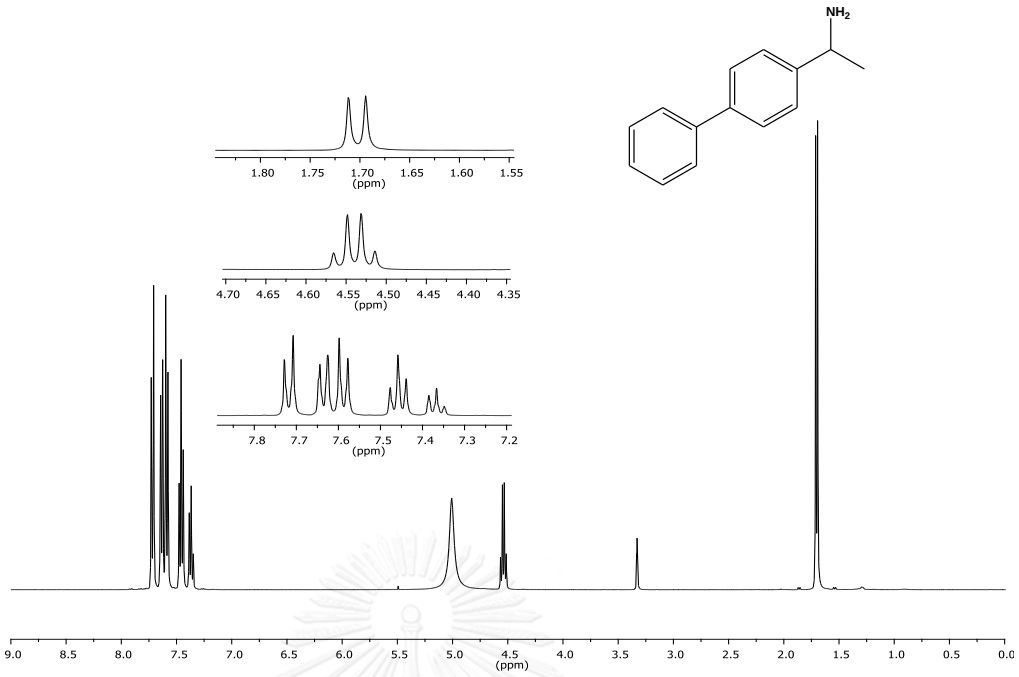

Figure B15 ^{1}H NMR of 4Ph (400 MHz, MeOD) δ (ppm): 7.72 (d, *J* = 7.8 Hz, 2H, Ar<u>H</u>), 7.61 (dd, *J* = 18.7, 7.8 Hz, 2H, Ar<u>H</u>), 7.46 (t, *J* = 7.8 Hz, 4H, Ar<u>H</u>), 7.37 (t, *J* = 7.8 Hz, 1H, Ar<u>H</u>), 5.01 (br s, 2H, CHN<u>H</u>$_2$), 4.54 (q, *J* = 6.9 Hz, 1H, C<u>H</u>CH$_3$), 1.70 (d, *J* = 6.9 Hz, 3H, CHC<u>H</u>$_3$).

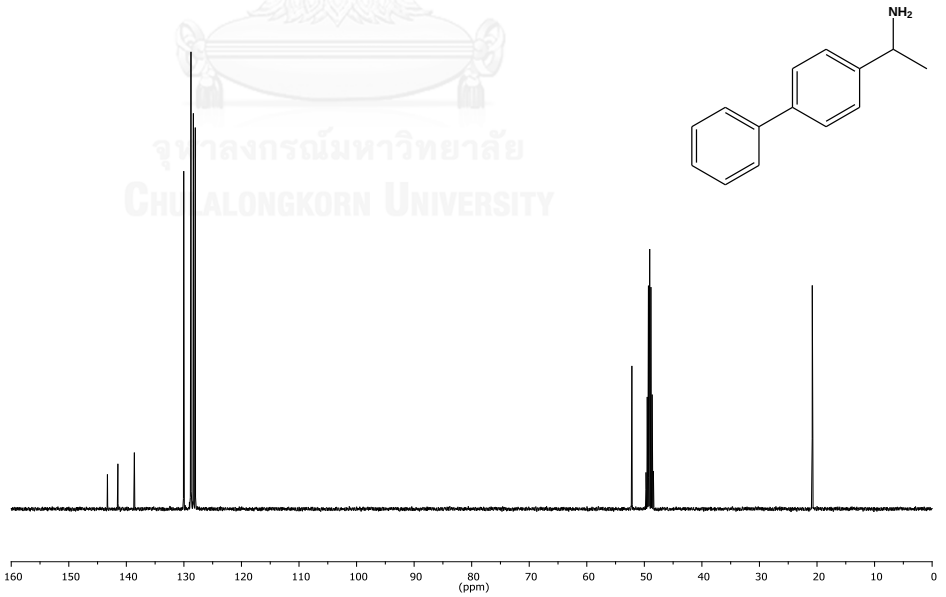

Figure B16 ^{13}C NMR of 4Ph (100 MHz, MeOD) δ (ppm): 143.3, 141.5, 138.6, 130.0, 128.8, 128.8, 128.4, 128.0, 52.2, 20.8.

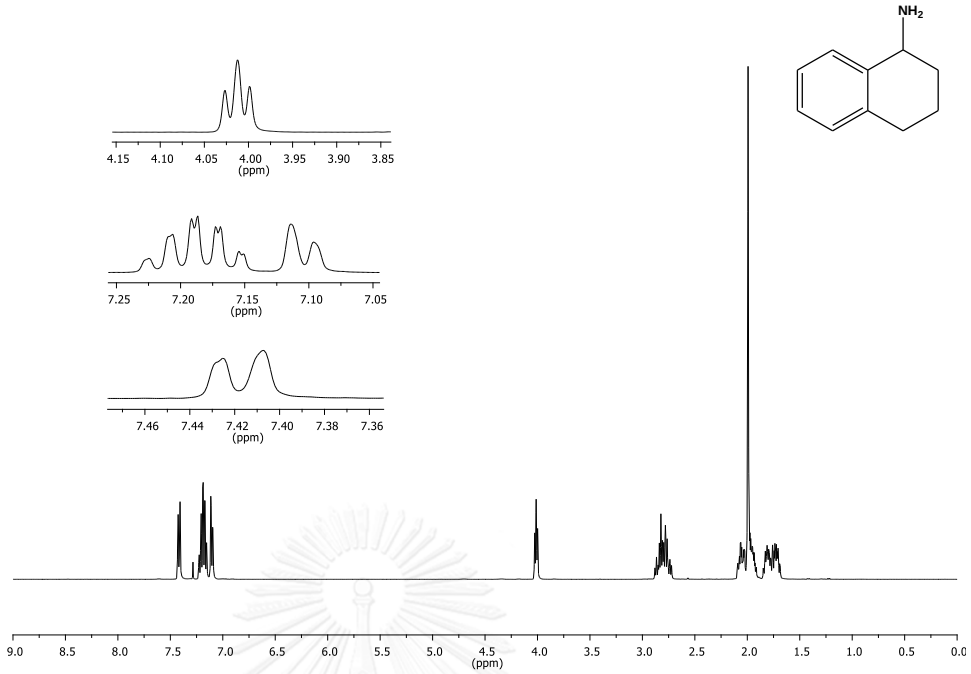

Figure B17 ^{1}H NMR of ATL (400 MHz, $CDCl_3$) δ (ppm): 7.42 (d, *J* = 7.2 Hz, 1H, ArH), 7.24–7.14 (m, 2H, ArH), 7.11 (d, *J* = 7.2 Hz, 1H, ArH), 4.01 (t, *J* = 5.6 Hz, 1H, CHCH$_2$), 2.89–2.71 (m, 2H, *c*-HxH), 2.13–1.90 (m, 2H, *c*-HxH), 1.99 (br s, 2H, CHNH$_2$), 1.86–1.66 (m, 2H, *c*-HxH).

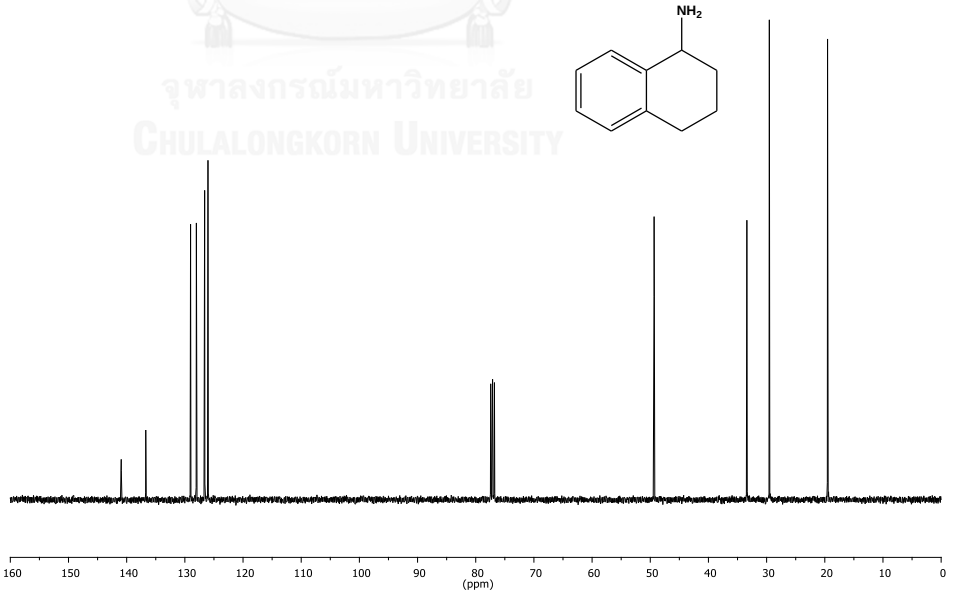

Figure B18 ^{13}C NMR of ATL (100 MHz, $CDCl_3$) δ (ppm): 140.9, 136.7, 129.0, 128.0, 126.6, 126.0, 49.3, 33.4, 29.5, 19.5.

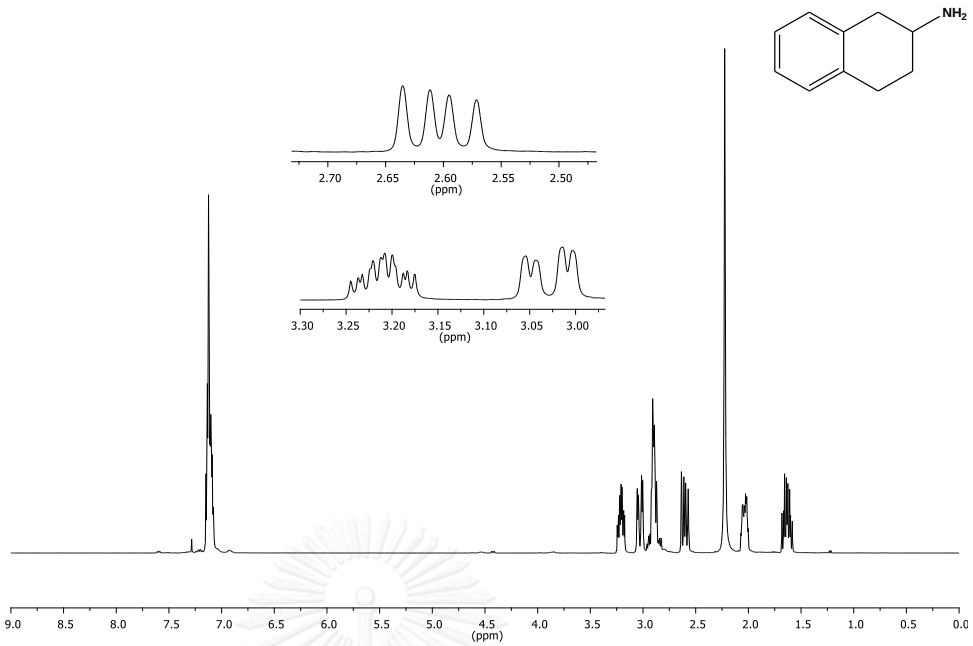

Figure B19 ^{1}H NMR of 2ATL (400 MHz, $CDCl_3$) δ (ppm): 7.18–7.04 (m, 4H, Ar<u>H</u>), 3.26–3.16 (m, 1H, C<u>H</u>NH_2), 3.03 (dd, *J* = 16.1, 4.3 Hz, 1H, *c*-Hx<u>H</u>), 2.97–2.81 (m, 2H, *c*-Hx<u>H</u>), 2.60 (dd, *J* = 16.1, 9.5 Hz, 1H, *c*-Hx<u>H</u>), 2.22 (br s, 2H, CHN<u>H_2</u>), 2.10–1.97 (m, 1H, *c*-Hx<u>H</u>), 1.73–1.51 (m, 1H, *c*-Hx<u>H</u>).

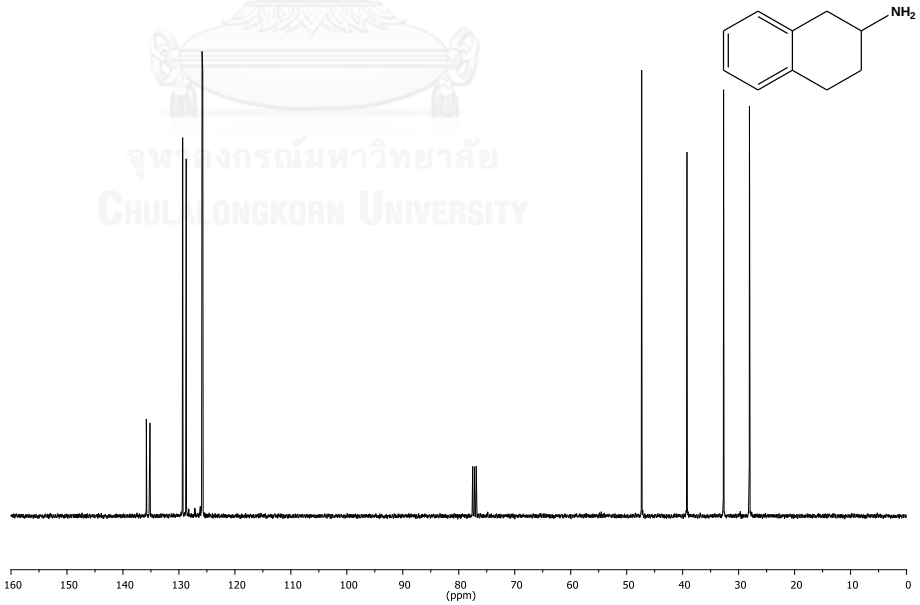

Figure B20 ^{13}C NMR of 2ATL (100 MHz, $CDCl_3$) δ (ppm): 135.8, 135.2, 129.3, 128.7, 125.9, 125.7, 47.3, 39.2, 32.7, 28.1.

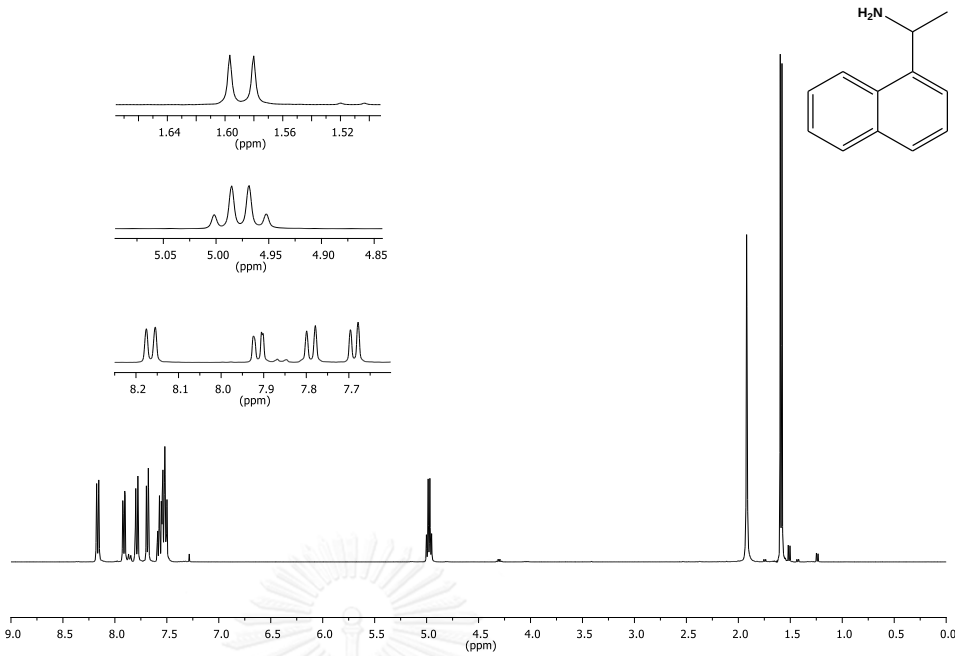

Figure B21 ^{1}H NMR of Nap (400 MHz, $CDCl_3$) δ (ppm): 8.17 (d, *J* = 7.9 Hz, 1H, Ar<u>H</u>), 7.91 (d, *J* = 7.9 Hz, 1H, Ar<u>H</u>), 7.79 (d, *J* = 7.9 Hz, 1H, Ar<u>H</u>), 7.69 (d, *J* = 7.9 Hz, 1H, Ar<u>H</u>), 7.60 – 7.48 (m, 3H, Ar<u>H</u>), 4.98 (q, *J* = 6.6 Hz, 1H, C<u>H</u>CH_3), 1.92 (br s, 2H, $CHN\underline{H}_2$), 1.59 (d, *J* = 6.6 Hz, 3H, $CHC\underline{H}_3$).

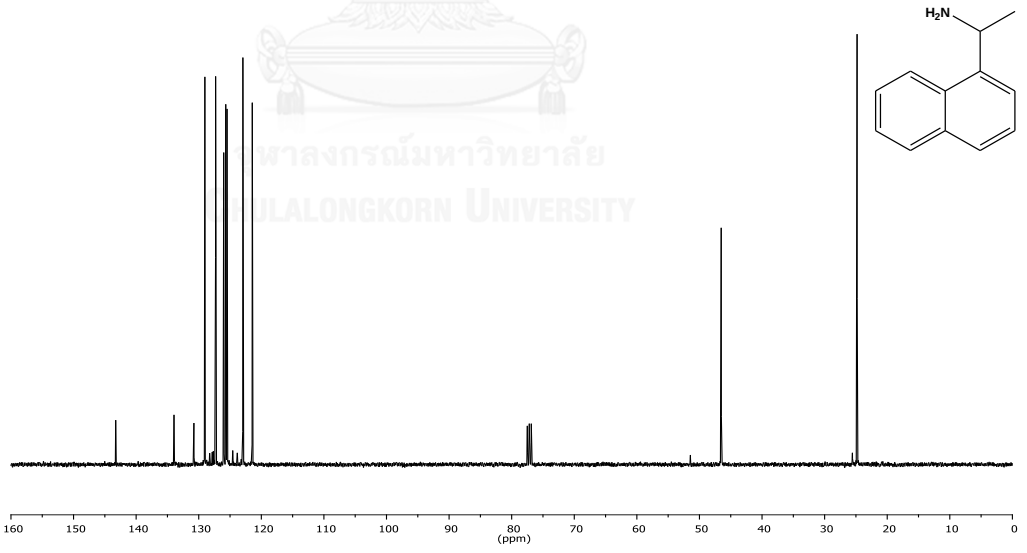

Figure B22 ^{13}C NMR of Nap (100 MHz, $CDCl_3$) δ (ppm): 143.3, 134.0, 130.8, 129.0, 127.3, 126.0, 125.7, 125.5, 123.0, 121.4, 46.5, 24.8.

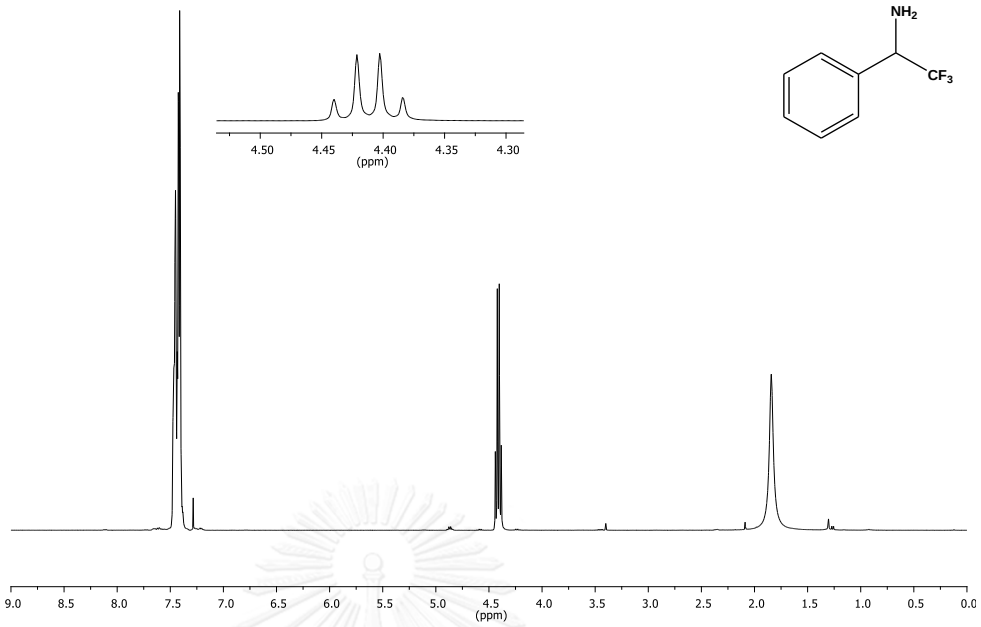

Figure B23 ^{1}H NMR of CF3 (400 MHz, $CDCl_3$) δ (ppm): 7.49–7.38 (m, 5H, Ar<u>H</u>), 4.41 (q, *J* = 7.5 Hz, 1H, C<u>H</u>NH_2), 1.84 (br s, 2H, CHN<u>H</u>$_2$).

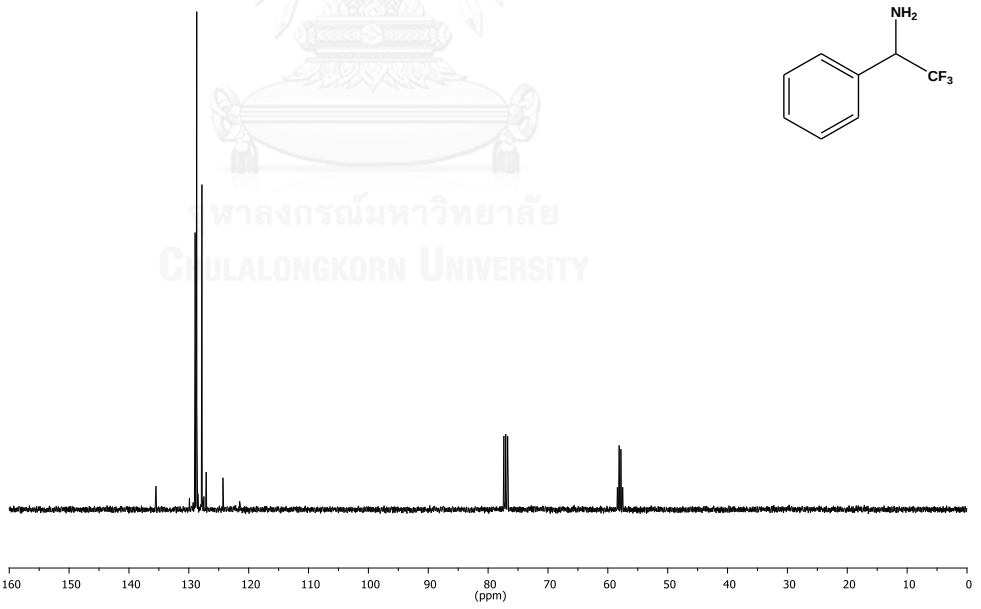

Figure B24 ^{13}C NMR of CF3 (100 MHz, $CDCl_3$) δ (ppm): 135.5, 129.0, 128.7, 127.8, 125.7 (q, *J* = 281.4 Hz), 58.0 (q, J_{CF} = 29.7 Hz).

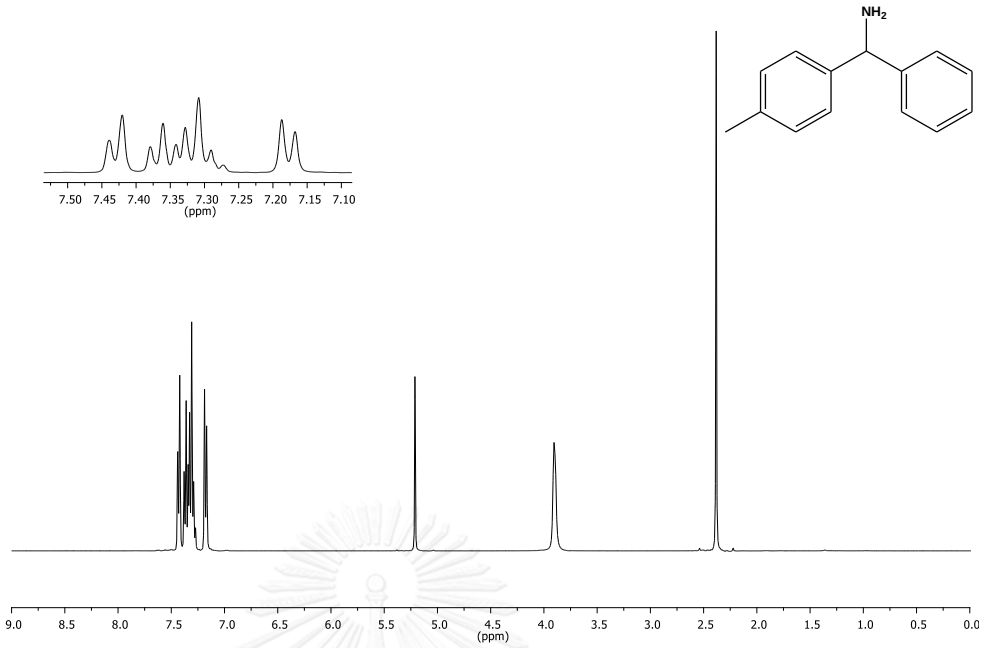

Figure B25 ^{1}H NMR of 4MePh (400 MHz, $CDCl_3$) δ (ppm): 7.52–7.24 (m, 7H, Ar<u>H</u>), 7.18 (d, *J* = 7.8 Hz, 2H, Ar<u>H</u>), 5.21 (s, 1H, C<u>H</u>Ar), 3.90 (br s, 2H, CHN<u>H</u>$_2$), 2.38 (s, 3H, ArC<u>H</u>$_3$).

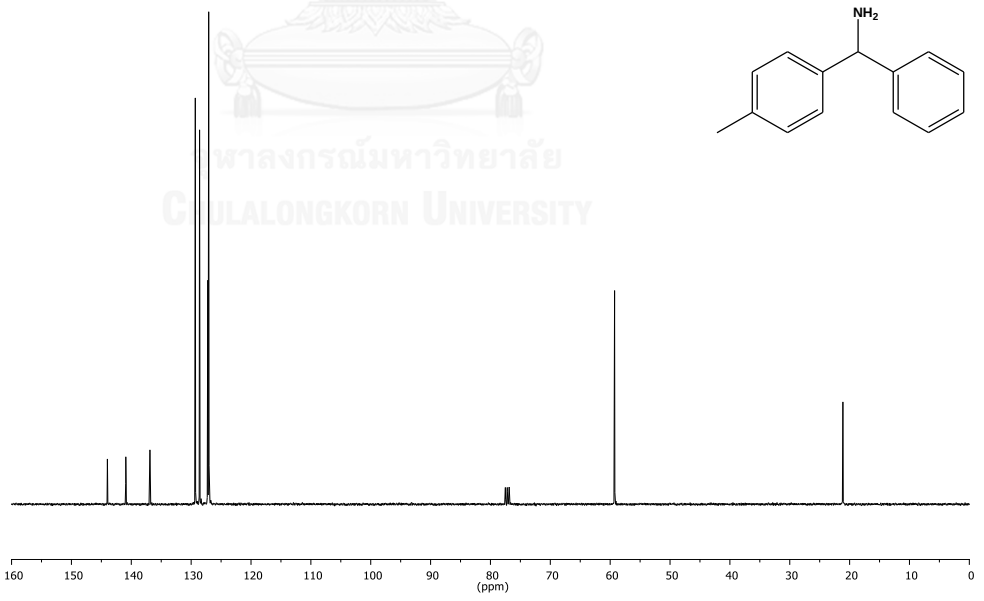

Figure B26 ^{13}C NMR of 4MePh (100 MHz, $CDCl_3$) δ (ppm): 144.0, 140.9, 136.9, 129.3, 128.6, 127.2, 127.1, 127.0, 59.3, 21.1.

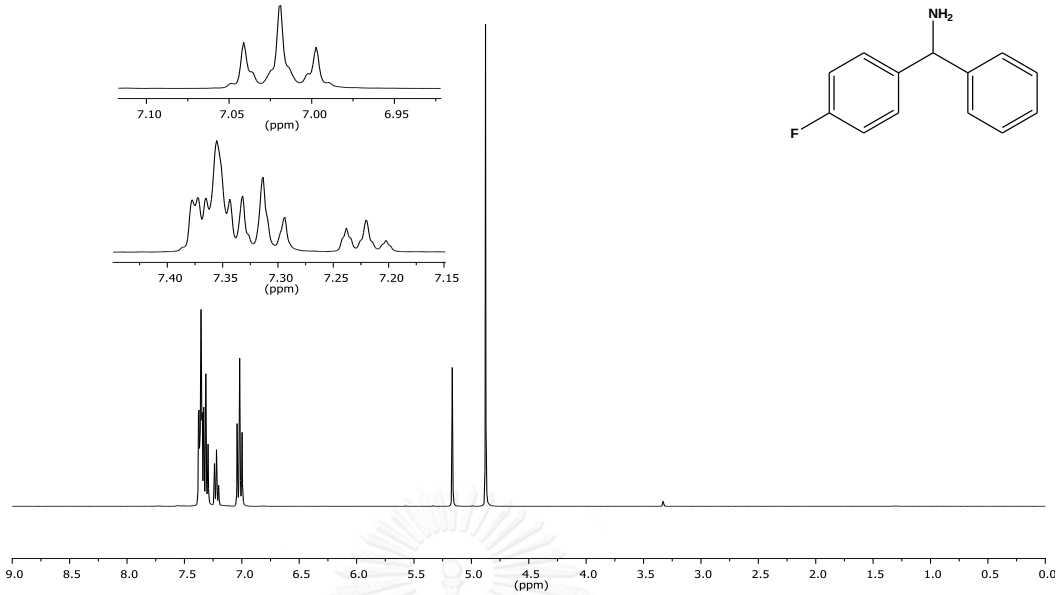

Figure B27 ^{1}H NMR of 4FPh (400 MHz, MeOD) δ (ppm): 7.39–7.28 (m, 6H, ArH), 7.22 (t, *J* = 7.2 Hz, 1H, ArH), 7.02 (t, *J* = 8.8 Hz, 2H, ArH), 5.17 (s, 1H, CHAr), 4.88 (br s, 2H, CHNH$_2$).

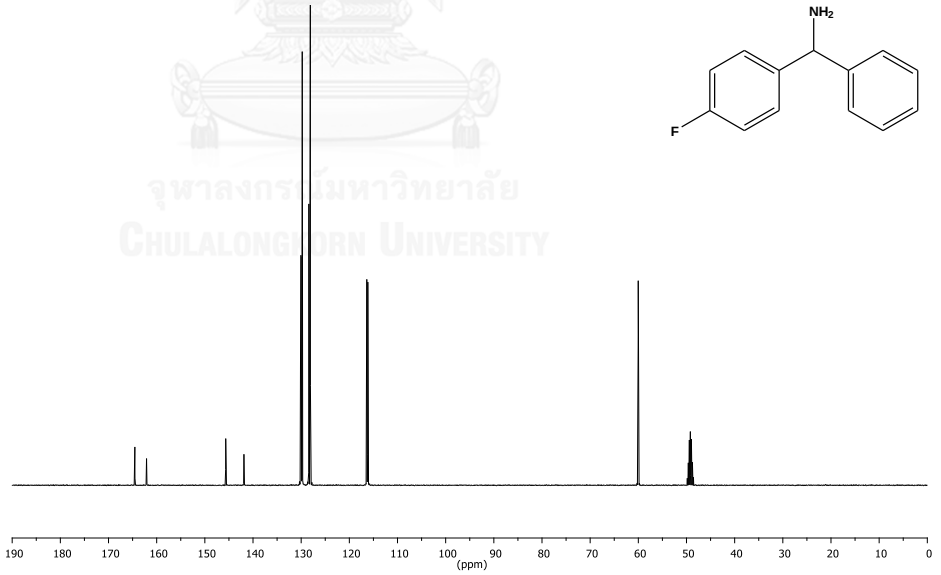

Figure B28 ^{13}C NMR of 4FPh (100 MHz, MeOD) δ (ppm): 163.3 (d, J_{CF} = 244.2 Hz), 145.7, 141.9 (d, J_{CF} = 3.1 Hz), 130.0 (d, J_{CF} = 8.1 Hz), 129.8, 128.4, 128.1, 116.3 (d, J_{CF} = 21.5 Hz), 60.0.

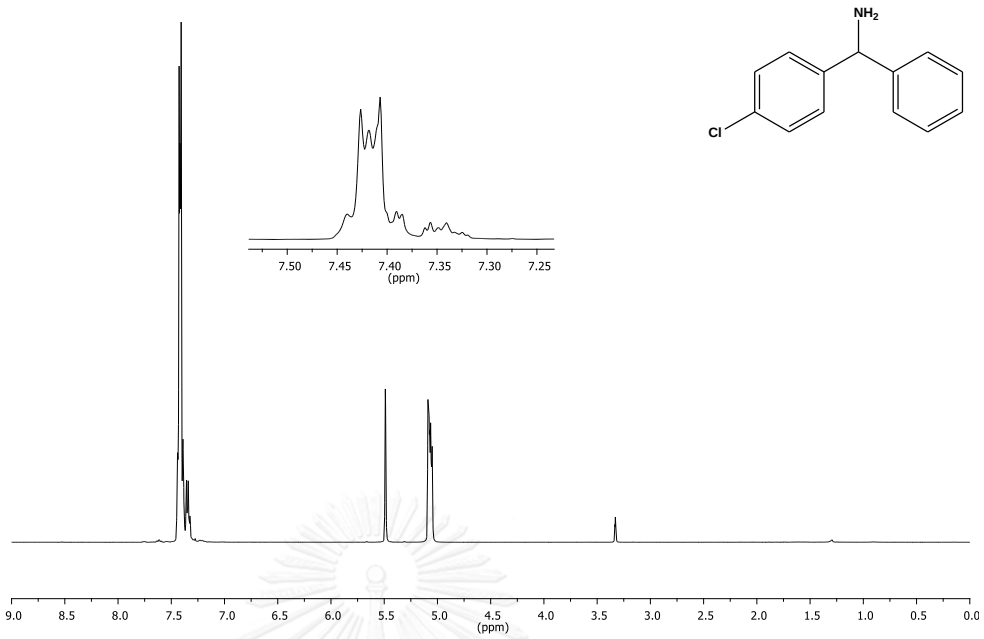

Figure B29 ^{1}H NMR of 4ClPh (400 MHz, MeOD) δ (ppm): 7.46–7.38 (m, 8H, Ar<u>H</u>), 7.37–7.31 (m, 1H, Ar<u>H</u>), 5.49 (s, 1H, C<u>H</u>Ar), 5.11–5.02 (br m, 2H, CHN<u>H</u>$_2$).

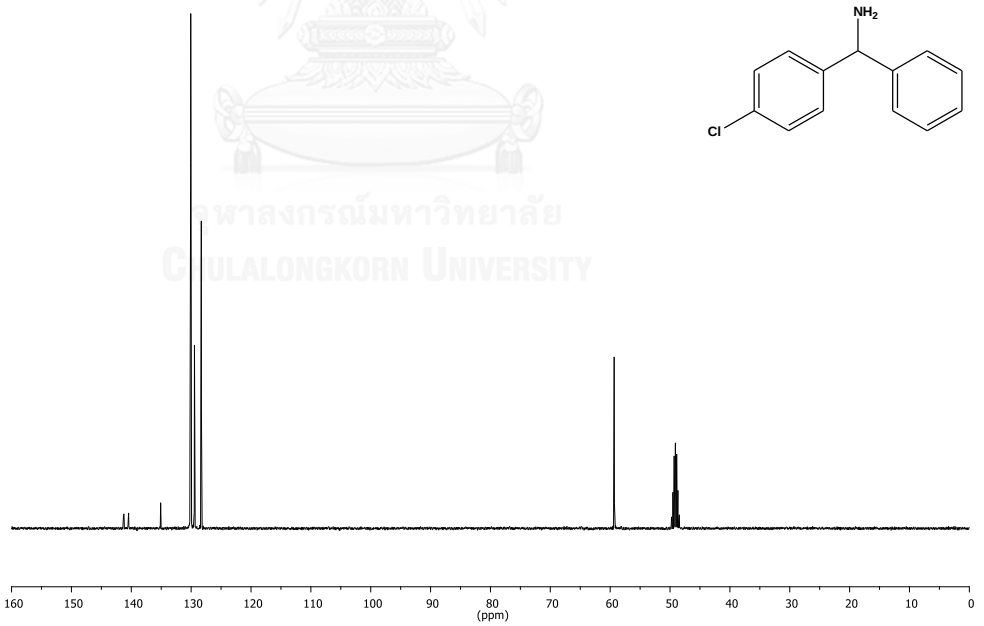

Figure B30 ^{13}C NMR of 4ClPh (100 MHz, MeOD) δ (ppm): 141.2, 140.5, 135.1, 130.1, 130.1, 130.1, 129.5, 128.3, 59.3.

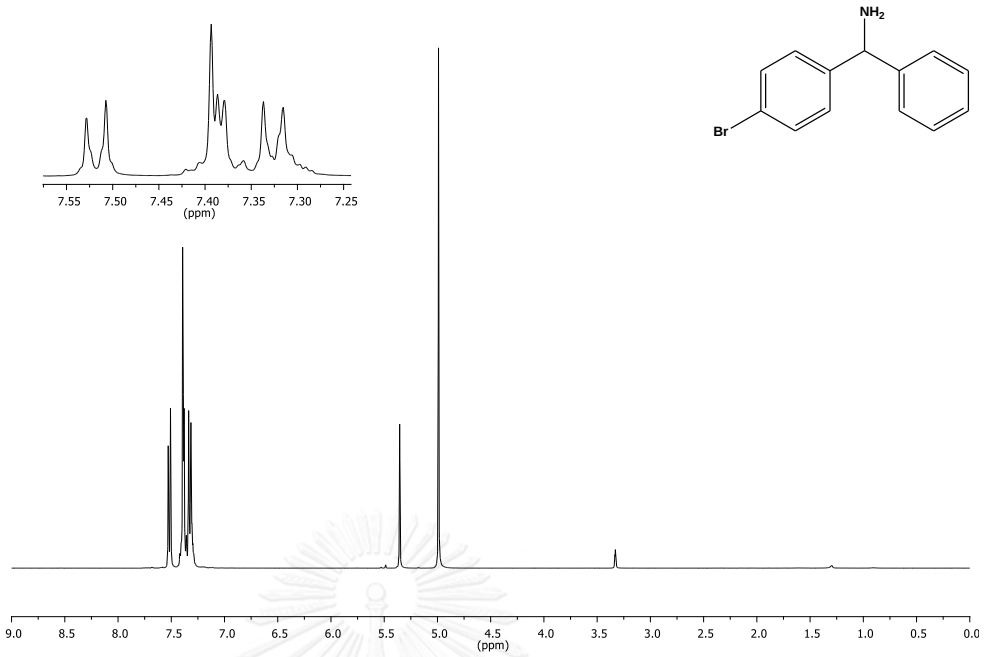

Figure B31 ^{1}H NMR of 4BrPh (400 MHz, MeOD) δ (ppm): 7.52 (d, *J* = 8.5 Hz, 2H, Ar<u>H</u>), 7.42–7.35 (m, 4H, Ar<u>H</u>), 7.35–7.28 (m, 3H, Ar<u>H</u>), 5.35 (s, 1H, C<u>H</u>Ar), 4.99 (br s, 2H, CHN<u>H</u>$_2$).

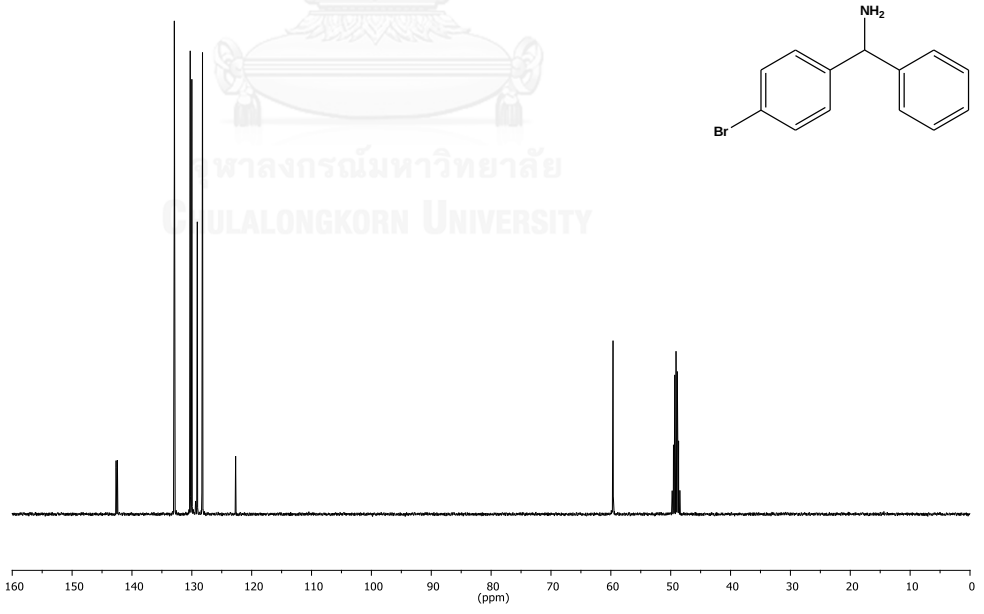

Figure B32 ^{13}C NMR of 4BrPh (100 MHz, MeOD) δ 142.7, 142.4, 132.9, 130.3, 130.0, 129.1, 128.2, 122.7, 59.6.

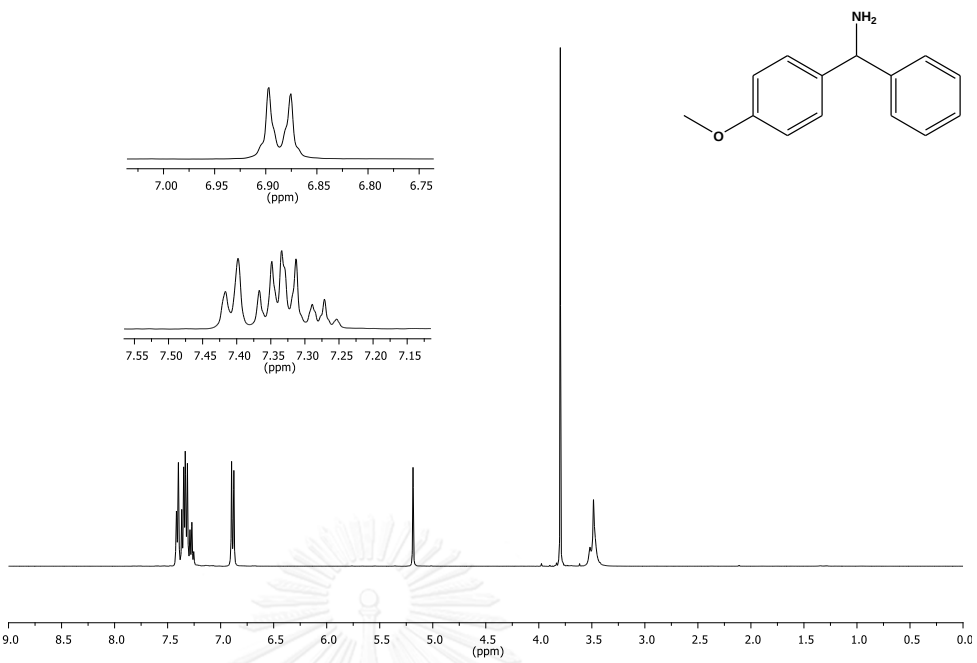

Figure B33 ^{1}H NMR of 4OMePh (400 MHz, $CDCl_3$) δ (ppm): 7.44–7.24 (m, 7H, Ar<u>H</u>), 6.89 (d, *J* = 8.6 Hz, 2H, Ar<u>H</u>), 5.19 (s, 1H, C<u>H</u>Ar), 3.80 (s, 3H, ArOC<u>H</u>$_3$), 3.48 (br s, 2H, CHN<u>H</u>$_2$).

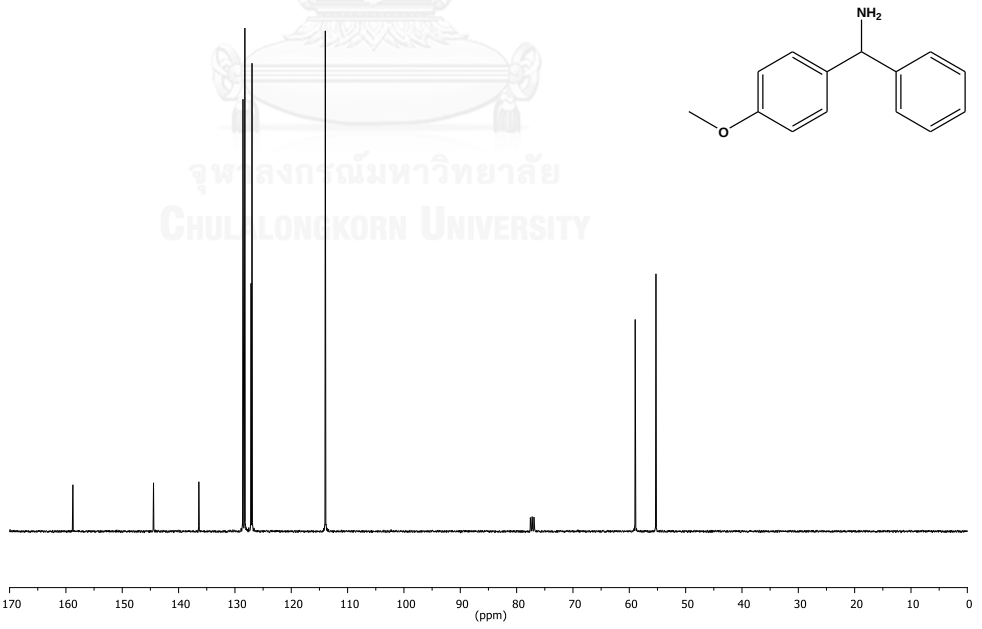

Figure B34 ^{13}C NMR of 4OMePh (100 MHz, $CDCl_3$) δ (ppm): 158.8, 144.5, 136.4, 128.6, 128.2, 127.1, 127.0, 114.0, 59.0, 55.3.

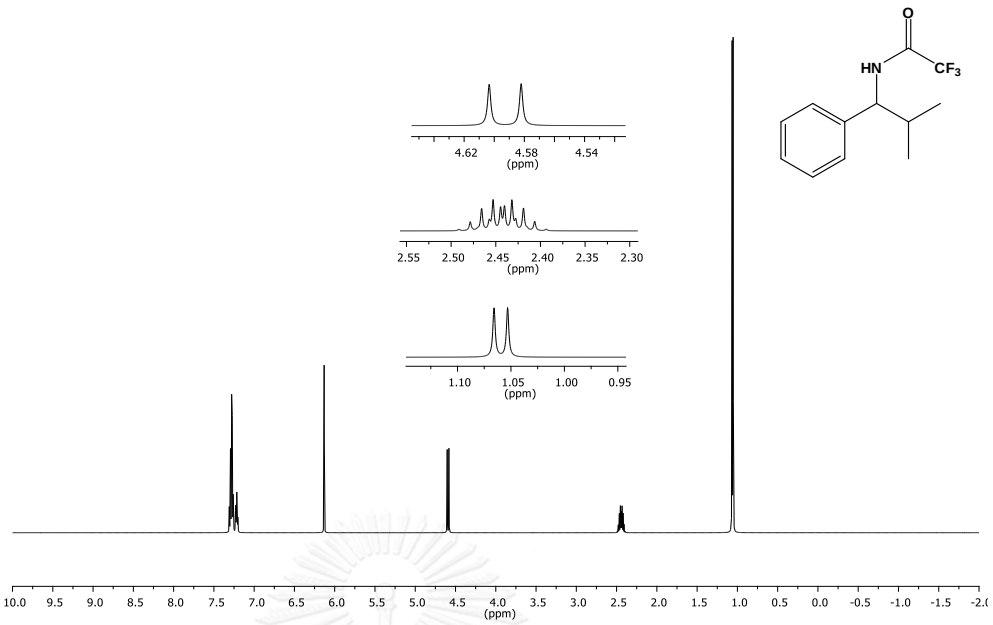

Figure B35 ^{1}H NMR of iBu-TFA (400 MHz, $CDCl_3$) δ (ppm): 7.45 – 6.97 (m, 5H, Ar<u>H</u>), 6.13 (br s, 1H, CHN<u>H</u>), 4.59 (d, *J* = 10.6 Hz, 1H, C<u>H</u>NH), 2.50 – 2.39 (m, 1H, C<u>H</u>$(CH_3)_2$), 1.06 (d, *J* = 6.3 Hz, 6H, CH$(C\underline{H}_3)_2$).

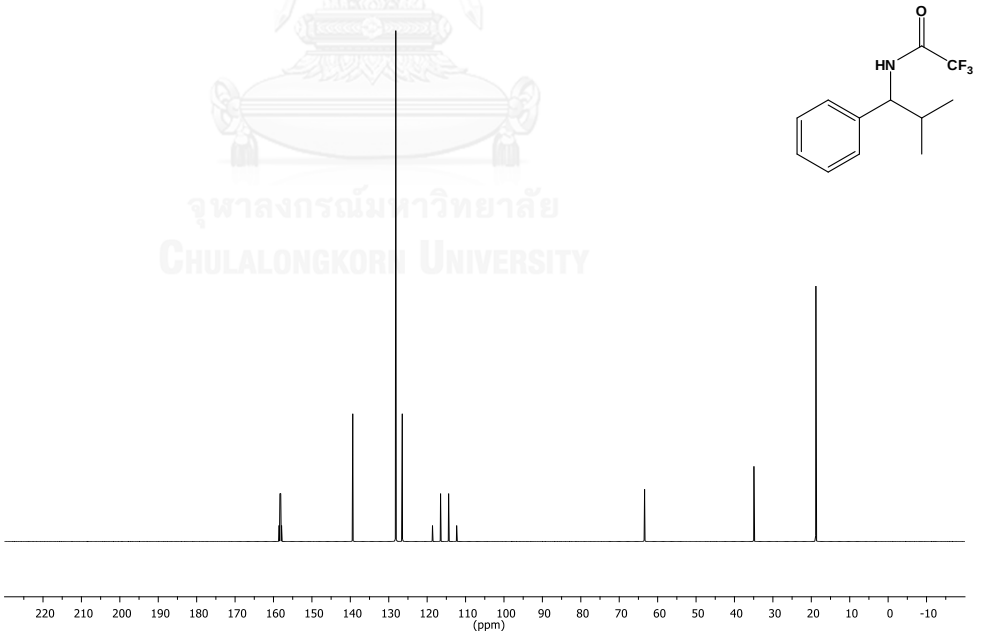

Figure B36 ^{13}C NMR of iBu-TFA (100 MHz,$CDCl_3$) δ (ppm): 158.2 (q, J_{CF} = 21.4 Hz), 139.4, 128.2, 126.5, 115.5 (q, J_{CF} = 209.8 Hz), 63.4, 34.9, 18.8.

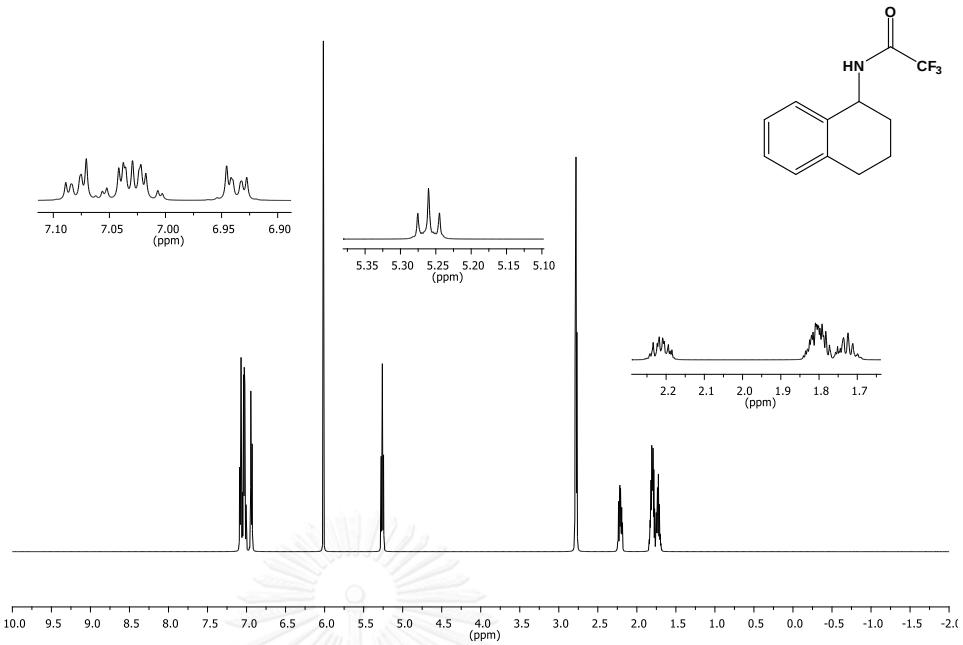

Figure B37 ^{1}H NMR of ATL-TFA (400 MHz, $CDCL_3$) δ (ppm): 7.17–6.85 (m, 4H, Ar<u>H</u>), 6.02 (br s, 1H, CHN<u>H</u>), 5.26 (t, *J* = 7.7 Hz, 1H, C<u>H</u>CH_2), 2.78 (t, *J* = 5.9 Hz, 2H, C<u>H</u>$_2$$CH_2$), 2.28–2.13 (m, 1H, C<u>H</u>$_2$CH), 1.88–1.66 (m, 3H, C<u>H</u>$_2$$CH_2$).

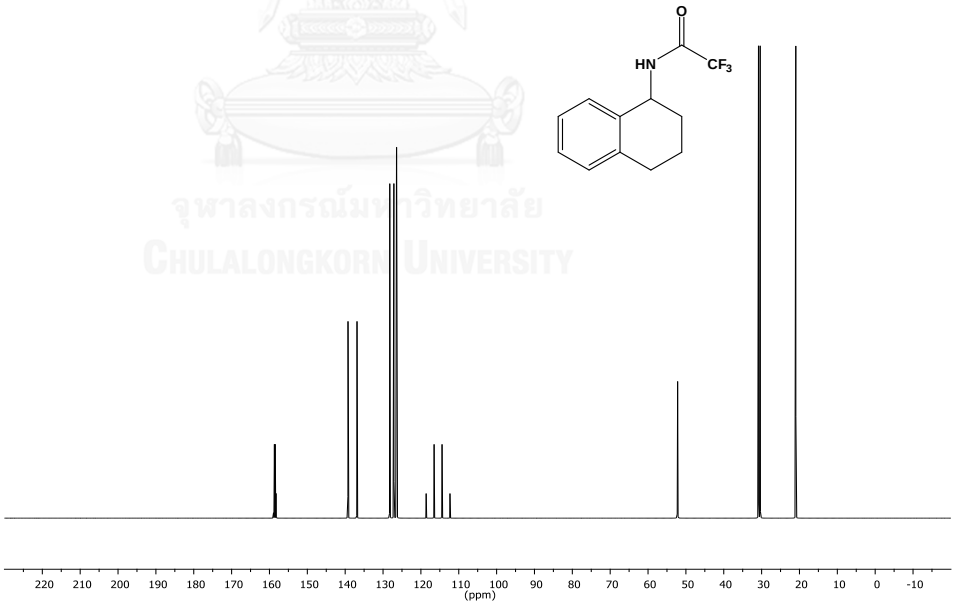

Figure B38 ^{13}C NMR of ATL-TFA (100 MHz, $CDCl_3$) δ (ppm): 158.6 (q, J_{CF} = 26.7 Hz), 139.3, 136.9, 128.2, 127.1, 126.4 (d, J_{CF} = 3.5 Hz), 115.5 (q, J_{CF} = 209.8 Hz), 52.2, 30.8, 30.4, 21.0

VITA

Miss Saithip Charoenchaiworakit was born on January 21, 1990 in Bangkok, Thailand. She graduated from Khema Siri Memorial School, concentration in Mathematic and Science in 2007. After that she entered the Department of Chemistry, Faculty of Science, Chulalongkorn University and received a Bachelor of Science degree in 2011. Then, she continued studying in analytical chemistry, focusing on the chromatographic separation at the same university. She completed her Master of Science Degree in 2015. Her current address is 305/66 Soi Pichai, Pichai road, Thanonnakornchaisri, Dusit, Bangkok, 10300 Thailand.